Microwave diagnostics of magnetoactive plasmas

František Žáček
Institute of Plasma Physics AS CR, v.v.i.
(1959 – 2009, 50-th anniversary)

(1977-84: tokamak TM-1-MH
1984-2007: tokamak CASTOR
2008->: tokamak COMPASS)

Plasma Physics in Science and Technology European Summer School,
Prague 17-28 August 2009

Outline:

- ***propagation*** of electromagnetic waves through a magnetoactive plasma (waves change phase, amplitude, polarization and even frequency)

I. ***active methods*** based mostly on dependence of the cold plasma refractivity index of the electron density (exception point 3)

1) direct measurement of electron density (including its space profile)

- *microwave interferometry* measuring the phase of the fix (or nearly fix) frequency probing O wave, passing the whole plasma perpendicularly to the direction of the confining magnetic field (homodyne or heterodyne systems, one or multichannel systems, moreover with possibility of polarometric determination of the current density j(r) profile) → line integrated method
- *microwave reflectometry* with fast frequency sweeping of the probing wave (change of location of the wave reflection with the frequency) -> edge, local

2) observation of local density turbulent characteristics and directed flows inside the plasma due to the *reflection/scattering* of constant frequency, well focused beam of probing wave (the spot of the beam determines the method space resolution), due to existence of the space localized inhomogeneities (study of anomalous transport and L→H transition, ELM's etc.)

- scattering (i.e. f→f+δf) of the probing beam in different observation direction → ω- as well as k-spectra of these turbulent formations can be obtained
- Doppler reflektometry (the beam is launched and also detected under not zero angle to the normal of the moving reflecting surface, i.e. scattering order m=-1 is observed) → → plasma rotation

3) ECA - Electron Cyclotron resonance wave Absorption measurements (based on thermal effect at the wave's resonance)

II. ***passive methods*** of electron temperature profile measurement by absolute calibrated ECE radiometer, based on electron thermal effect at ECR (see ECA as well) (in additional to the thermal radiation suprathermal radiation of group of non maxwellian particles and EBW mode conversion can be also observable); simple "sniffers" (correlation characteristics of the heating RF wave)

Microwaves - frequencies and generators used

f [Hz]	λ[mm]	
10^9	300	klystrons, BWO, TWO, Gunn oscillators, avalanche diodes
10^{10}	30	- „ -
10^{11}	3	mm waves (doublers, triplers, …) ➜ submm waves ➜
		➜ FIR lasers
	1,22	$C^{13}H_3F$ isotropic methyl fluoride
	0,432	HCOOH formic acid (RTP – 2x40mW, optically pumped)
	0,381	DCOOD deuterized formic acid
$8{,}9.10^{11}$	0,337	HCN cyanide hydrogen (electrically pumped)
$> 10^{12}$	0,119	DCN
	0,118	CH_3OH methyl alcohol

increasing frequencies -> transition from basic to the oversized waveguides and finally to the quasioptics and open resonators (lasers)

Propagation of the waves through a medium

(plasma dispersion equation ➜ effect of the plasma parameters)

- fields and medium properties are coupled (through Maxwell equations) by two quantities ε a μ (permittivity, $D=\varepsilon E$ and permeability, $B=\mu H$)
  - isotropic medium ⇨ ε, μ are scalars
  - anisotropic medium ⇨ ε, μ are generally complex tensors of the 3rd order
- relation between local values of ε, μ characterizing medium as a whole and local microscopic parameters of the plasma (distribution function and density of all kinds of particles) is derived by plasma kinetic theory
- plasma in magnetic field ⇨ $\varepsilon = \varepsilon_{rel}.\varepsilon_o$ is a complex tensor ($\varepsilon_o = 8{,}85.10^{-12}$ F /m), while $\mu \doteq \mu_o = 4\pi.10^{-7}$ H/m is practically constant
- using Maxwell equations and supposing a harmonic plane wave ($\sim e^{-i(\omega t - k.r)}$), the following wave equation (i.e. possible time and space oscillating electromagnetic fields) can be easily derived (for space discharge $\rho=0$):

$$\Delta E + (\omega/c)^2 \varepsilon_{rel} E = 0 \qquad \text{(knowing that } \varepsilon_o \mu_o = 1/c^2\text{)}$$

- if we denote z as direction of the wave propagation then solution of this equation can be written as follows:

$$E = E_o.\exp[-i(\omega t - k.z) - \alpha z] \quad \rightarrow v_{ph} = dz/dt = \omega/k \quad (= c/n,\ n<1 \rightarrow v_{ph} > c)$$

- where $\mathrm{Re}\mathbf{k} = k = (\omega/c).n = 2\pi/\lambda$ denotes the wave number and n index of refractivity, determining the phase velocity and in an inhomogeneous plasma also the wave trajectory – Ray tracing (note that generally n, as well as k, are vectors, which components and therefore also the amplitudes depend on direction of the wave propagation with regards to the density gradient and if magnetic field is present, also to direction of the magnetic field !!!)
- and $\mathrm{Im}\mathbf{k} = \alpha$ is absorption coefficient (determining the wave attenuation)

- relation between the index of refractivity of the wave with a given frequency and microscopic parameters of the plasma is given by dispersion equation
- dispersion equation can be derived as condition for a non-trivial solution of three equations for all three components of the wave equation for the plane wave electric field $E \sim e^{ik.r}$ (determinant of the equations coefficients equals zero), overwritten in the vector form:

  $$n \times n \times E + \varepsilon_{rel}(\omega,k).E = 0$$ (again, $n=(c/\omega).k$ is a vector)
- if we put direction of the magnetic field B in z axis and direction of the wave propagation k in the plane z,x, then vector n has only two components (parallel $n_{\parallel}$ and perpendicular $n_{\perp}$ to B)
- in such case the condition of the non-trivial E solution can be written as an algebraic equation of the sixth power for the vector n amplitude (the third power for $n^2 = n_{\parallel}^2 + n_{\perp}^2$):

  $$n^6.A + n^4.B + n^2.C + D = 0 ,$$

  where all coefficients are known function of components of the tensor ε_{rel} and of the wave propagation direction, whereas coefficient $A \sim v_T^2/c^2$, therefore in the cold plasma $A \rightarrow 0$
- it may be seen that in the cold plasma dispersion equation becomes to be quadratic equation for n^2 ; its two solutions $n_1^2 < n_2^2$ (n_1 fast, n_2 slow) are two different branches of the transverse electromagnetic waves (with different polarization), which can propagate through the cold magnetoactive plasma
- in the case of a cold plasma, solution of dispersion equation are entering plasma density, collision frequency and cyclotron frequency of all charged particles (i.e. value of the magnetic field), further direction of the wave propagation;
- nearly all microwave diagnostics are based on the n_2 cold collisionless plasma approximation; attention in the case of resonances, where $n \rightarrow \infty$!!! and the thermal velocity of particles must be added ➜ T_e from ECE or ECA

Dispersion equation of a cold collisionless plasma in the region of high frequencies ($\omega >> \omega_{ci}$ and even $\omega > \omega_{ce}$)

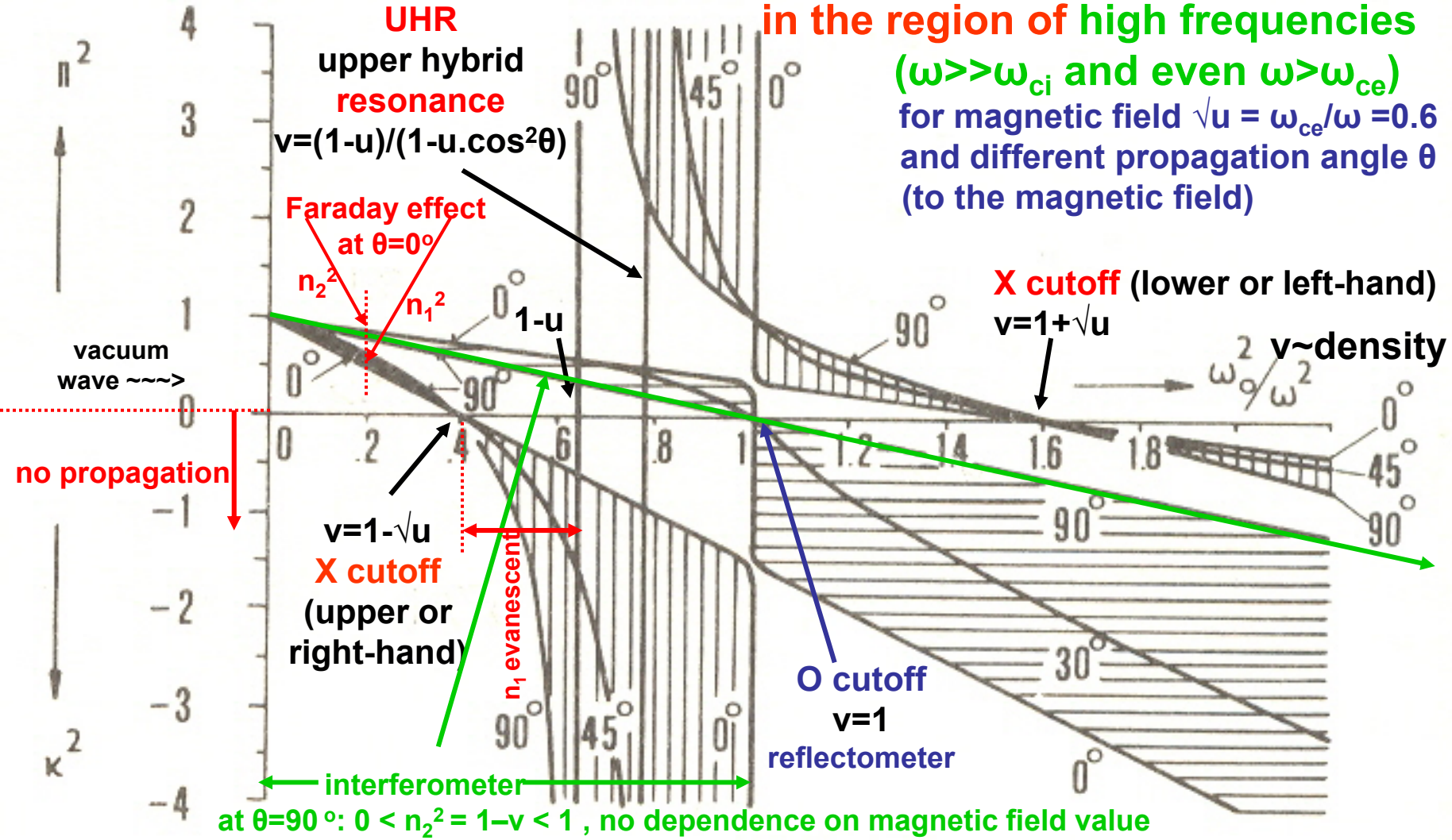

at θ=90°: $0 < n_2^2 = 1 - v < 1$, no dependence on magnetic field value

$(\omega_o/\omega)^2 = v = N/N_{crit}$ ~density

here ω_o=plasma frequency

$(\omega_{ce}/\omega)^2 = u$ ~mag. field

Terminology:

slow wave n_2

($n_2 > n_1 \rightarrow v_2^{ph} < v_1^{ph}$)

fast wave n_1

propagation angle arbitrary

$E \parallel B$ ordinary wave LHCPW

$E \perp B$ extraordinary wave RHCPW

θ= 90° θ=0°

Cold plasma wave classification (Allis diagram)

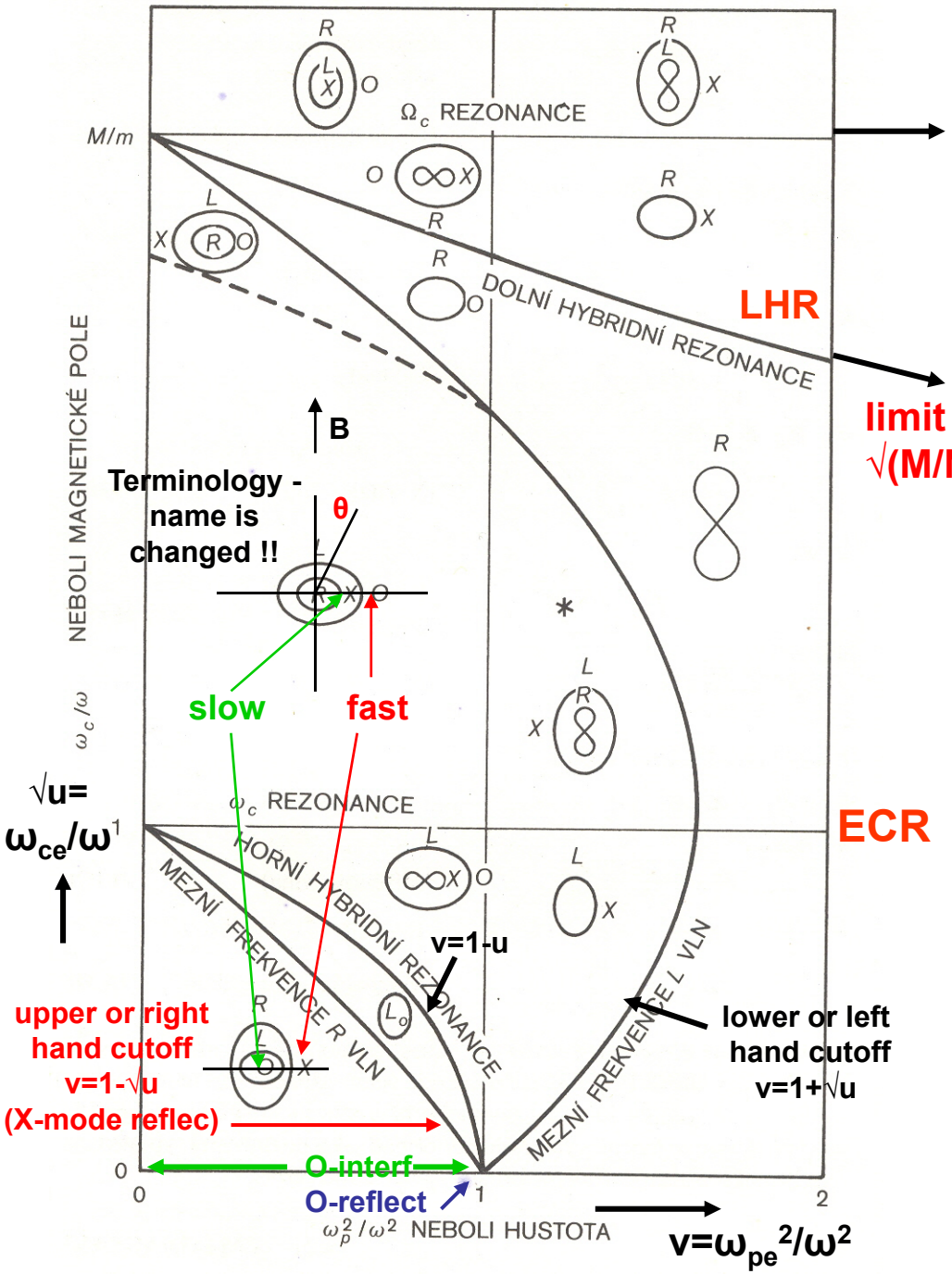

ICR ($\omega_{pe} \gg \omega_{pi} \sim \omega$)

Diagram of normalized magnetic field versus normalized density (normalized to the wave frequency

- fragmented into a set of regions, mutually separated by cut-offs (limit frequencies) and wave resonances

Closed curved (one, two or also no) inside the regions show, which waves (fast and slow) can propagate in this region and simultaneously give, in polar coordinates, dependence of the phase velocity of these waves (as curve radius) on the angle θ of the wave propagation with regards to the magnetic field (zero angle must be put in the vertical axis)

Remark.: diagram is sometimes called also CMA diagram (Clemmow-Mullaly-Allis)

Refractivity index frequency dependence of O-wave - comparison of the effect of all other particles presented

- there are *three groups of particles*, which influence the wave refractivity index:
  free electrons, free ions and neutrals (through the bounded electrons)
- the contributions of all these groups to the total refractivity index can be written symbolically in cumulative form as follows:
  $n = 1 + \delta n_e + \delta n_i + \delta n_n$
- we will shown further that for the *cold collisionless* plasma with $N_e << N_{crit}(\lambda)$
  $\delta n_e = -4{,}48.10^{-14}\lambda^2 N_e < 0$ [cm, cm^{-3}]
  (quite different situation arises in the case of strong collisions !!! - see the next slide)
- it is clear that $\delta n_i = (Z^2.m)/M \,.\, \delta n_e \leq 5.10^{-4}.\, \delta n_e$ (for H), i.e. $\delta n_i \ll \delta n_e$ (both are negative)
  ➜ effect of ions can be neglected
- contribution of the neutral particles is given by ability of these particles to be polarized;
  this contribution has two parts
  - the first is frequency dependent, the second doesn't depend on the frequency:
    $\delta n_n = \alpha(1 + \beta/\lambda^2).N_n > 0$ (positive)
    here α and β are tabulated constants of single gases;
    δn_n is often also expressed, using only one constant K (so called Gladstone-Daley constant, however depending on frequency) in the form $\delta n_n = K.\rho$
    (here ρ [g/cm^{-3}] is the gas mass density
  - contribution of the neutral particles has the opposite sign than contribution of those charged particles !!!

Note the important fact:
Contributions of the charged and the neutral particles to the index of refractivity exhibit (in the *collisionless* plasma) quite opposite frequency dependence (δn_e decreases, while δ_n increases at transition from microwaves to FIR and farther to the IR and visible light)
➜ $n<1$ as well as $n>1$ is possible to measured in low ionized gases at highest frequencies !!!

Dependence of the power transmission coefficient and phase shift of the ordinary wave having frequency ω on the normalized electron density N/N_{crit} of the high collisional plasma

(high pressure discharges)

(Musil, Žáček: Z. f. Naturforsch. 30a (1975) 947)

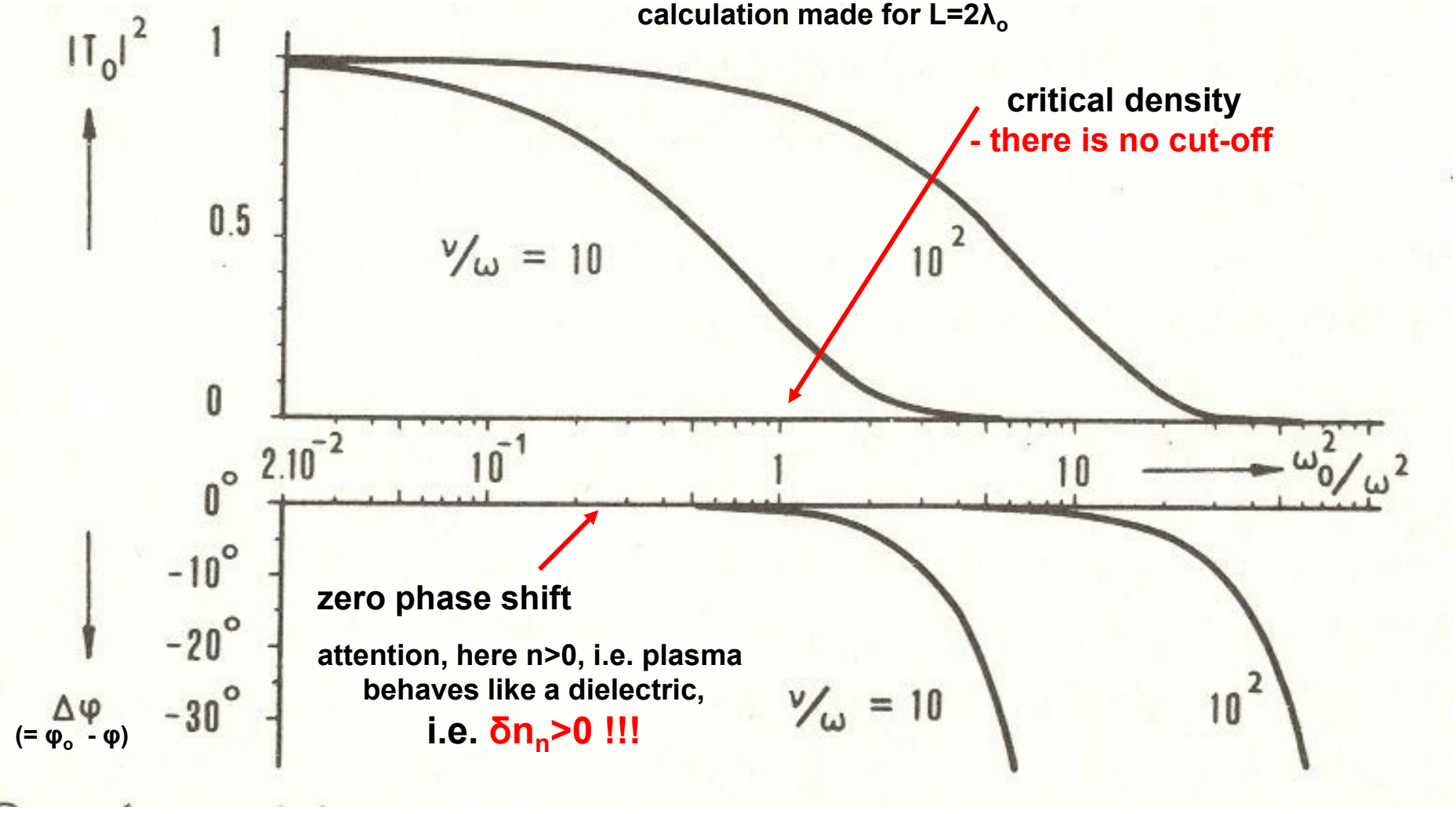

Phase shift of the O-mode wave when the plasma layer L is created

- phase of the wave with frequency ω and vacuum wavelength λ_v after passing the distance L in vacuum: $\varphi_v = 2.\pi.(L/\lambda_v)$
- phase of the same wave after passing of the same distance L in a medium with index of refractivity n(x) changing along the wave trajectory x:

$$\varphi = 2.\pi.(1/\lambda_v).\int_0^L n(x).dx$$

$n^2=1-v$

- for ordinary wave is valid: $n(x) = (\varepsilon_{rel})^{1/2} = (1-N/N_{crit})^{1/2}$ $[\varepsilon_{rel}=1-(\omega_o/\omega)^2,$
- if $N \ll N_{crit}$ is valid, then: $n(x) = 1 - (1/2).(N/N_{crit})$ where $\omega_o^2=N.e^2/m\varepsilon_o]$
- if plasma is created, we can write the phase difference (shift) as following

$$\Delta\varphi = \varphi - \varphi_v = 2.\pi.(1/\lambda_v).\left(L - (1/2).\int_0^L (N/N_{crit})dx - L\right)$$

- after introduction of the line averaged value of density N

$$\langle N\rangle = (1/L).\int_0^L N(x).dx \quad \rightarrow \quad \Delta\varphi = -\pi.(L/\lambda_v).(\langle N\rangle/N_{crit})$$

COMPASS ~500/2.3=220, $2.10^{20}m^{-3}$

Conclusion: the phase shift measured by interferometer increases linearly with λ_v of the probing wave used (doesn't increase with the second power λ_v as the N_{crit}, due to decreasing relative path L/λ_v of the wave due to the L=const)

Dependence of the relative phase shift ε = Δφ/2π, related to 1cm trajectory, on the electron density for different frequency of the probing wave

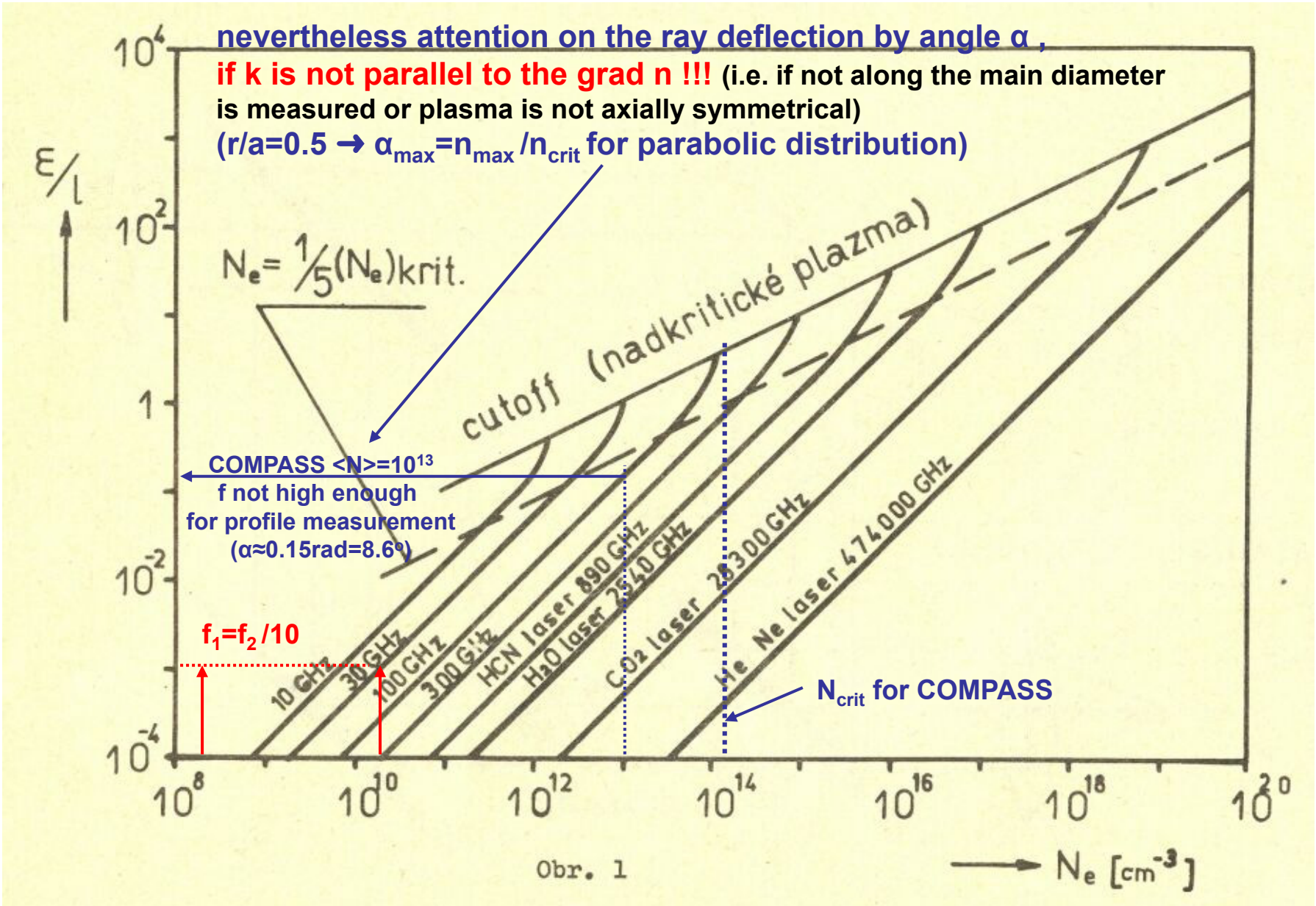

Obr. 1

Distortion of the probing wave phase by two dielectric walls surrounding the plasma

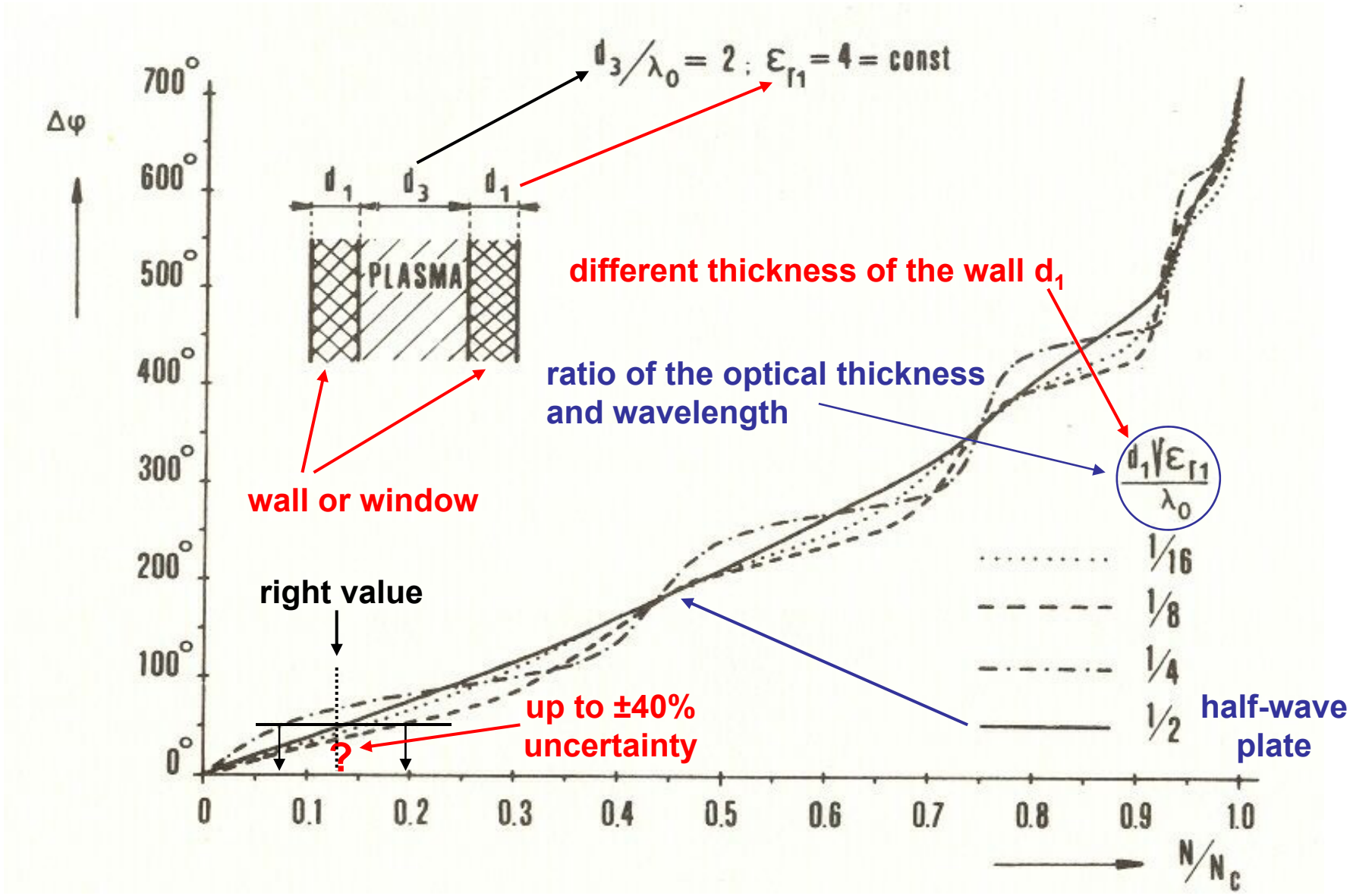

Density dependence of the wave power transmission coefficient if the plasma is surrounded by two dielectric walls

again see the half-wave plate (important for RF generators)

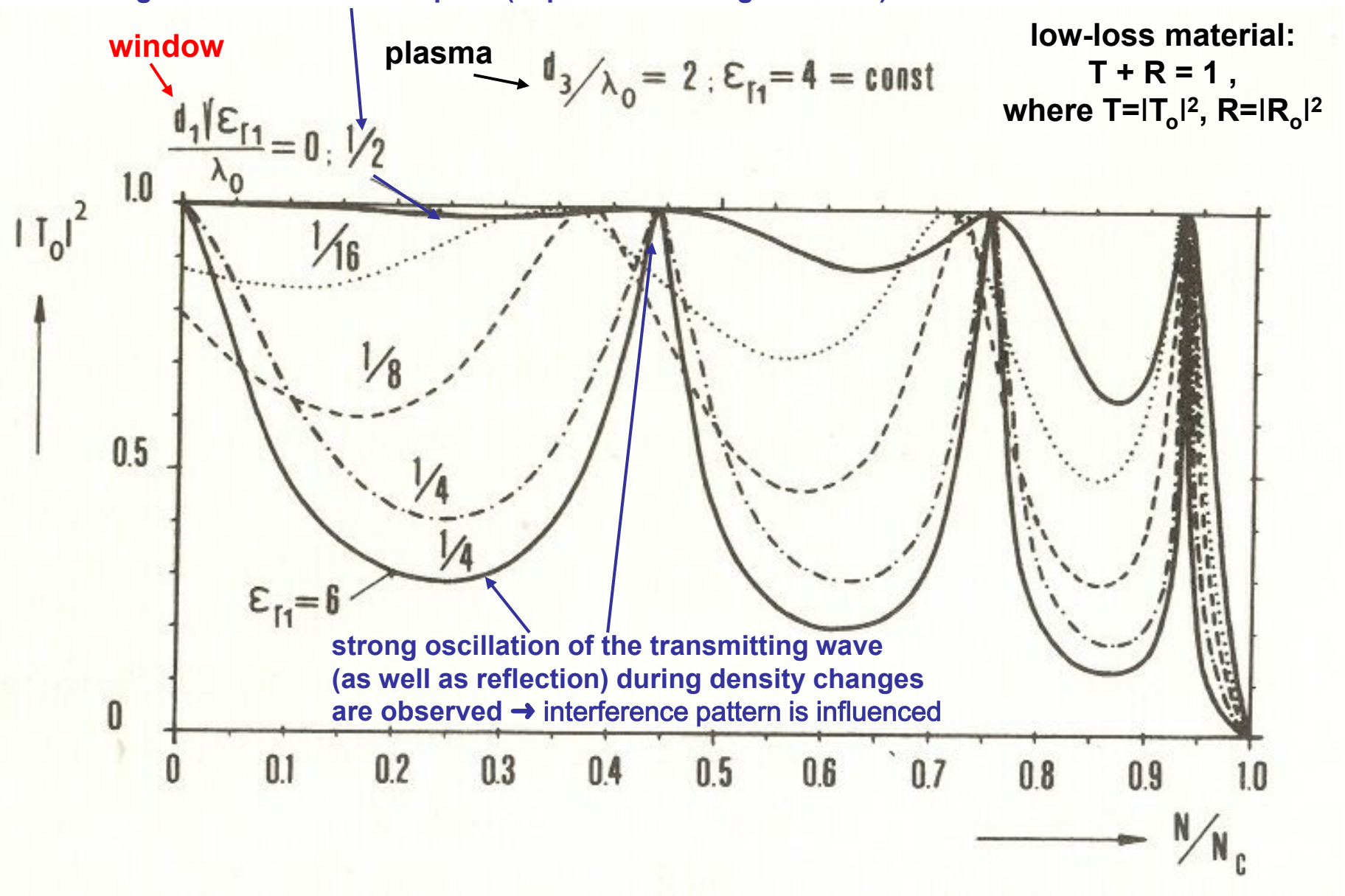

low-loss material:
T + R = 1 ,
where $T=|T_o|^2$, $R=|R_o|^2$

strong oscillation of the transmitting wave (as well as reflection) during density changes are observed → interference pattern is influenced

70GHz ← O-mode interferometer 70GHz ($f > f_p^{max}$)

(but mostly in vertical direction, i.e. B=const.)

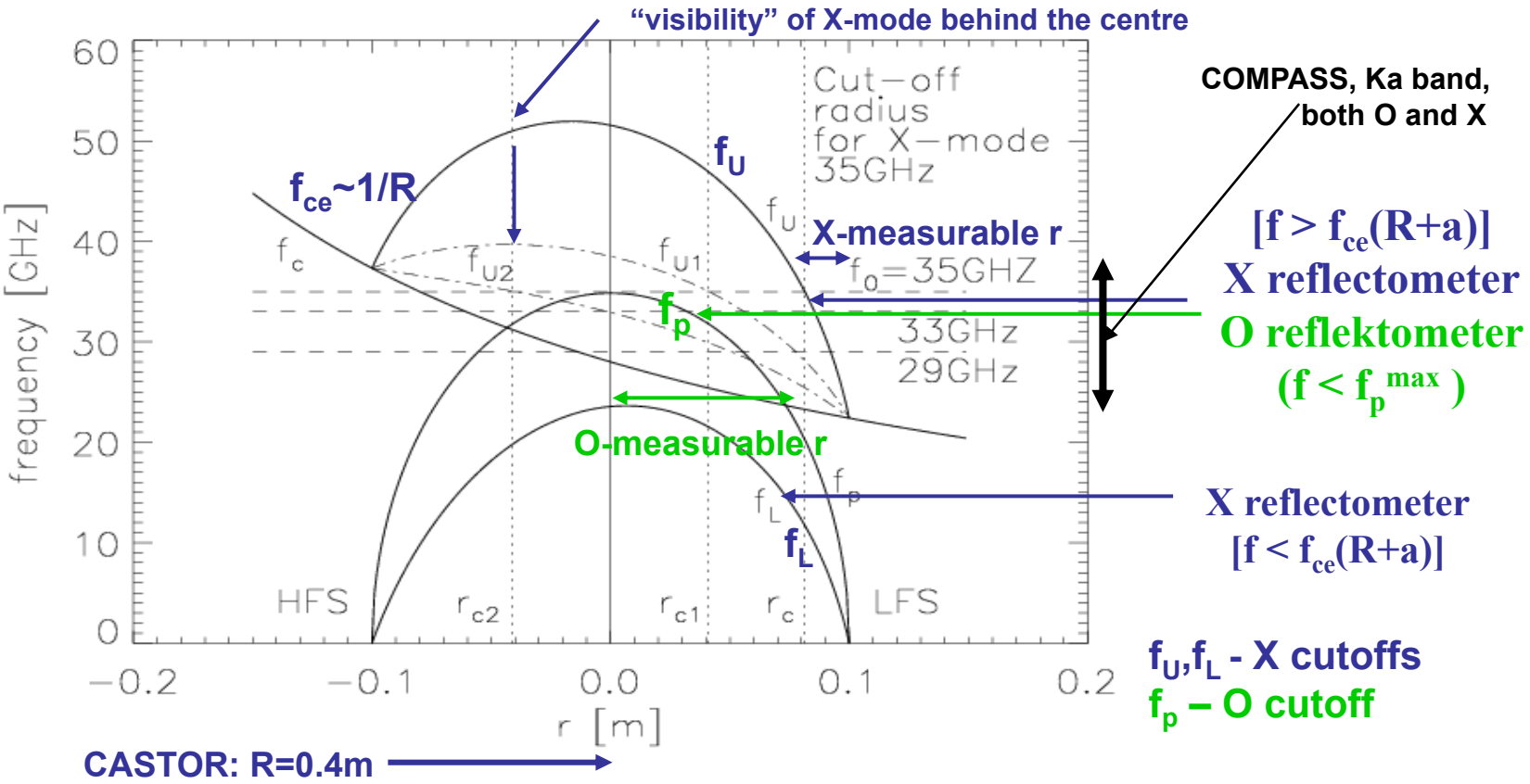

Radial profiles of cut-off frequencies and resonances in CASTOR tokamak (but generally valid for all tokamaks)

for the magnetic field 1T and parabolic density profile (f_p~ √N)

(f_U, f_L for n(0)=$10^{19}m^{-3}$, f_{U1} , f_{U2} for n(0) stepwise decreasing)

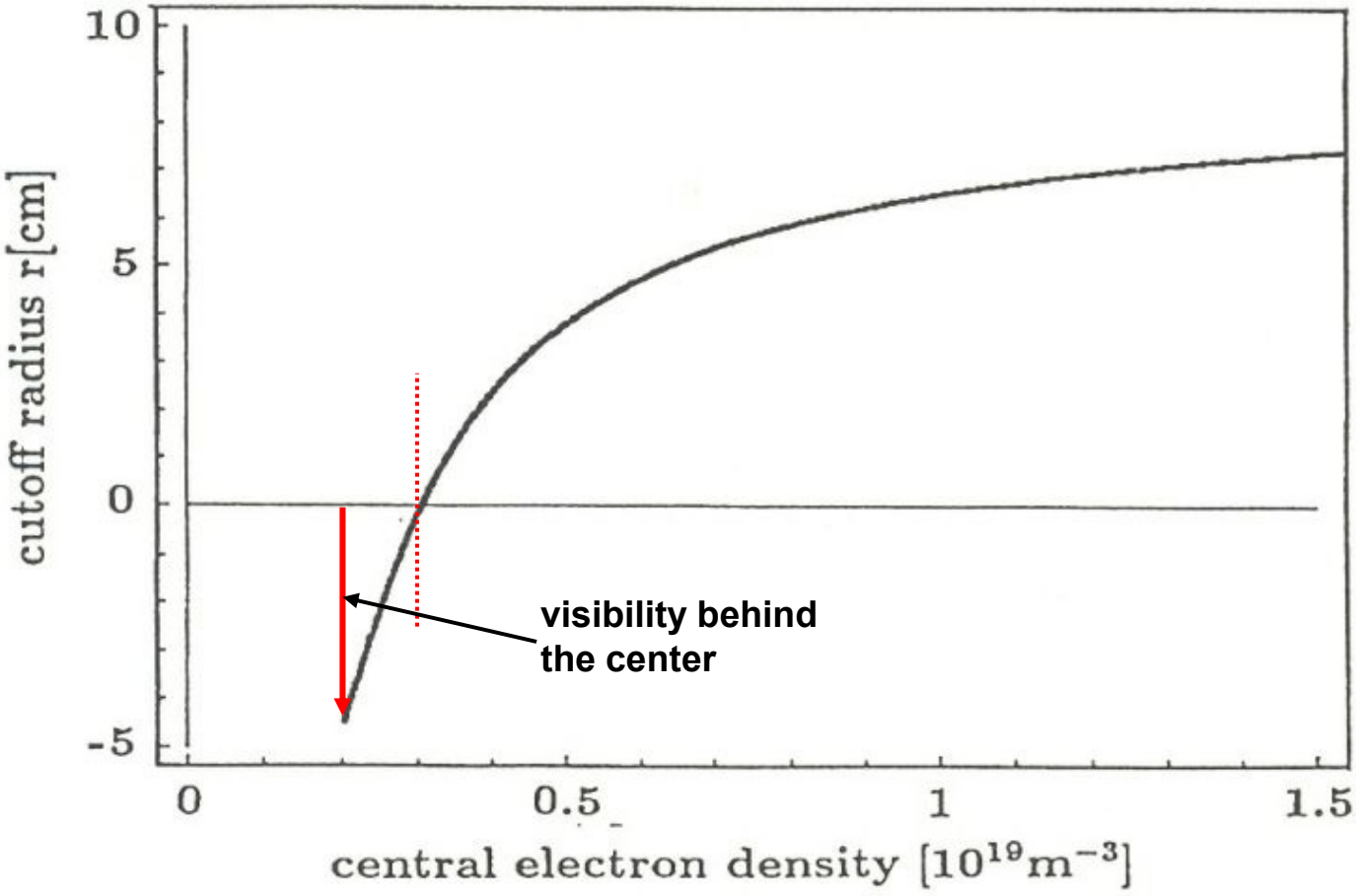

Figure 2: Dependence of the cut-off radius r_c on the central plasma density in CASTOR.

(Using the X-mode reflectometer working on the frequency 35GHz, if B(0)=1T)

Scheme of the microwave homodyne interferometer for measurement of the transmitted as well as reflected waves complex amplitude

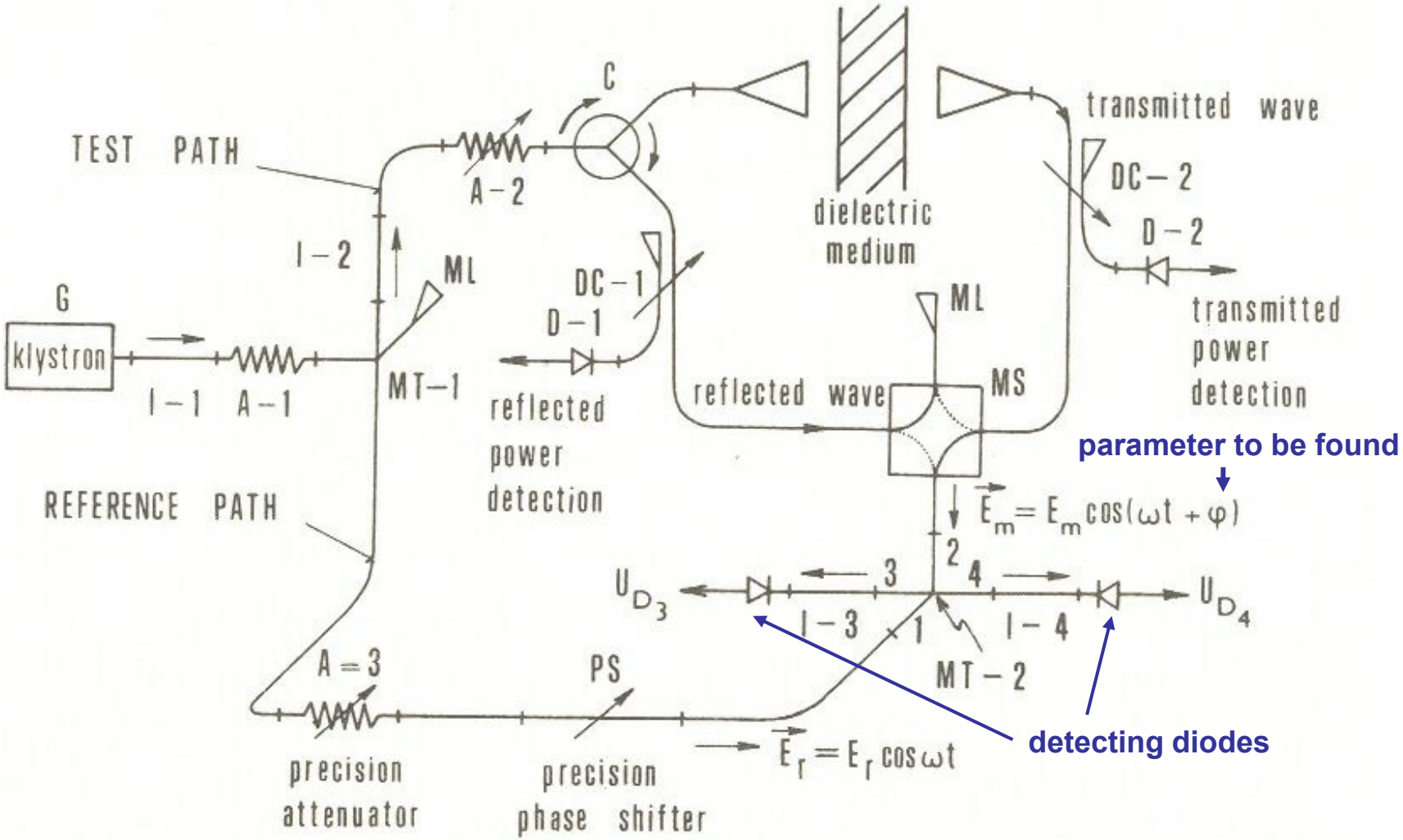

Dependence of normalized voltage U_{D3} and U_{D4} of detection diodes D3 and D4 of the mixing Magic-T junction on the phase difference φ between the reference E_o^{ref}=const and measuring $E_o^m(t,\varphi)$ waves

diodes are quadratic → $U_3 \sim E_3^2=(E_o^{ref})^2/2.[1+(E_o^m/E_o^{ref})^2+2(E_o^m/E_o^{ref}).\cos\varphi]$

usually $E_o^m<E_o^r$, therefore $(E_o^m/E_o^r)^2<<1$

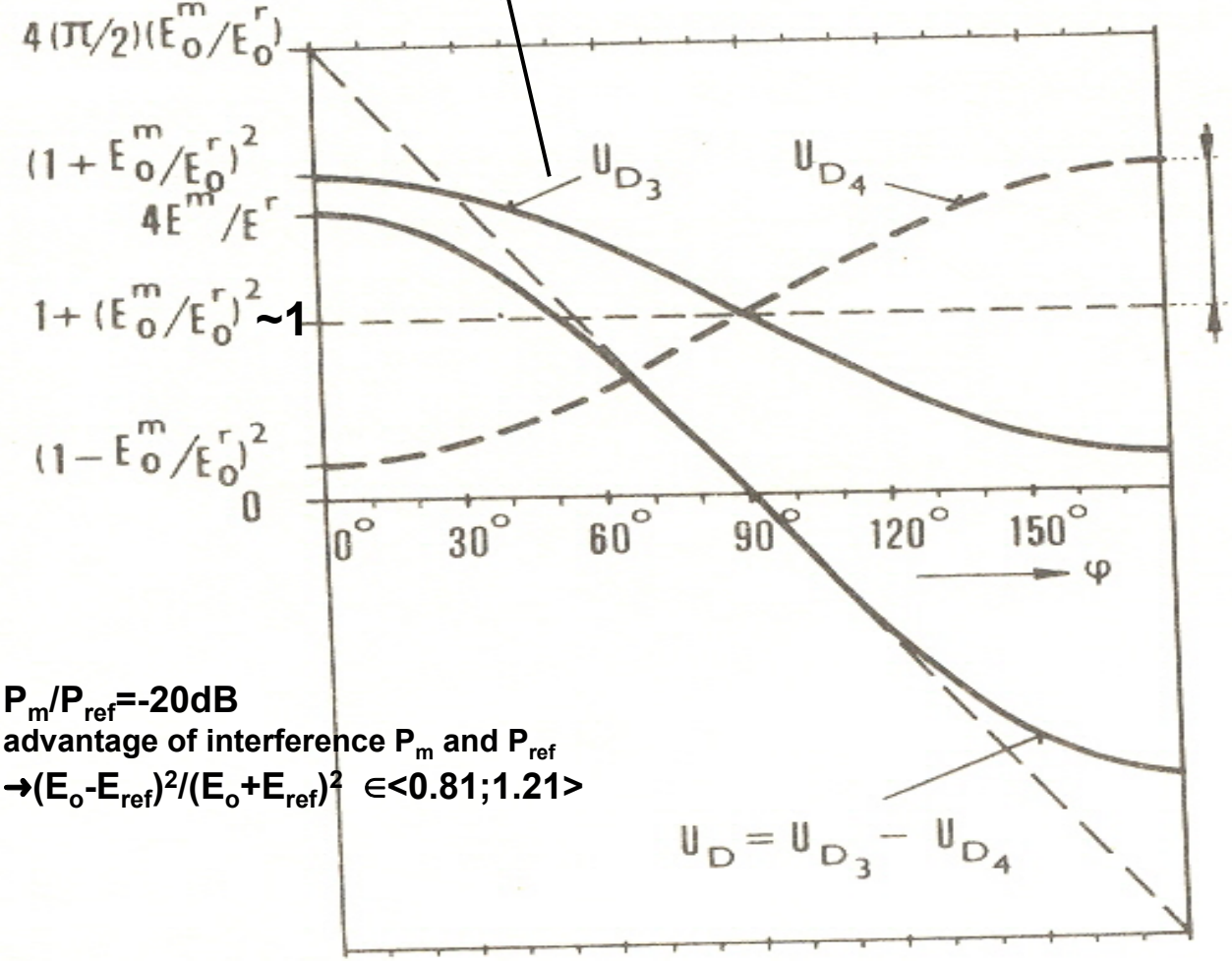

P_m/P_{ref}=-20dB

advantage of interference P_m and P_{ref}

→$(E_o-E_{ref})^2/(E_o+E_{ref})^2 \in$<0.81;1.21>

Conclusions:

1) Amplitude of the interference signal is function not only of the waves phase difference, but also of the wave amplitude (which is changing in the time)

2) Only passages through center of the interferometric picture (φ=π/2, 3π/2, …) are on the measuring wave amplitude independent.

4-beam interferometer with double elliptical cylinder mirrors

(8mm, Musil, Žáček: Czech.J. Phys.B 16 (1966) 782)

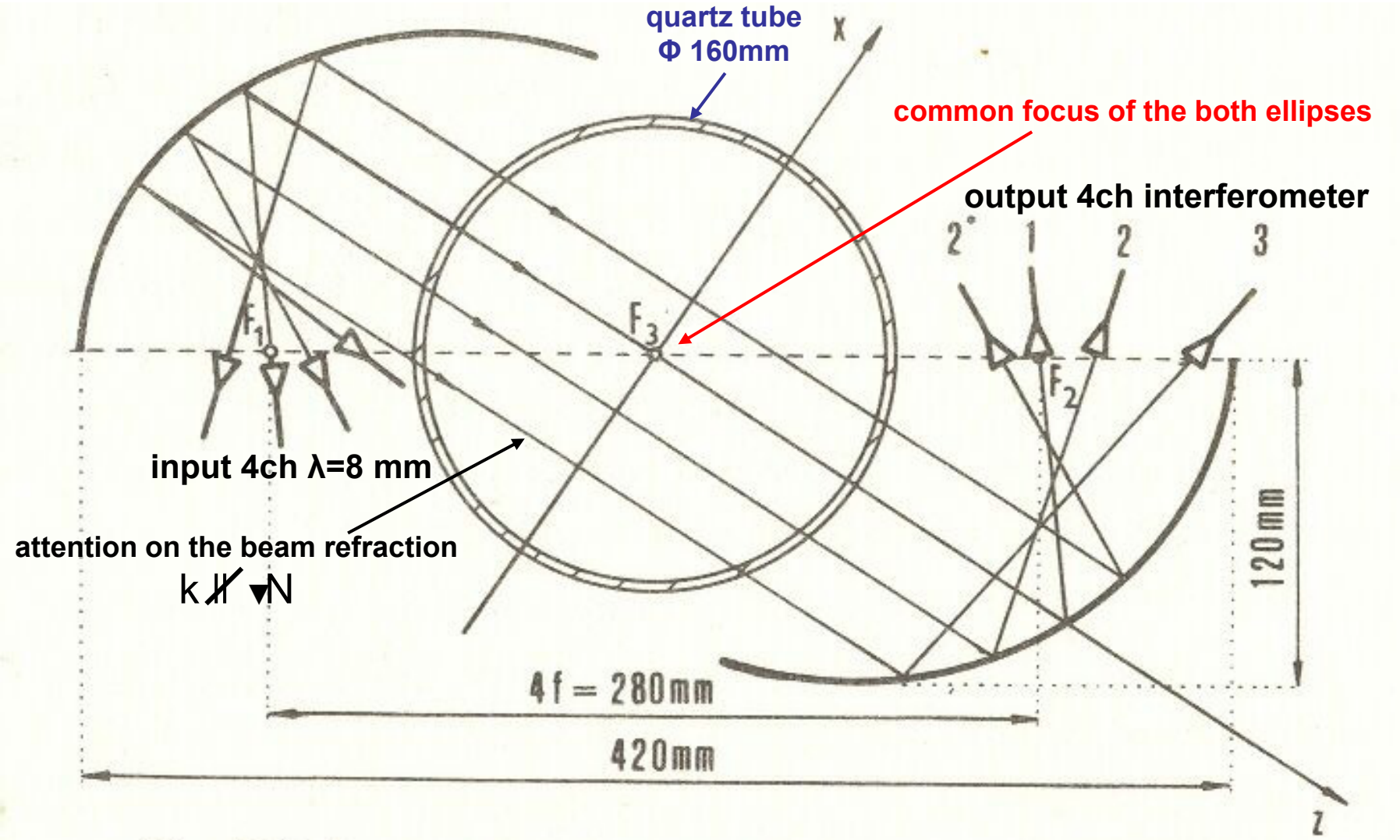

Fig. 5.32 Antenna system of a multiple-beam interferometer.

Radial power profiles of 4 beams of 8mm interferometer, formed by double elliptical mirrors

- no overlapping of the channels

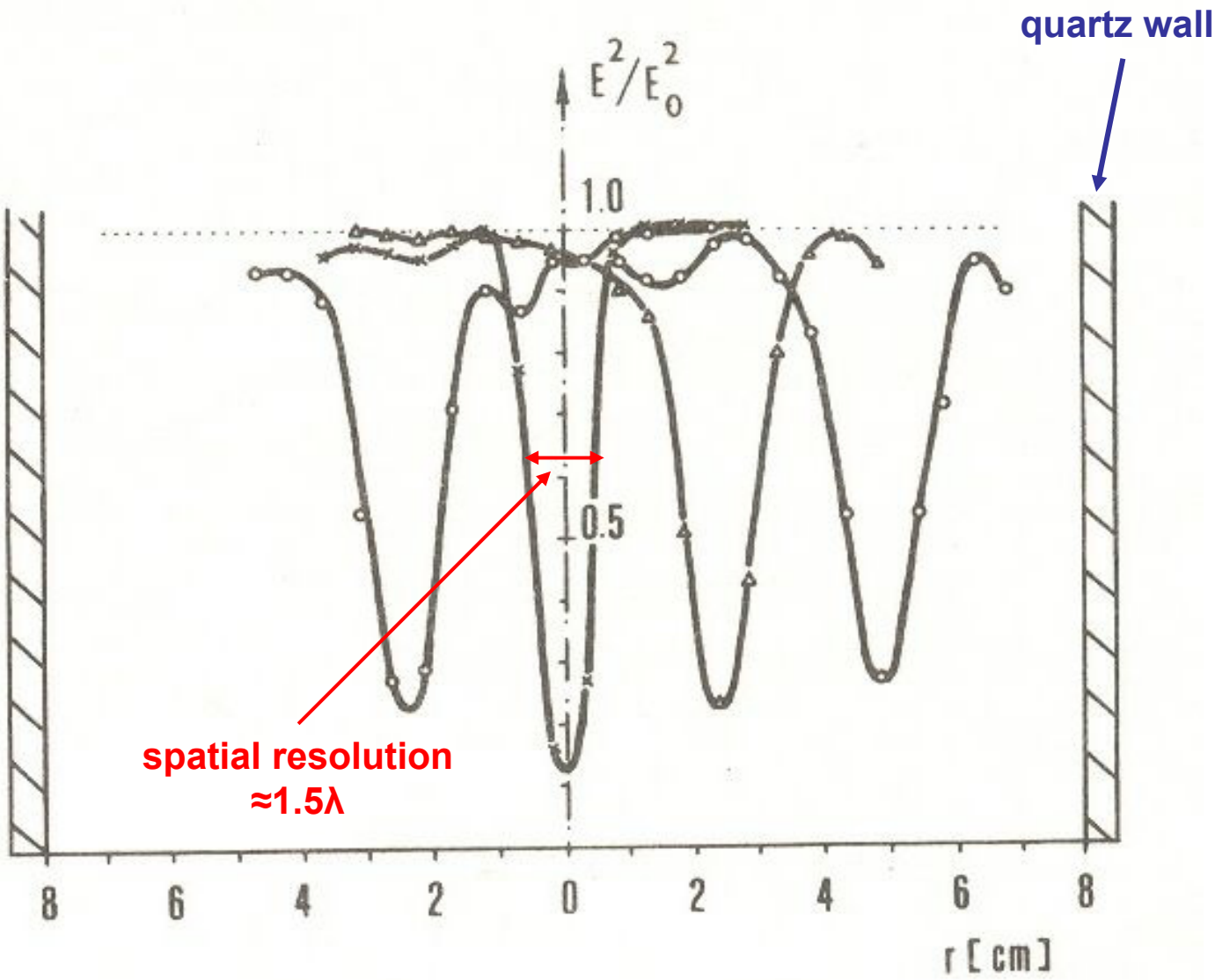

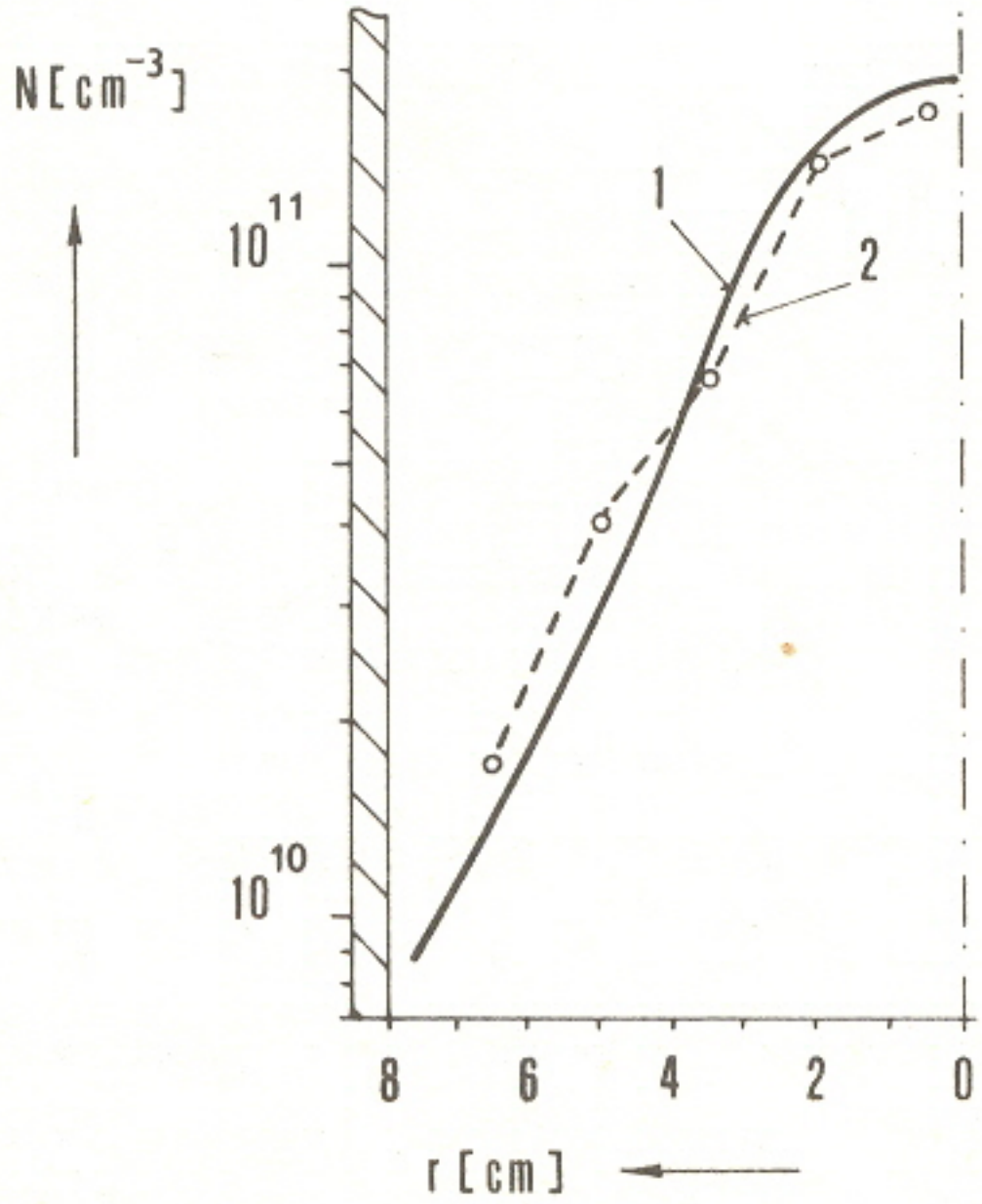

Comparison of the radial profile of the electron density in a cylindrical argon reflex discharge plasma

full line 1 – microwaves (fit from the 4 channels)
dashed line 2 – Langmuir probes

Stationary discharge with following parameters:
current 2A
mag. field 0,05T
pressure $1{,}3.10^{-3}$Pa

Line average density in TM-1-MH with a different impulse gas puffing

(evaluated still by laborious method by the zero crossing points of the interferogramme)

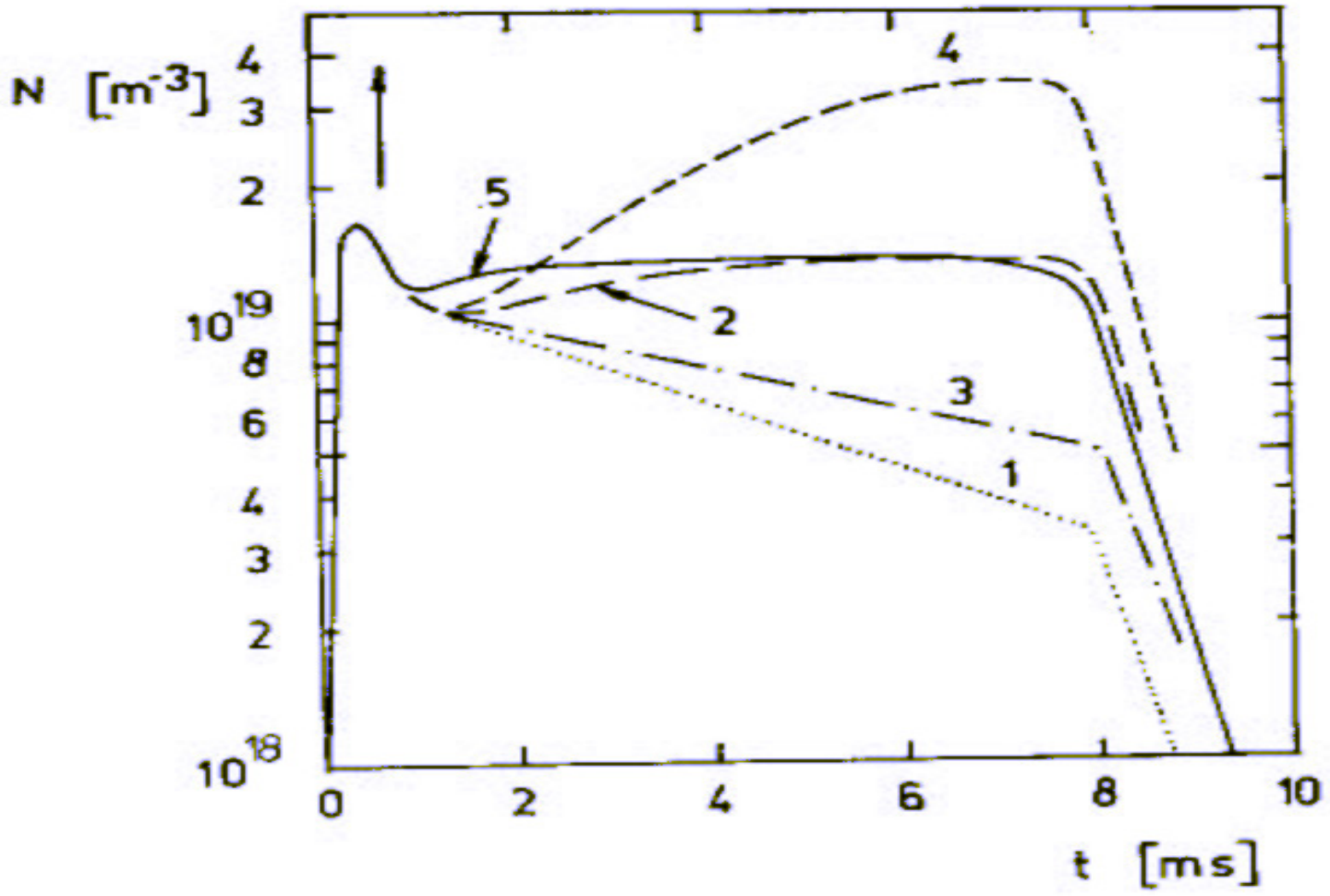

Direct reading interferometer on CASTOR tokamak

- homodyne, frequency modulated

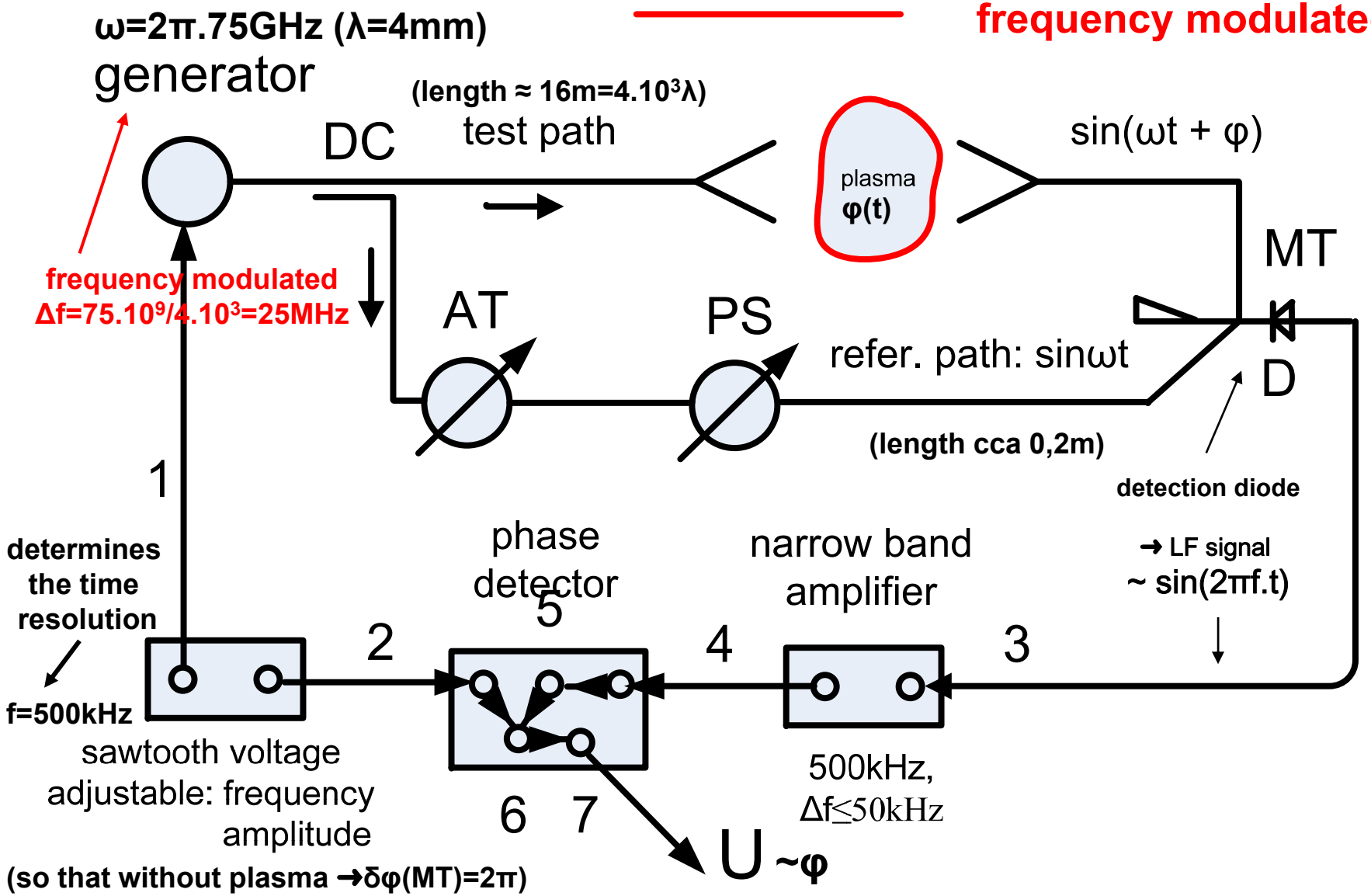

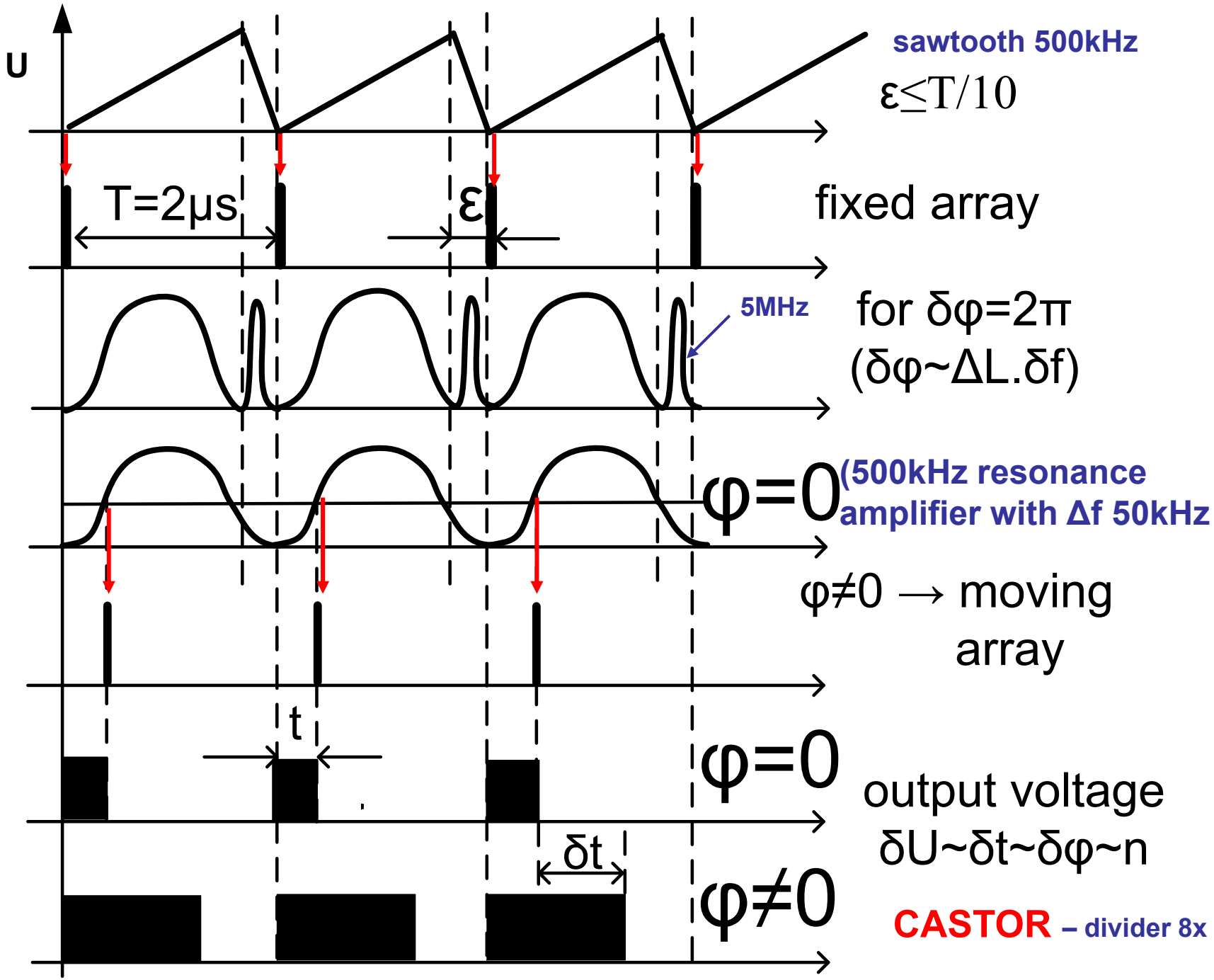
U
sawtooth 500kHz
ε≤T/10
T=2μs
ε
fixed array
5MHz
for δφ=2π
(δφ~ΔL.δf)
φ=0
(500kHz resonance
amplifier with Δf 50kHz
φ≠0 → moving
array
t
φ=0
output voltage
δU~δt~δφ~n
δt
φ≠0
CASTOR – divider 8x

Loop voltage U_{loop}, plasma current I_p, line averaged density n, incident LH power P_{inc} and non-inductively generated LH current I_{LH} in a typical CASTOR discharge with LHCD (shot #5581)

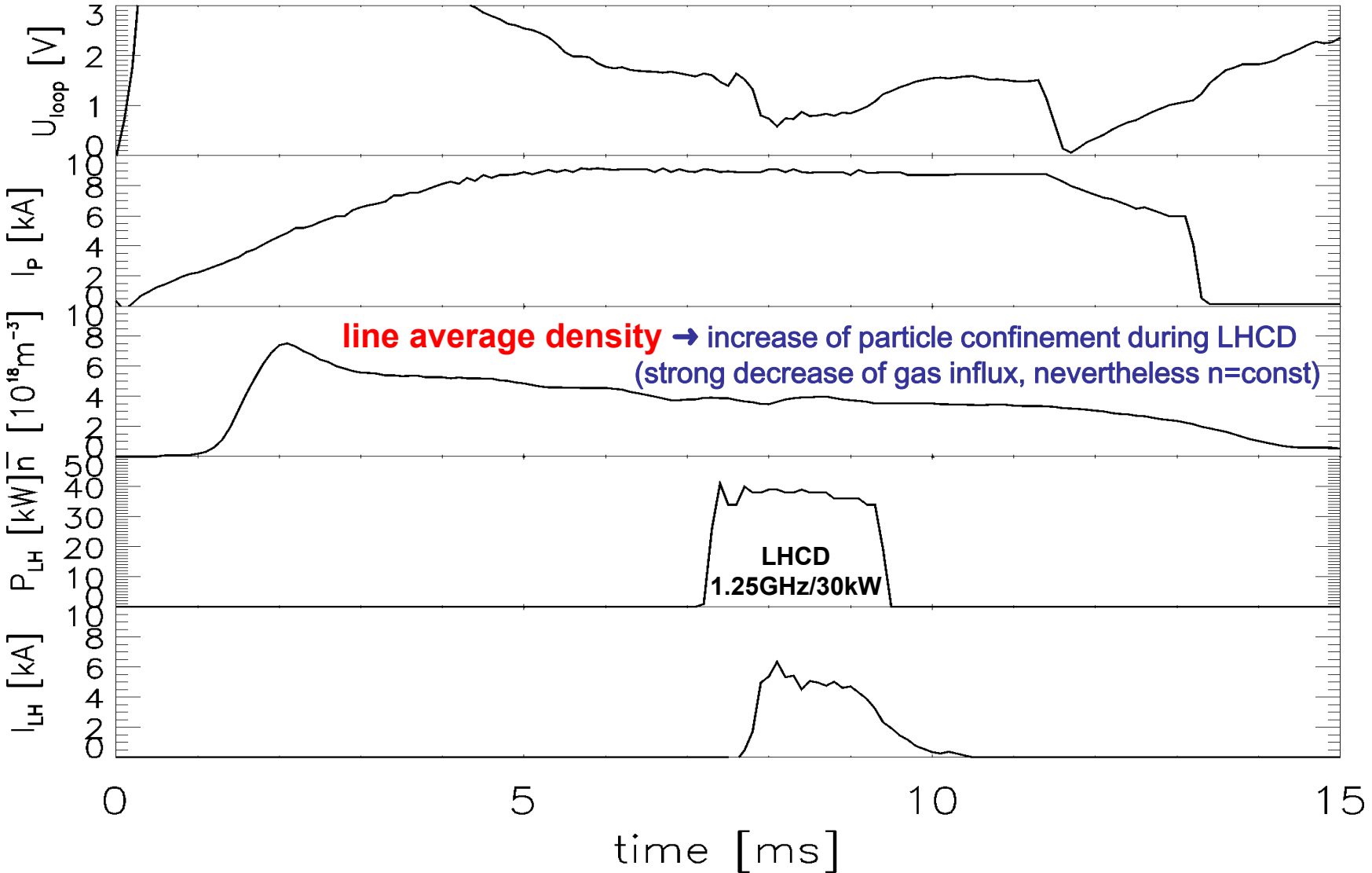

Double (unambiguous) interferometer for tokamak COMPASS-D

(heterodyne system, where the *both* waves with constant frequencies are measuring waves)

(see e.g. Annual Rep. of the EURATOM/UKAEA Fusion Programme 2000/01, p.108)

(will be used for feed-back control of the density averaged along diameter)

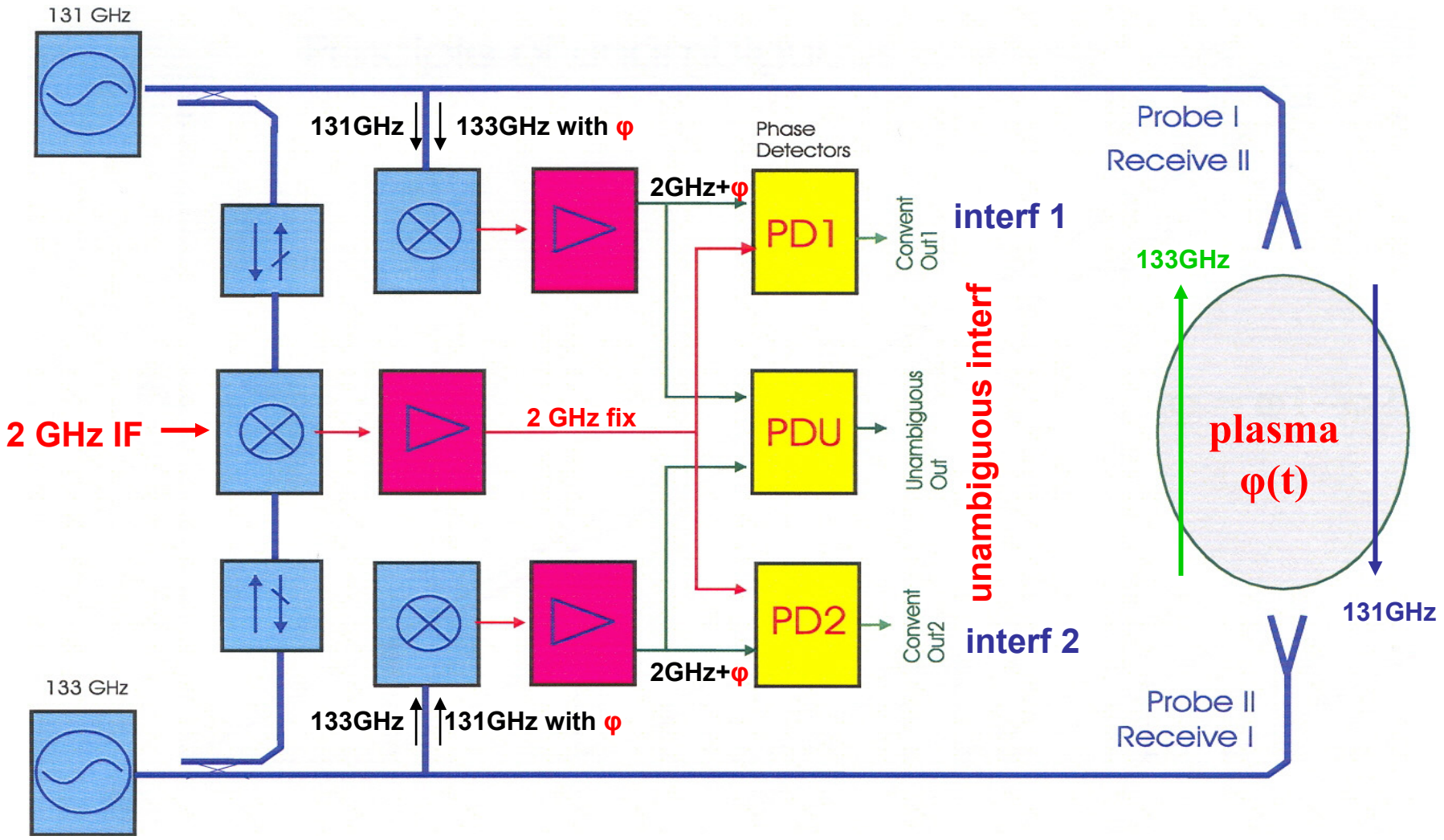

Principle of unambiguous interferometer

(with two probing waves with a little shifted, but fixed frequencies)

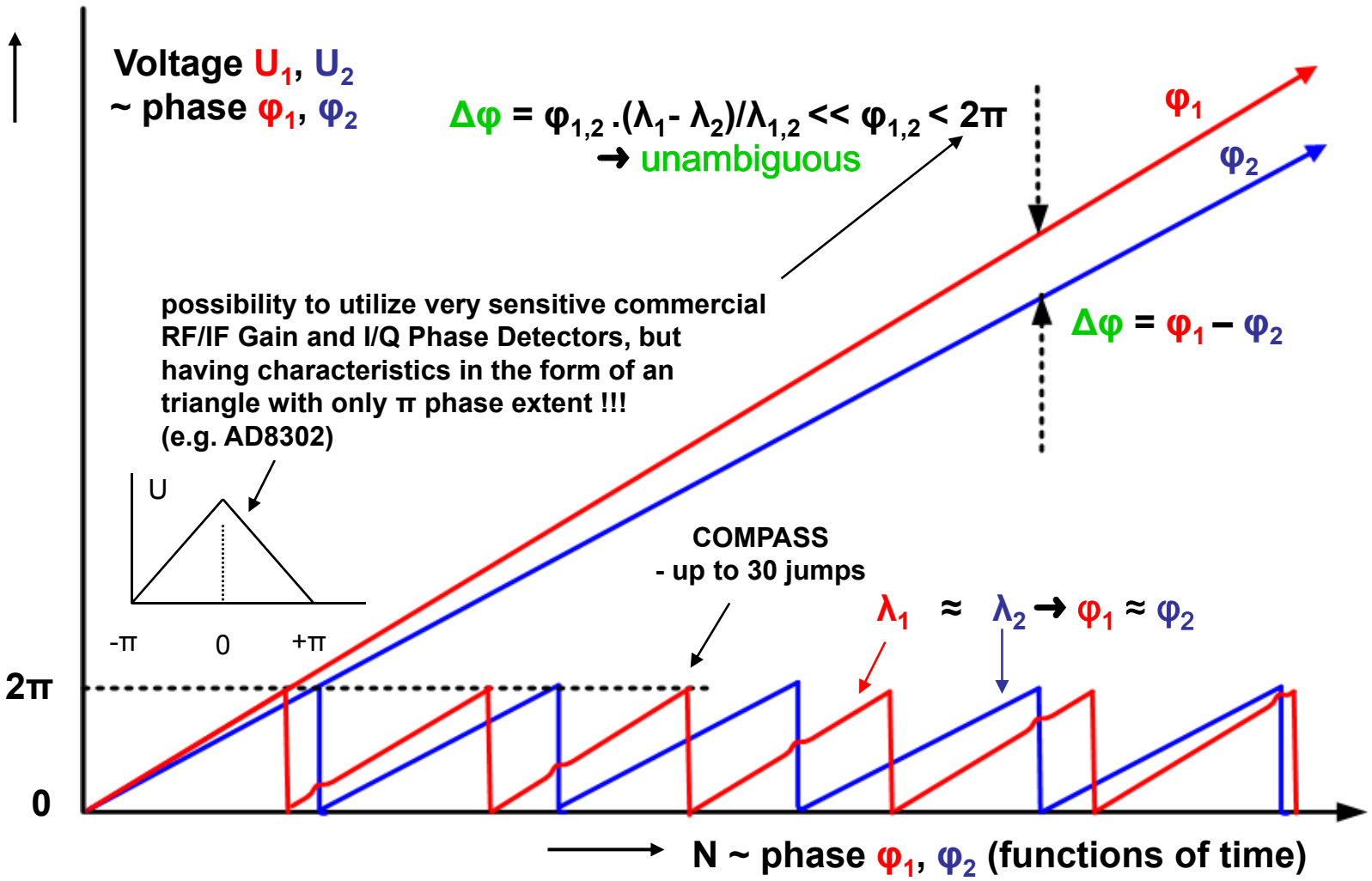

Double (unambiguous) interferometer for tokamak COMPASS-D

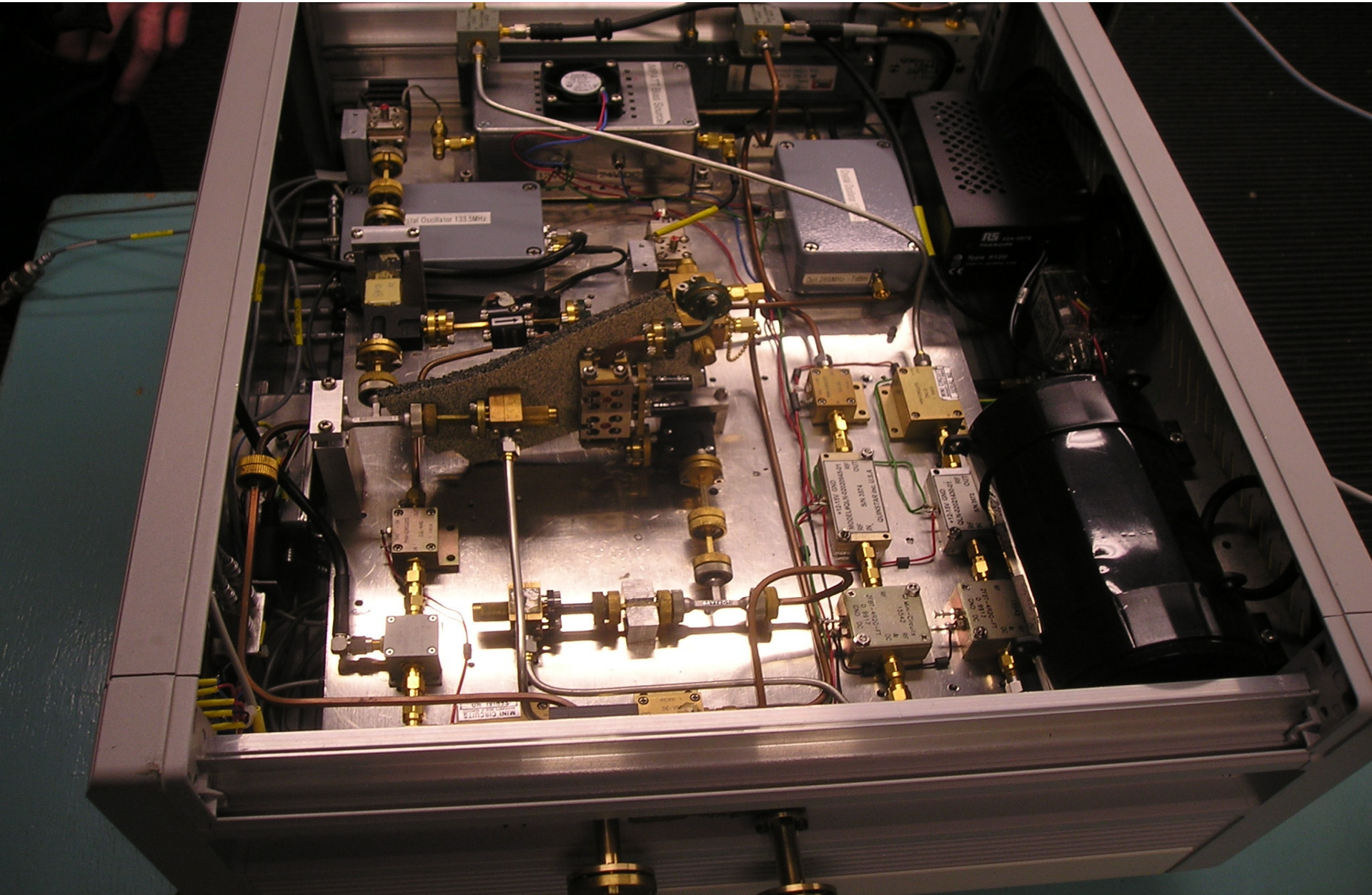

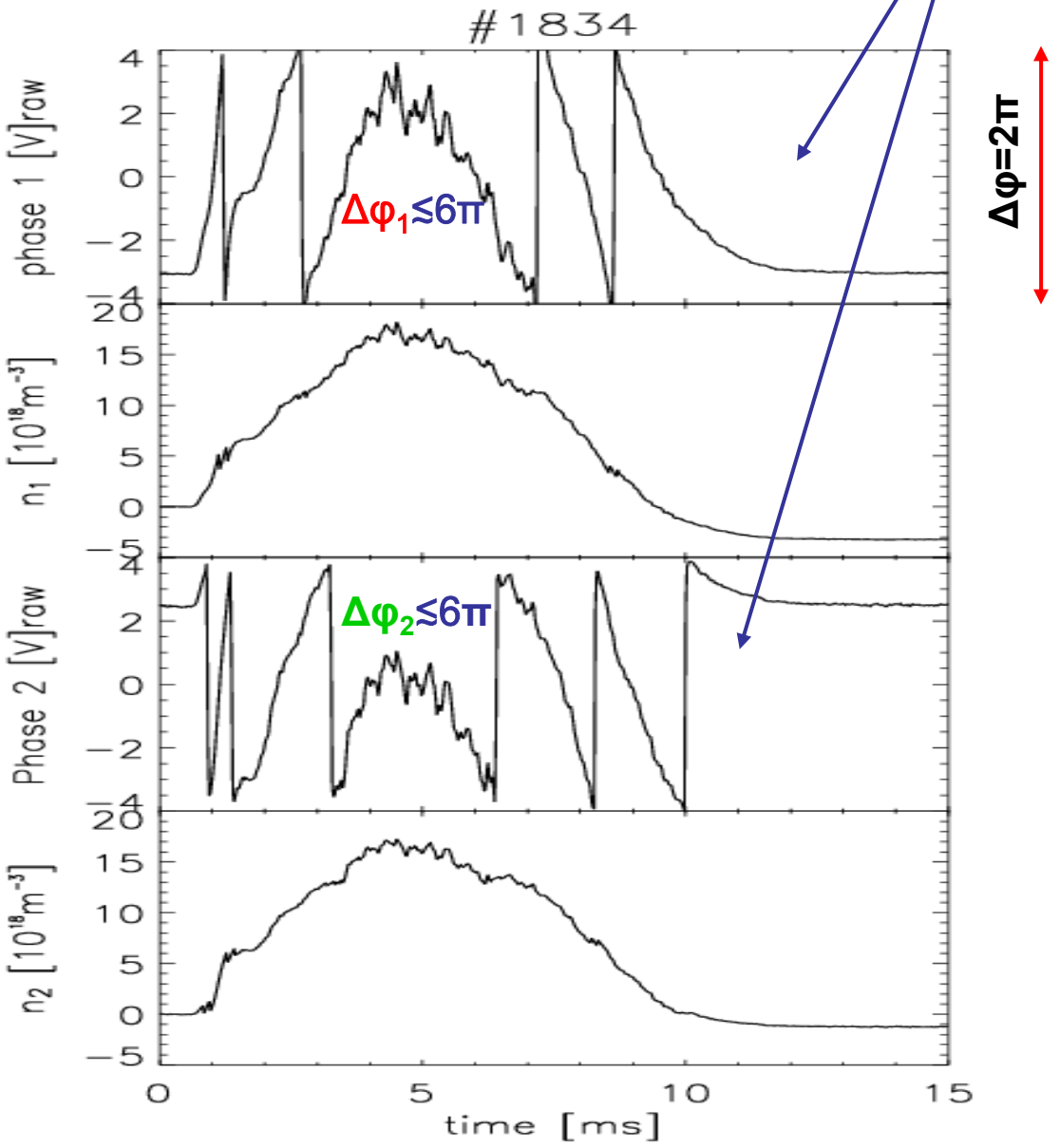

mutual phase shift $\Delta\varphi_1$-$\Delta\varphi_2$ changes 2/132=65.5times slower than $\Delta\varphi_1$ or $\Delta\varphi_2$ itself

→ unambiguous interferometer (maximum shift never exceeds 2π)

$\Delta\varphi=2\pi$

CASTOR

calibration of

double interferometer

f=131 and 133 GHz

(developed in Culham for tokamak COMPASS)

($\Delta\varphi=2\pi \Rightarrow 8V$)

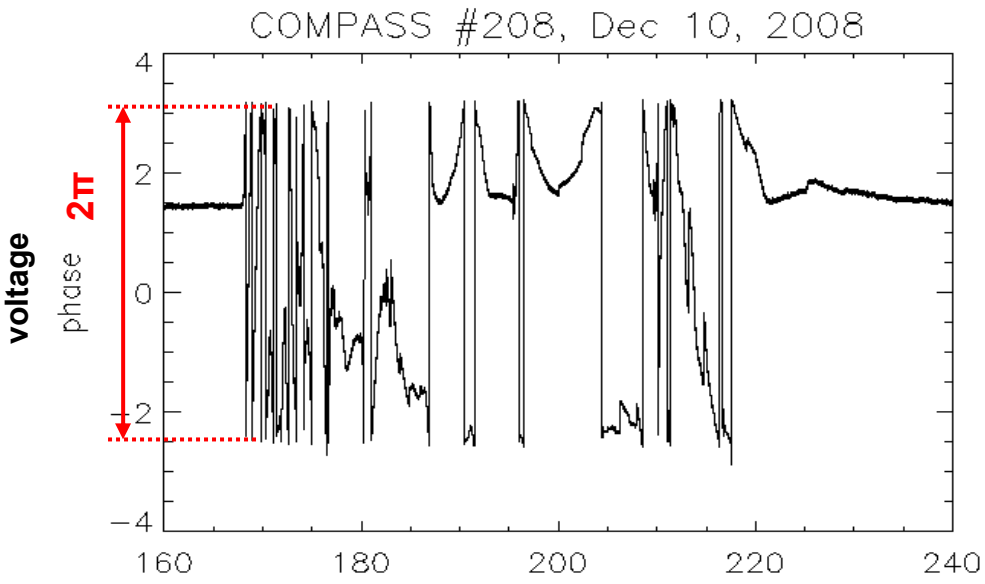

COMPASS
line averaged density

start of operation, Dec 10, 2008
(without plasma position feed-back)

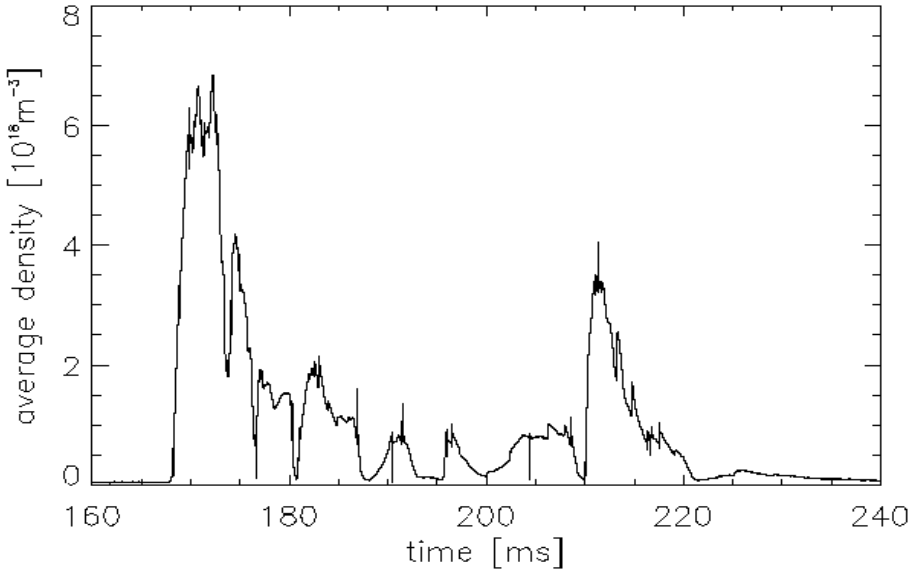

evaluated from only one interferometer by SW program under two conditions:
a) if $\varphi_{i+1} - \varphi_i < -\pi$, then $\varphi_{i+1} = \varphi_i + 2\pi$
b) if $\varphi_{i+1} - \varphi_i > +\pi$, then $\varphi_{i+1} = \varphi_i - 2\pi$

RTP tokamak - double FIR interferometer (Δf = 1 MHz)

2x50mW/432μm (HCOOH – formid acid)
optically pumped by IR CO_2 laser (150W CW)
(heterodyne system, where only one wave is measuring)

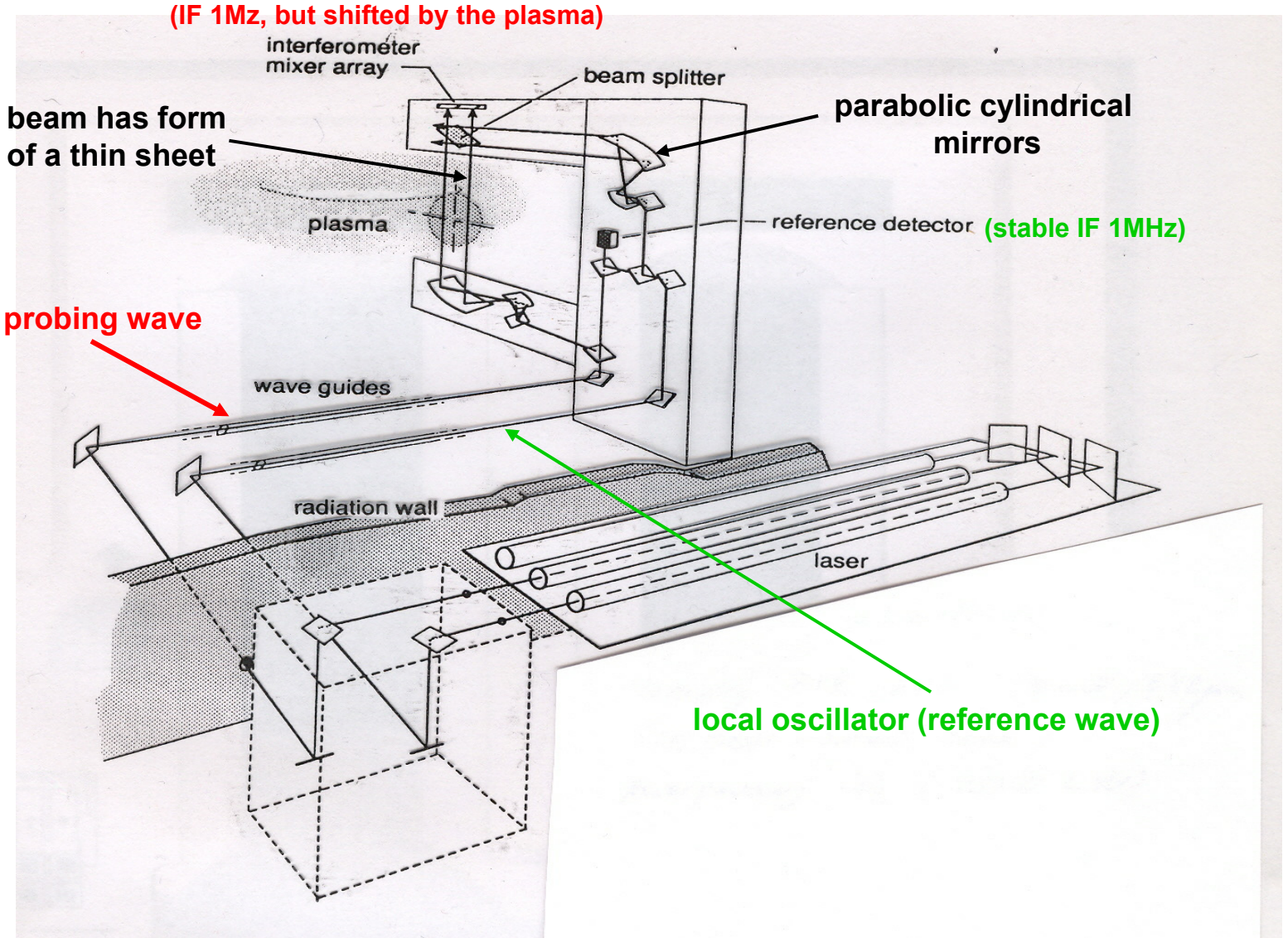

Principle of heterodyne detection

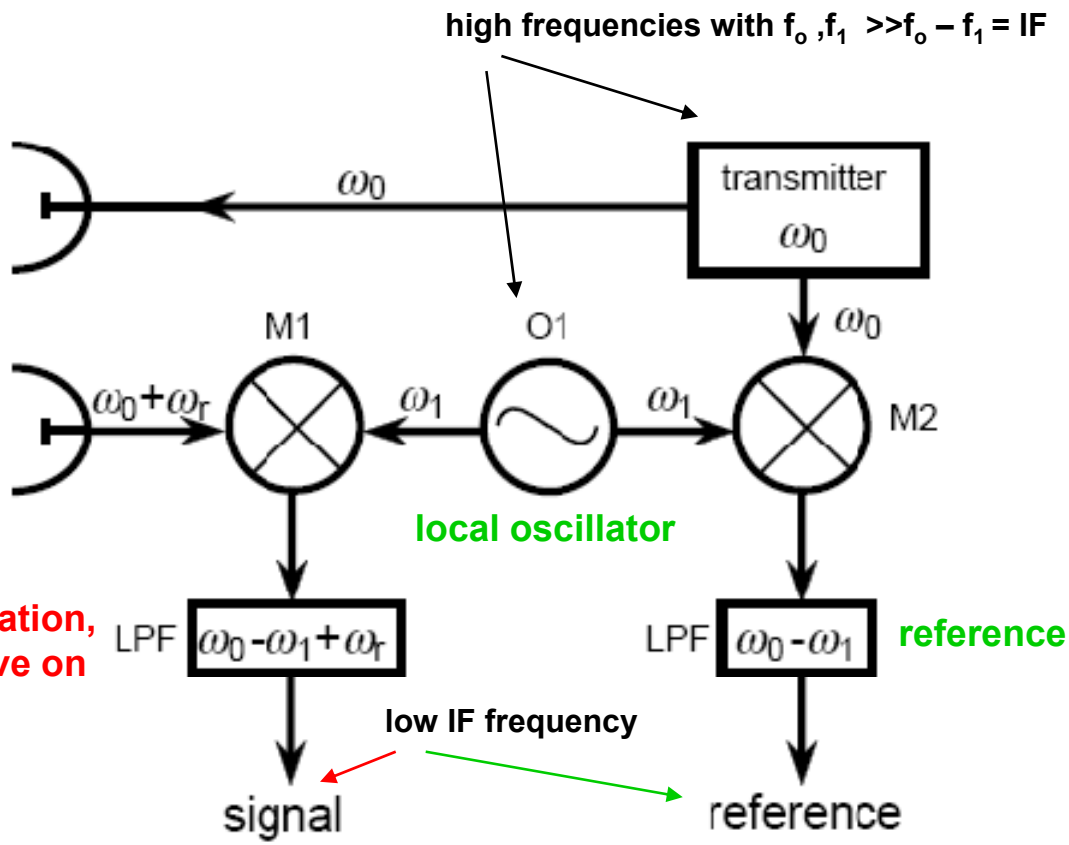

IF carrying phase information, acquired by probing wave on its frequency ω_o

Time development of the density profile for ECRH heated RTP discharge

(RF is switched on from 80 to 121ms)

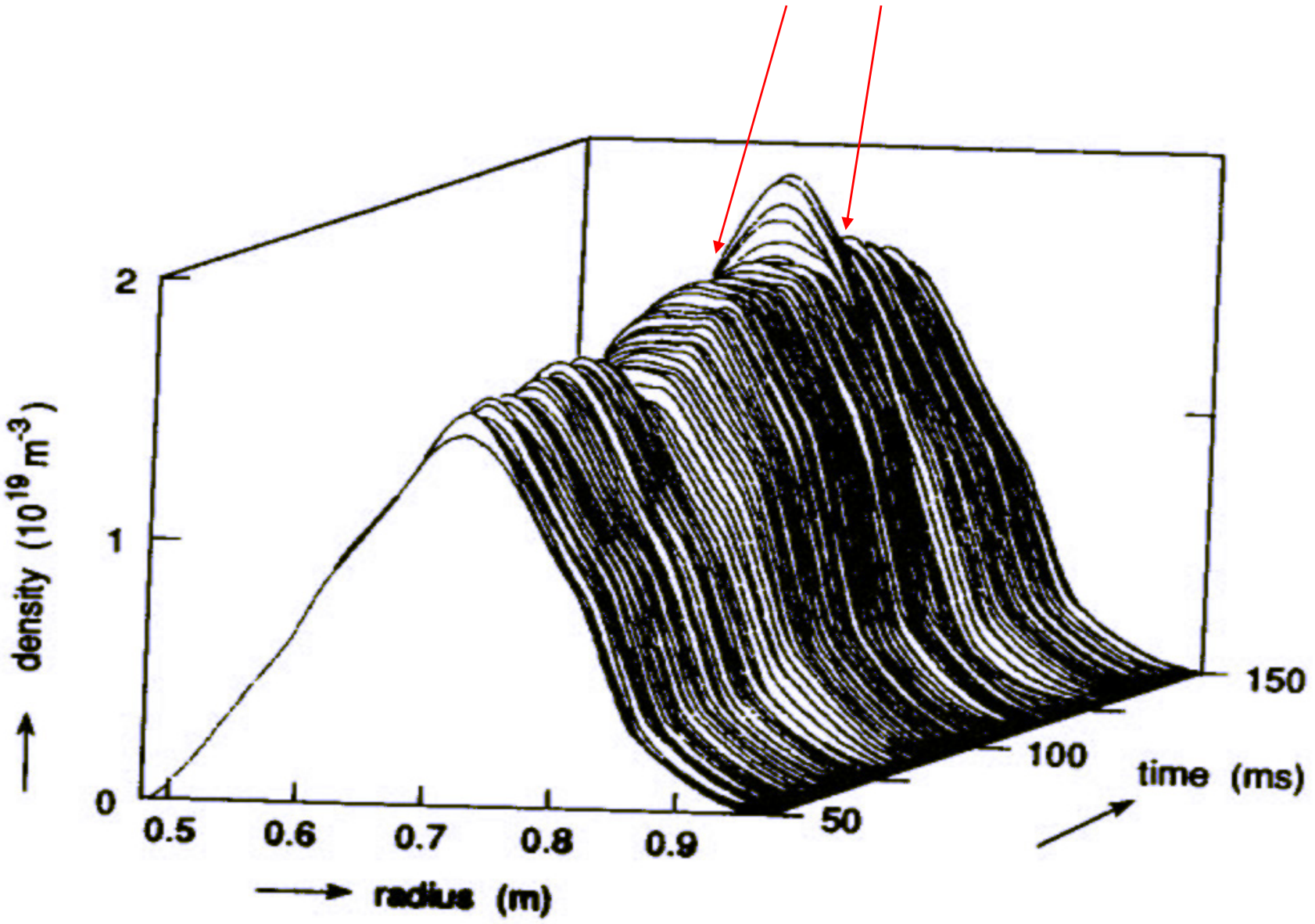

Sin – cosin reflektometer on CASTOR

(X-mode, 35GHz/200mW, resolution hundreds of kHz)

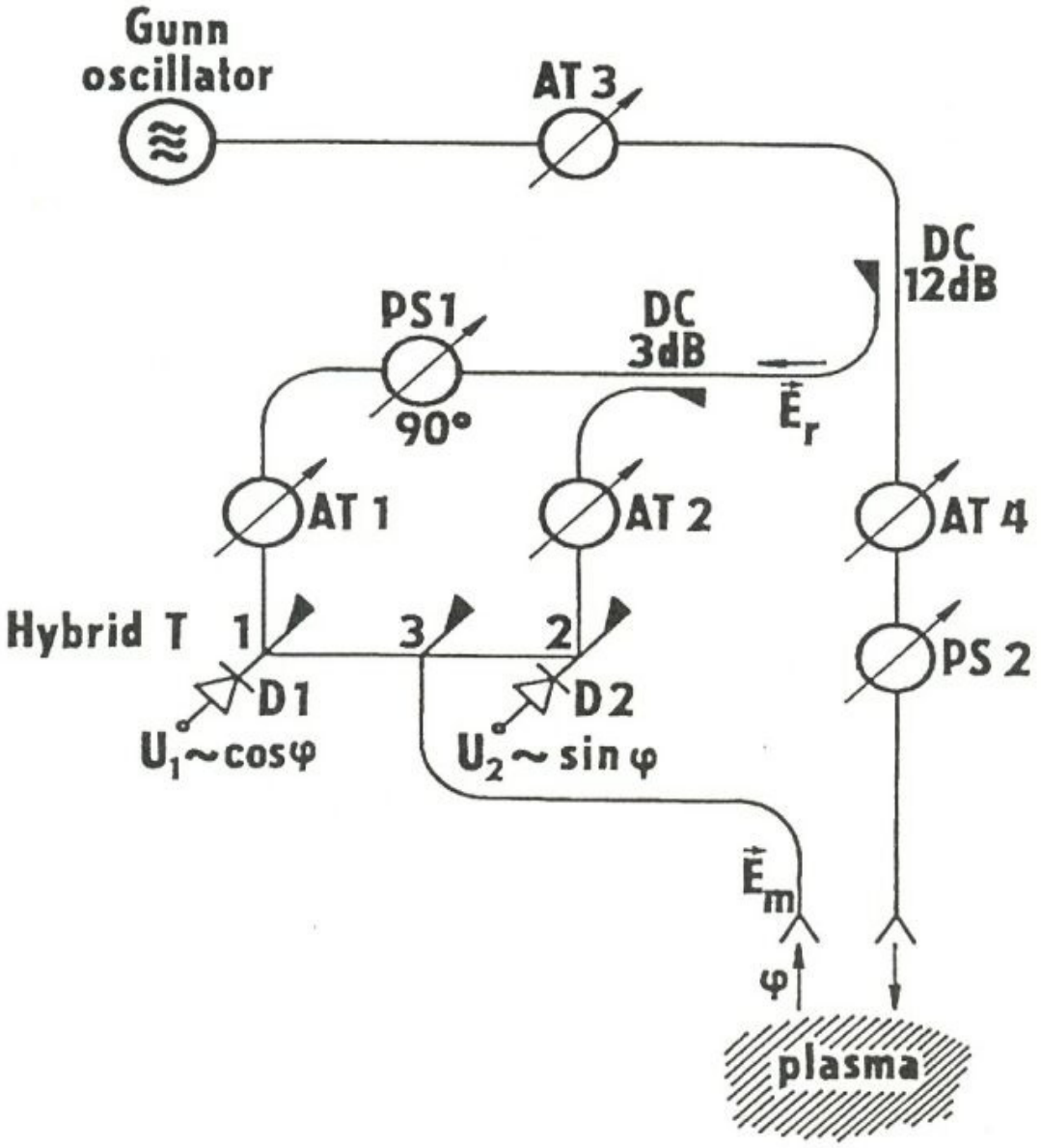

$$\mathbf{E_m}=E_m(t).\sin[\omega t+\varphi(t)]$$
$$\mathbf{E_r}=E_r.\sin\omega t$$

quadratic diodes, $\varepsilon(t)=E_m(t)/E_r$:

$$U_1(t) = E_r^2(1+\varepsilon^2(t)+2\varepsilon(t)\cos\varphi)$$
$$U_2(t) = E_r^2(1+\varepsilon^2(t)+2\varepsilon(t)\sin\varphi)$$

assumption:

1. **diodes are identical**
2. **diodes are quadratic**
3. **$E_m \ll E_r$ (i.e.. $\varepsilon^2 \lll 1$, e.g. for -20db the error $\delta\varphi=4^o$)**

then without AC component we obtain:

$$\varphi(t) = \mathrm{arctg}(U_2(t)/U_1(t))$$

I/Q phase detection scheme ($\varphi(t)=\int\Delta\omega.t'=\int\omega_r.t$)

using a commercial electronics

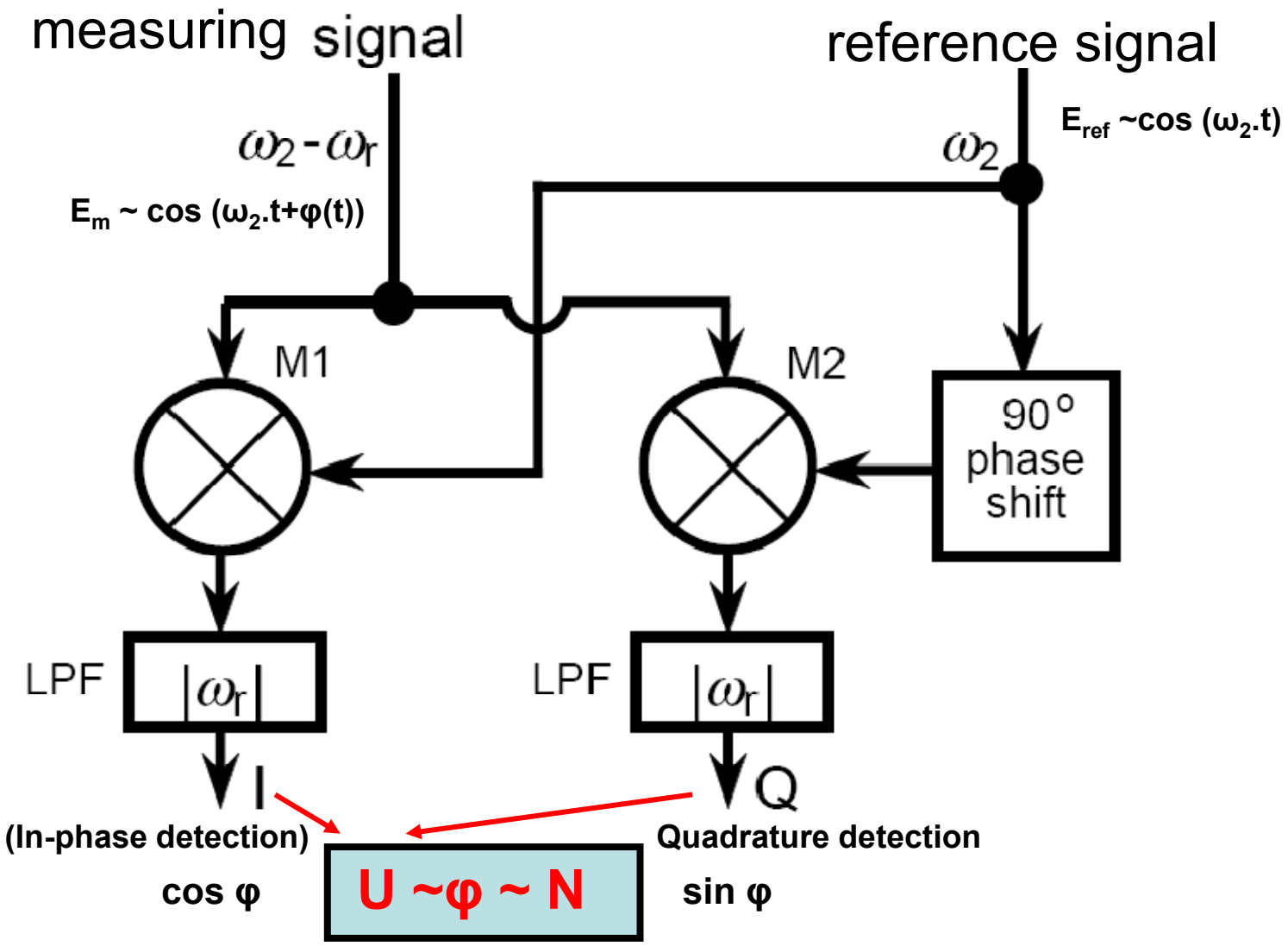

Three-frequencies reflectometer on CASTOR

(possibility of poloidal as well as toroidal correlation measurements)

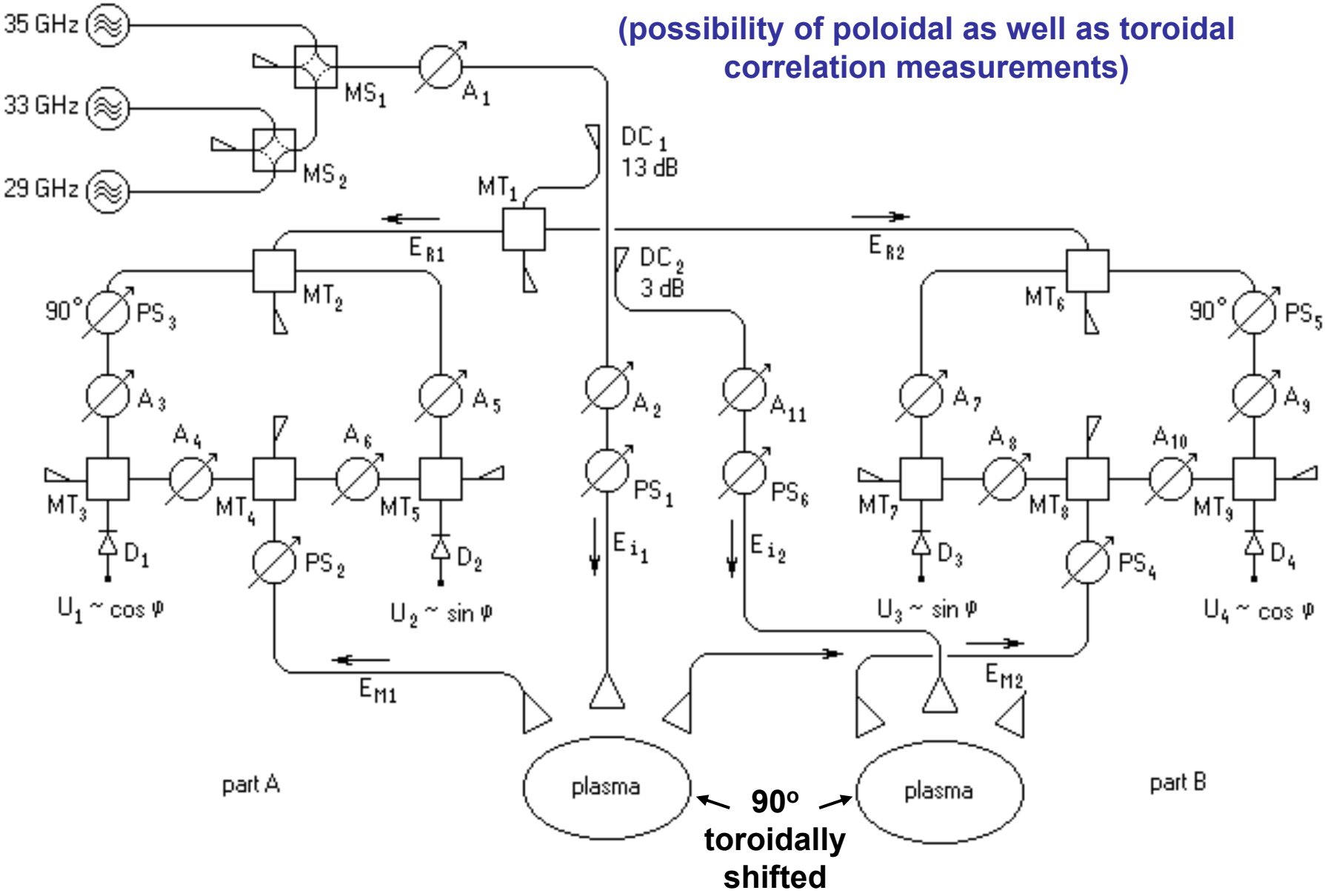

Antenna system of reflectometer used on tokamak CASTOR

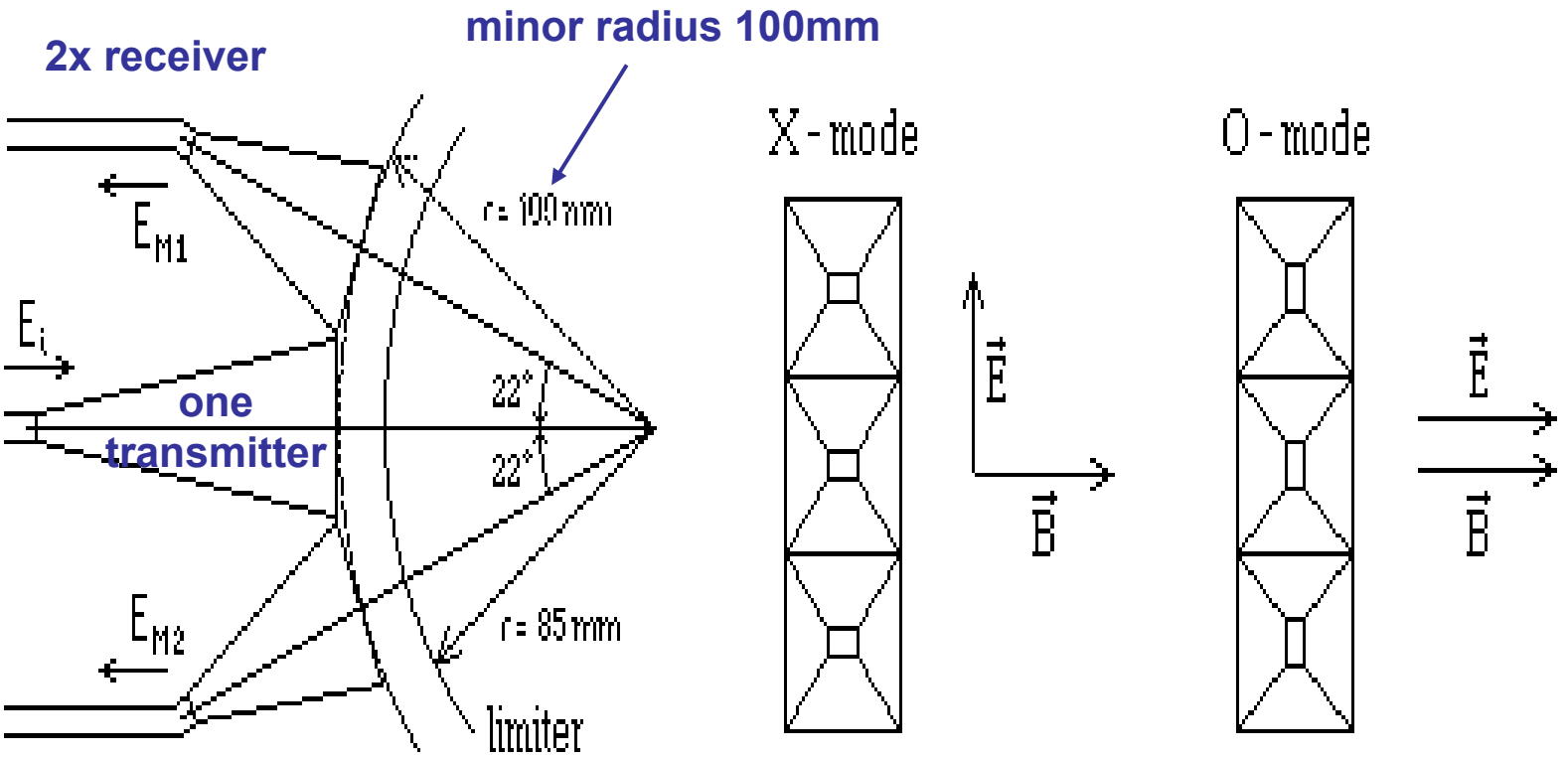

CASTOR – 8mm microwave diagnostic antennas:

1 … rectangular hog-horn for HFS measurements
2 … circular for 4mm interferometer
3 … system of three rectangular antennas of reflectometer working in v O-mode

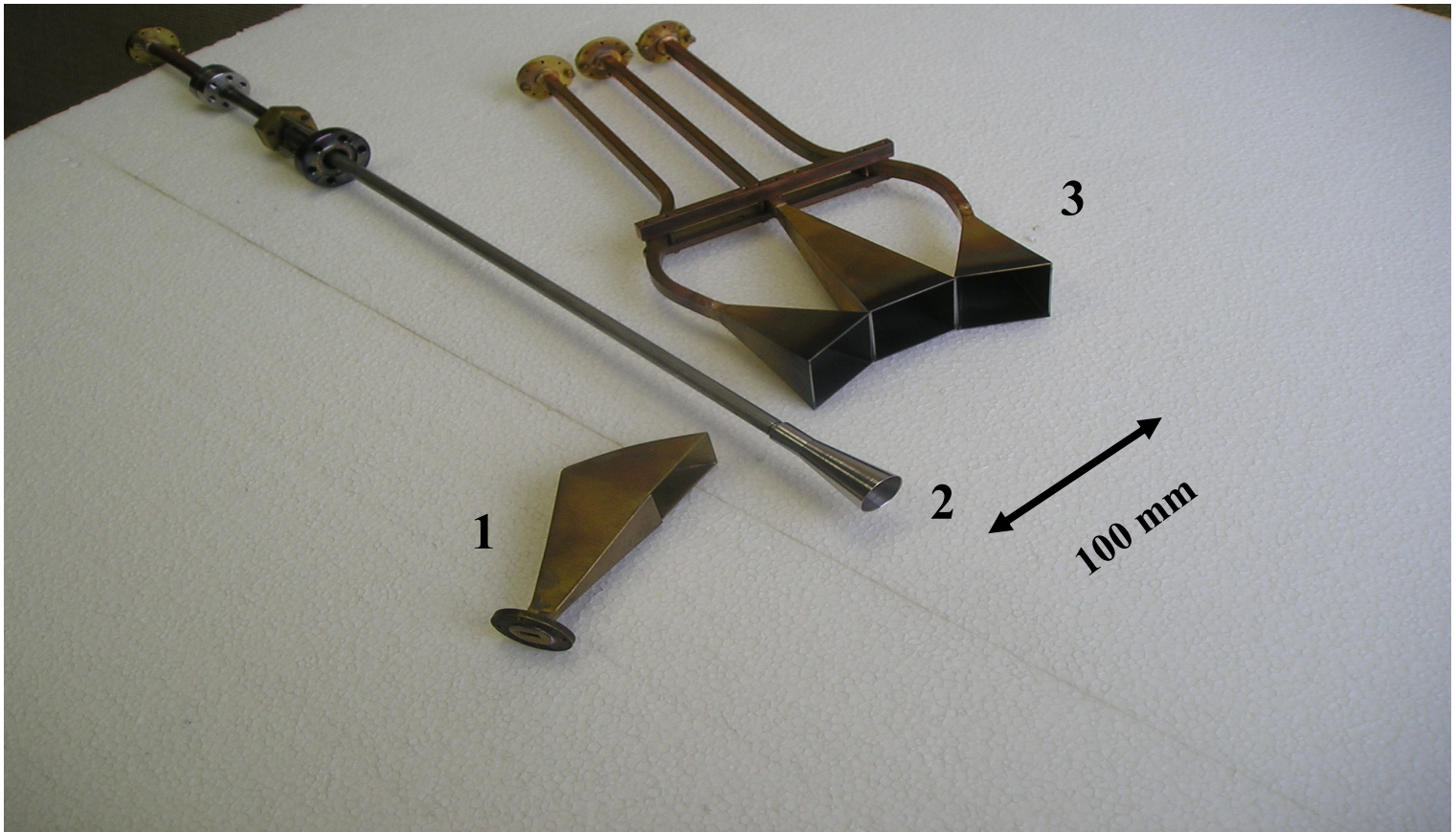

Three-frequencies reflectometr on CASTOR

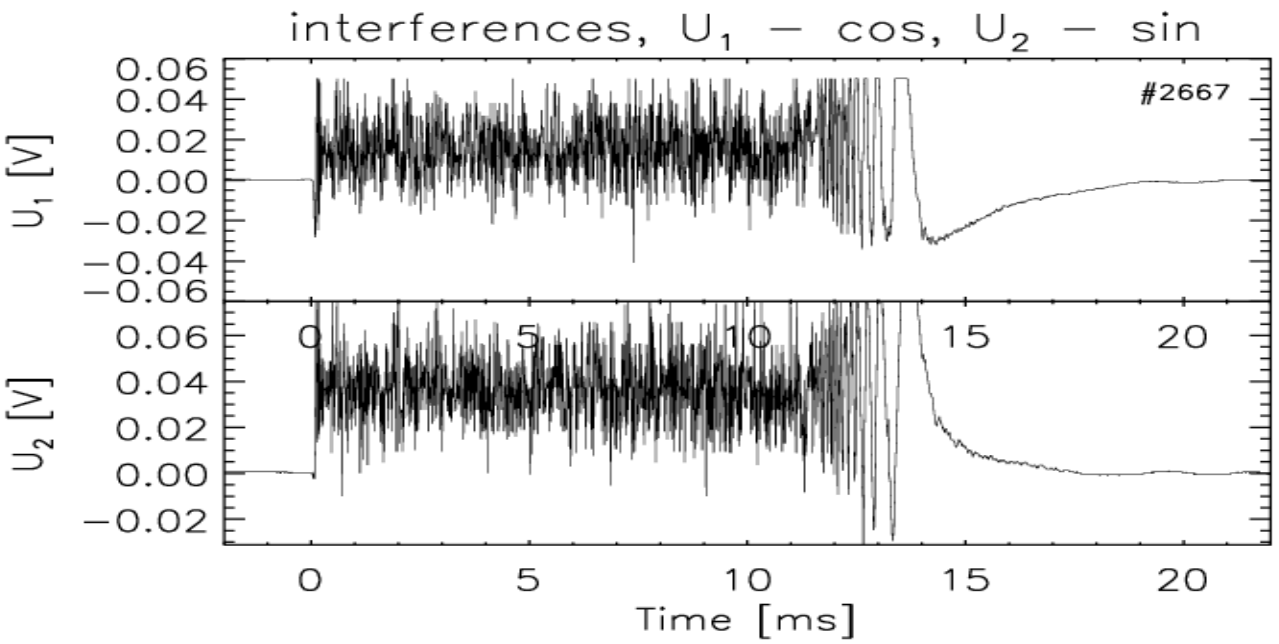

Record of the CASTOR 33GHz reflectometer signal

(AC input)

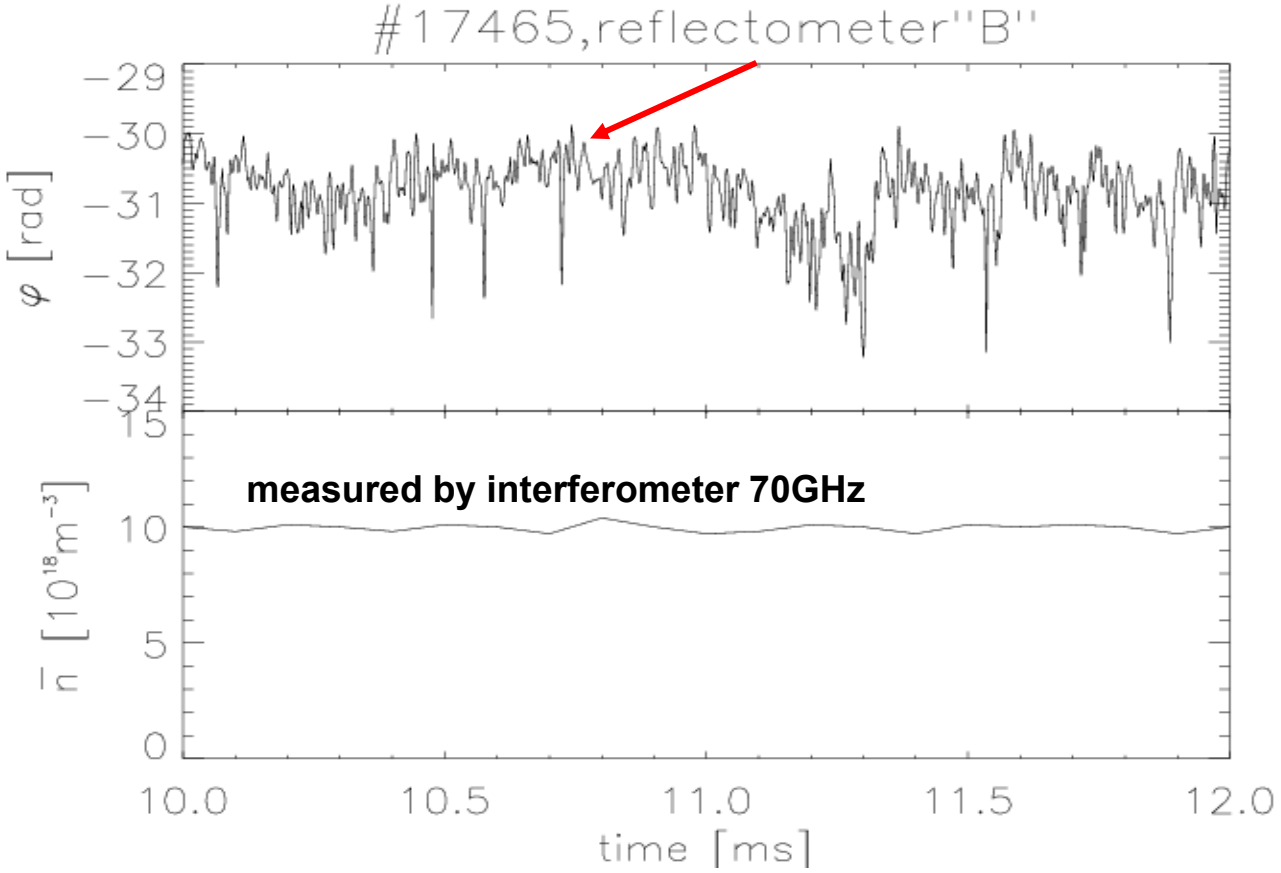

Phase fluctuations of the reflected wave during the stationary phase of tokamak CASTOR discharge

(δn/n from measured φ, depending on the gradient n supposed in the place of reflection, has been estimated to be about 2-5%)

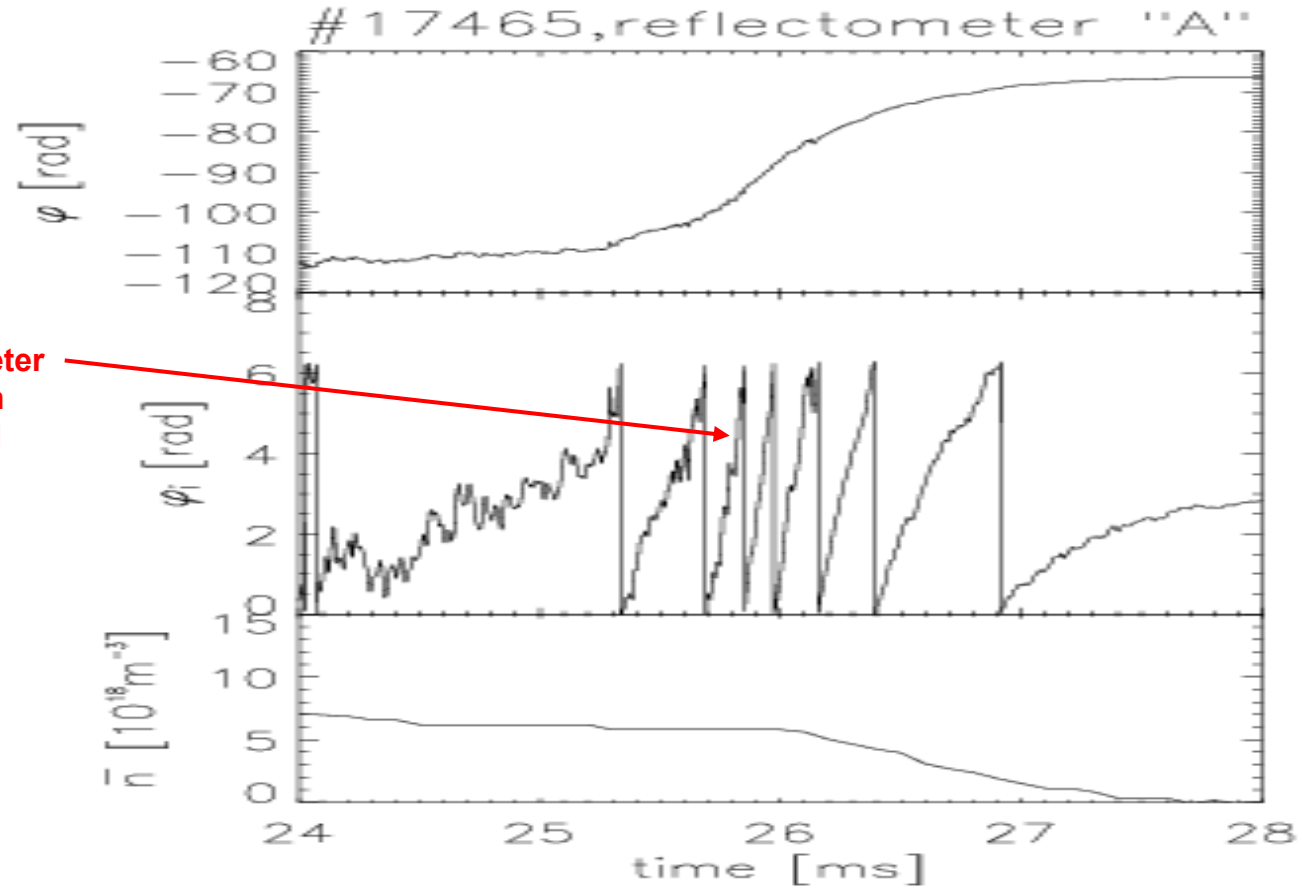

double-pass interferometer on 8mm (reflection on the tokamak HFS wall

Reflectometry phase measurement in the end discharge phase

CASTOR – „Phase runaway“ phenomenon, result of Doppler shift of reflected signal by plasma turbulence

(Zacek F., …: 18th SPPT, 1997, 42)

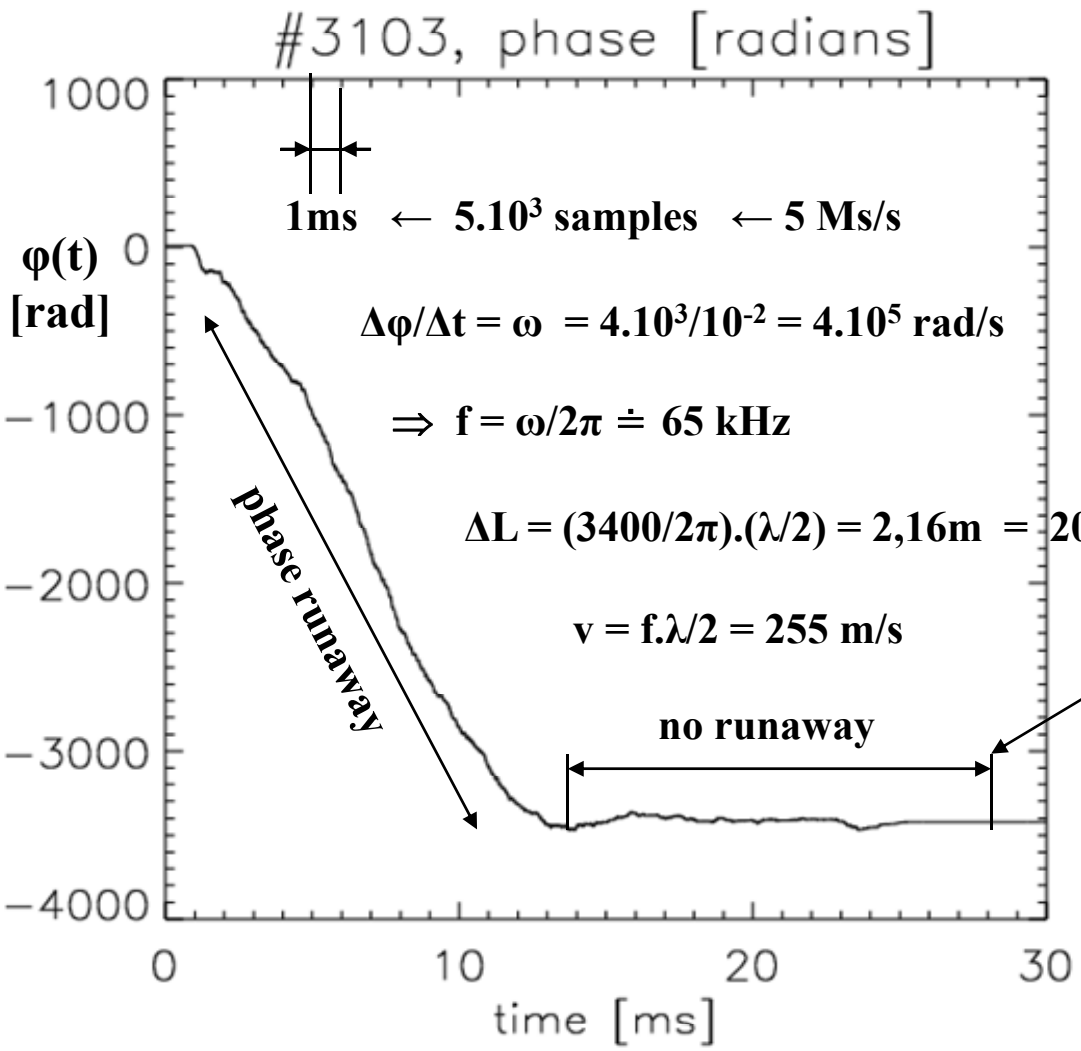

$\varphi(t) = (\omega_{30GHz}+\omega).t$

Doppler shift

(rectified by diode)

transmitting and receiving antennas under certain angle

Principle of fluctuating plasma density profile measurement using a method of fast swept reflectometry

Principle of **classical reflectometry** – measurement of the phase φ of the reflected wave (by interfering with the reference wave with φ_o):

1. if generator frequency $f = const$ (homodyne or heterodyne reflectometry) and reflection occurs on a fixed metal plane, then $\varphi - \varphi_o = const$ and also interference signal $U = U(E_{ref}, E_m, \varphi) = const$, but periodically depending on φ, i.e. on the reflection plane distance L
2. if frequency f is swept (f has a saw tooth form in a certain frequency range), i.e. $f = k.t$ and reflection occurs on the fixed mirror in a distance L, then $\varphi = const.t$ and interference signal U will show beats ~ $\sin(\omega_b.t)$ with constant frequency $\omega_b = 4.\pi.(L/c).df/dt$

Important: Beat frequency is function of two parameters:

- distance L of the reflection point
- and speed of the sweeping df/dt *only* (it is not function of the frequency f itself !!!).

Note: For L determination (commercial FMCW radars), $df/dt = const$ is needed (high linearity f with time must be assured)

3. In plasma is the situation concerning fast swept reflectometry much more complex - from two reasons:

a) the point of the reflection in the plasma, i.e. also ω_b, depends on the actual wave frequency → L is increasing with increasing frequency and just this effect (increase of ω_b by $\Delta\omega_b$) can be used for the profile measurement (through localization of the reflection point in the corresponding density)

b) but, due to the density δn fluctuations, the point of the reflection L (even at f = *const* and density $\langle n \rangle$ = *const*) is not localized all the time on the same radius, but it is fluctuating together with density fluctuations in the place of the wave reflection – this disturbing effect results also in broadening of ω_b (let us denote it by $\delta\omega_b$)

4. The problem is, how to eliminate that undesirable effect δn of density fluctuations on ω_b and so how to determine that searched $\Delta\omega_b$;

it is enabled by statistical correlation methods of the receiving signal (sampling rate tens of MHz is needed, nevertheless „sliding FFT“ needed for the signal frequency analysis has windows longer than they are typical plasma fluctuations and a „proper“ $\Delta\omega_b$ must be therefore found from “time history” of the measurement

Effect of fluctuations on reflected electric field

(taken from a lecture of M. Manso, Association EURATOM/IST, Lisboa, Portugal)

no turbulence

with turbulence

fluctuating side lobes (wave front)

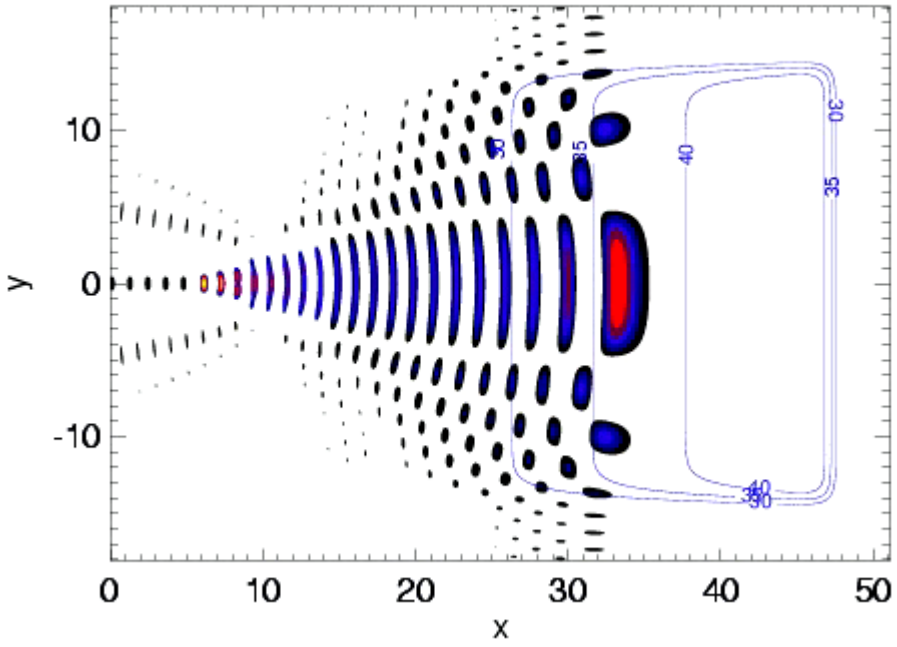

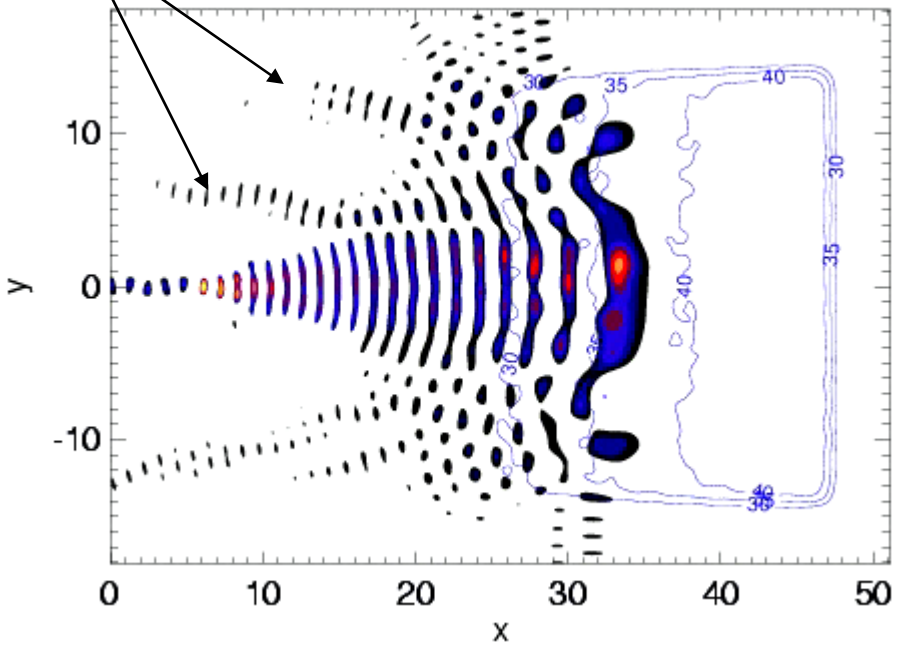

➜ the plasma density perturbations strongly distort the spatial electric field pattern causing scattering of probing wave energy.

Comparison of impulse radar and fast swept reflectometry

- **classical impulse radar - time of the short pulse return, after its reflection on the objection, is measured (pulse propagate with group velocity, which equals phase velocity only in non-dispersive medium)**
- **by application for detection of small distances has the classical radar (= pulse reflectometry) problems with the time (and therefore also with the space) resolution, due to the non zero pulse length**

- **reflectometry with the fast frequency sweeping is nothing else than CW radar (commercial products are also called FMCW radar), because generator transmits wave continuously and the phase of the wave reflected on the objection is continuously detected (the phase propagates with phase velocity)**
- **if the wave enter plasma at $x=x_o$ and the critical density is located at $x=x_c(\omega)$, then the phase φ of the reflected wave after its return can be written as follows:**

$$\varphi(\omega) = 2(\omega/c).\int_{x_o}^{x_c(\omega)} n(\omega,x).dx \; + \varphi_o(\omega)$$

- it may be easily shown that in inhomogeneous plasma the frequency derivative of the phase $d\varphi(\omega)/d\omega$ of the reflected wave (frequency, not the time derivative) equals the total group delay of the wave τ_g propagating from the plasma edge x_o to the point of the critical density $x_{crit}(\omega)$ and back, i.e.:

$$d\varphi(\omega)/d\omega = \tau_g = \int_0^{\tau_g} dt = 2.\int_{x_o}^{x_{crit}(\omega)} dx/v_{gx} \quad ,$$

  and therefore, $d\varphi/d\omega$ determines the actual distance of the reflected point (i.e. in tokamaks radial position of the frequency corresponding density).
- so, the group velocity, not phase velocity, is directly measured
- much more complicated interferometric measurement of the phase wave φ, which can be moreover "interrupted", must not be performed because a direct output of the measurement – an analysis of the beat frequency behavior– can be used.
- a small departure $\Delta\omega_b$ with frequency increasing in time, caused by dependence of the reflection point in the plasma on the frequency (in the case of reflection on a fixed mirror would be $\omega_b = const$), must be distinguished from $\delta\omega_b$ caused by density fluctuations).

Radial profiles of frequencies in tomamak AUG

fp … O wave cutoff **fu, fl … X wave cutoffs**
fh … upper hybrid resonance **fc … electron cyclotron frequency**
magnetic field on the device axis 2,4T
density on the device axis 7,6.$10^{19}$$m^{-3}$ (profile determined by TS)

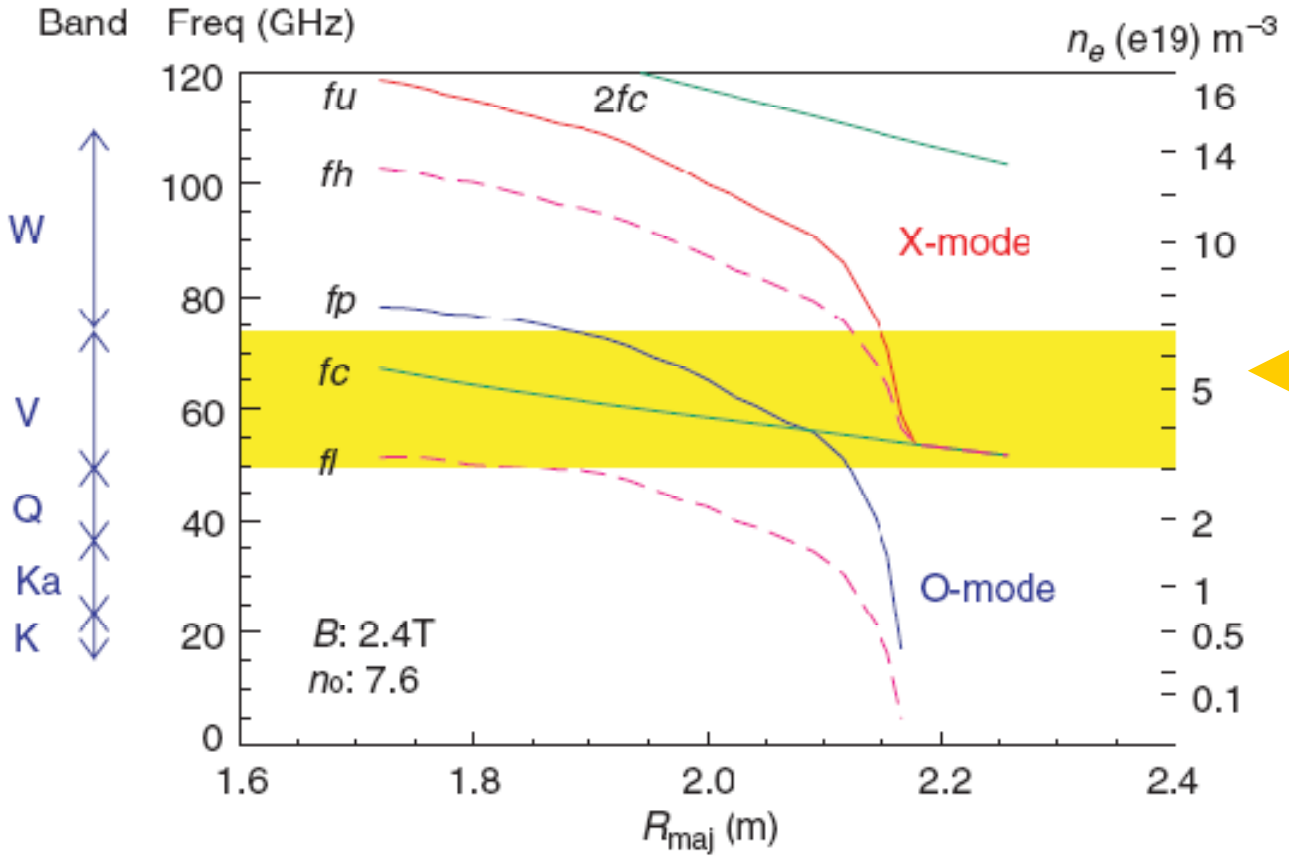

yellow band is frequency band V

ASDEX Upgrade – broadband FM-CW reflectometry - observation of ELMs

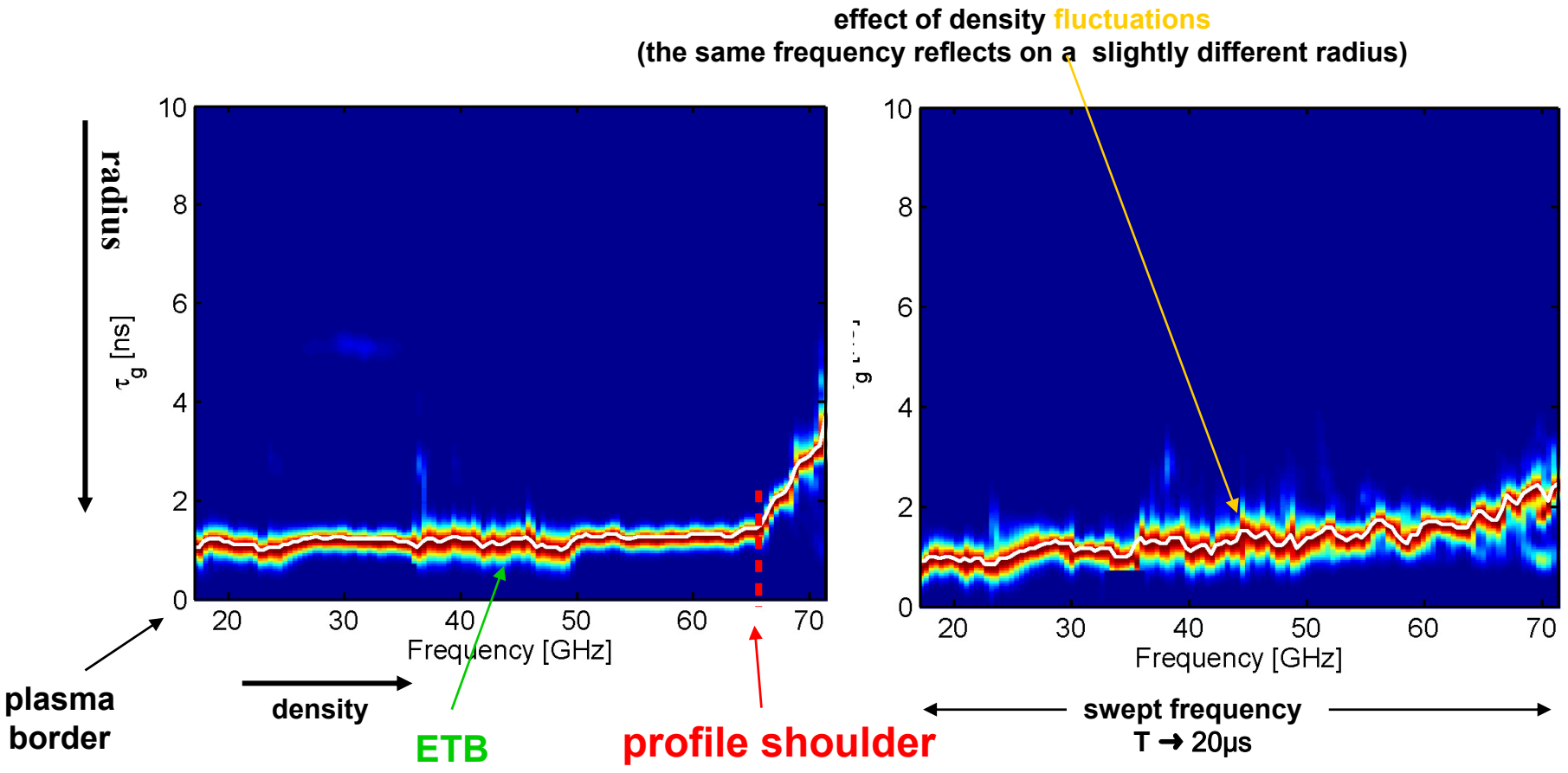

- **Between ELMs**
- **During ELMs**

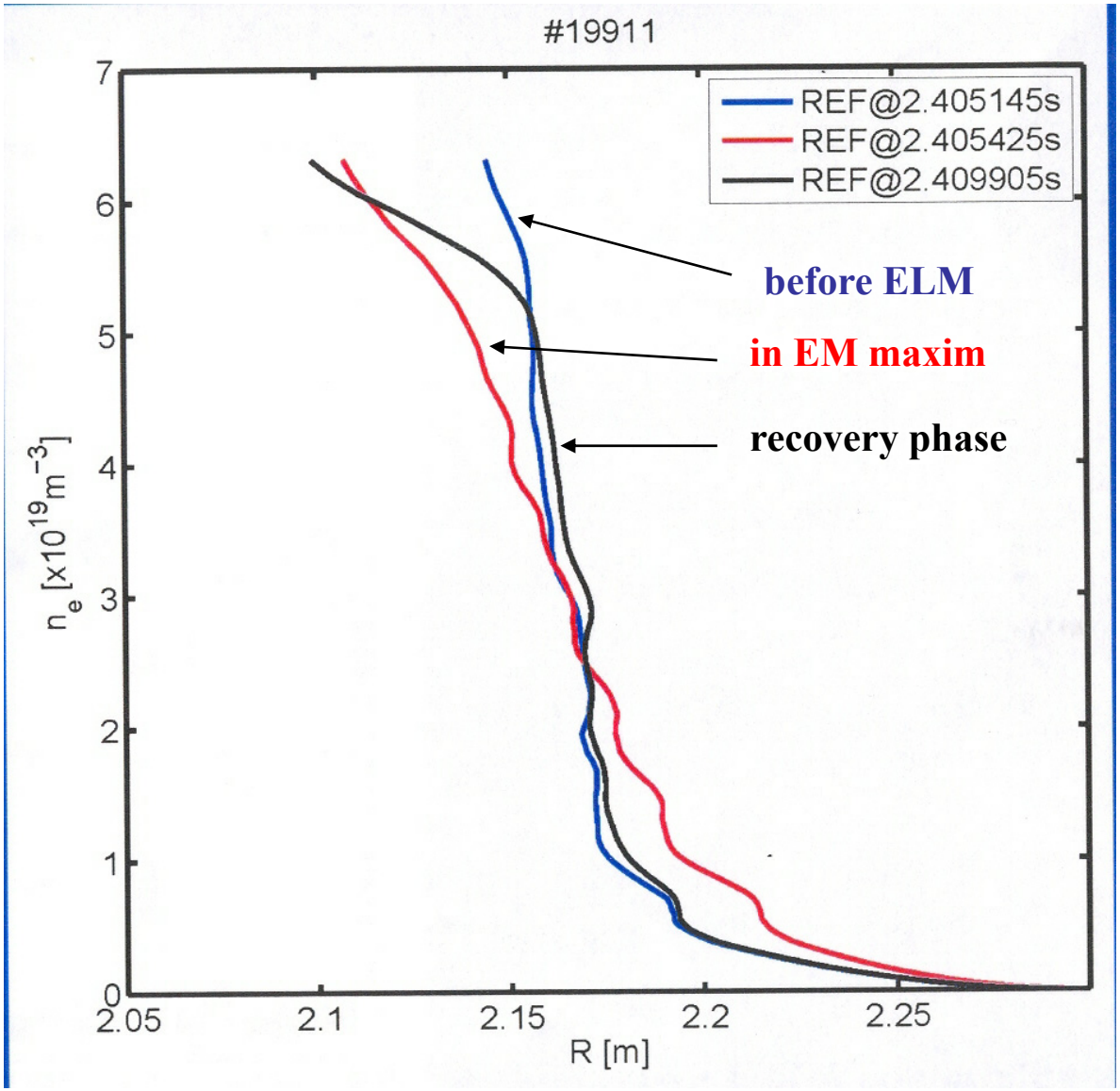

ASDEX-UG reflectometric measurement of density profile

in different ELM phase

ASDEX-UG, reflectometry measurement of HFS and LFS density profiles before (red) and after ELM (blue)

ELM start is put in t=0
after ELM start a collapse of density profile occurs:
- **region of pedestal steps back inside the chamber**
- **SOL broadens towards HFS as well as LFS**

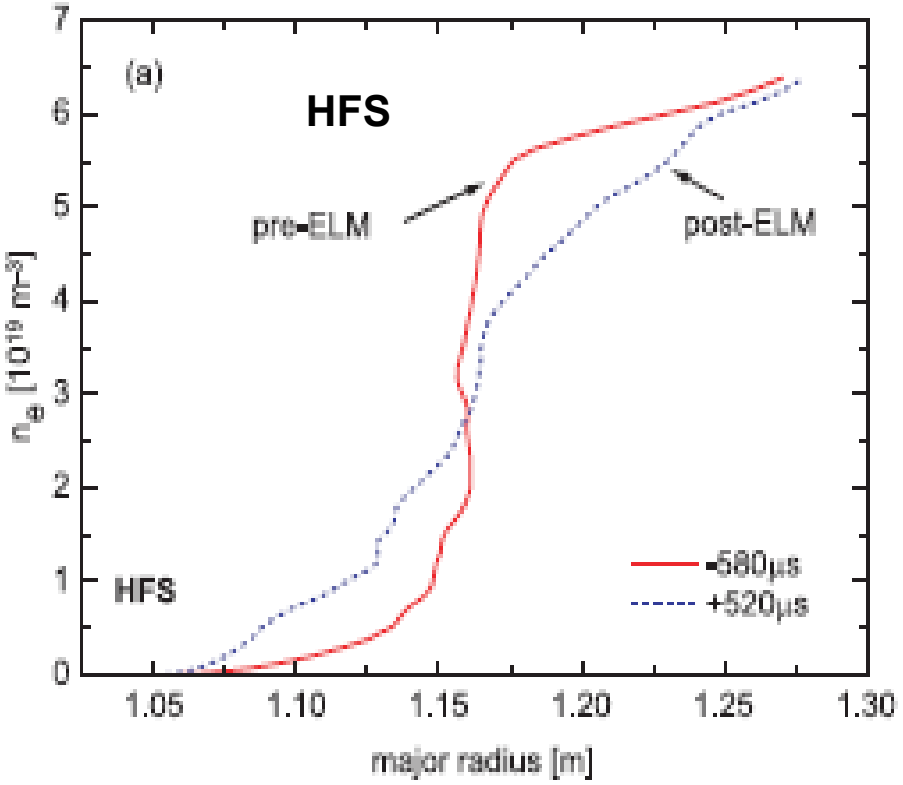

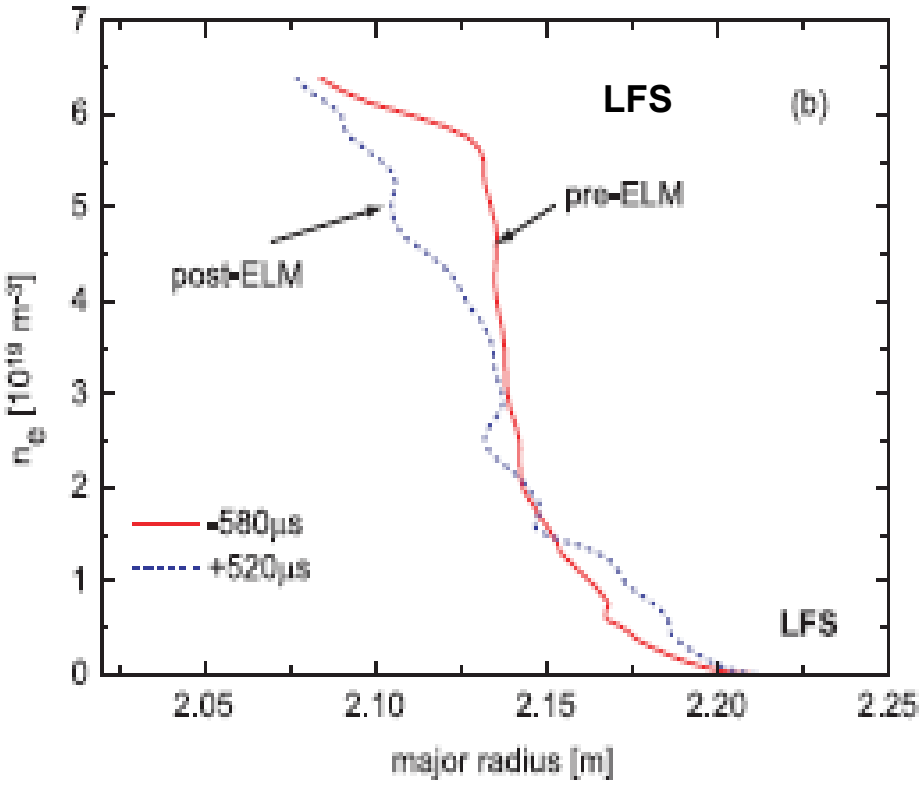

JET – „sewing“ of density profile from the measurements of two different diagnostic method (LIDAR - core and fast swept XM reflectometer - edge)

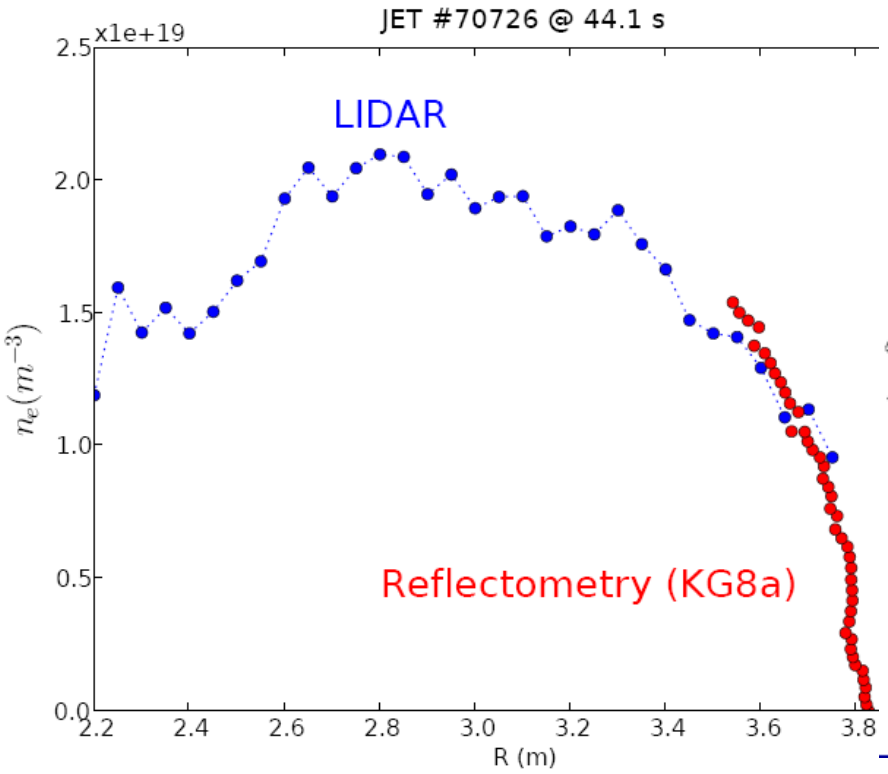

L mode

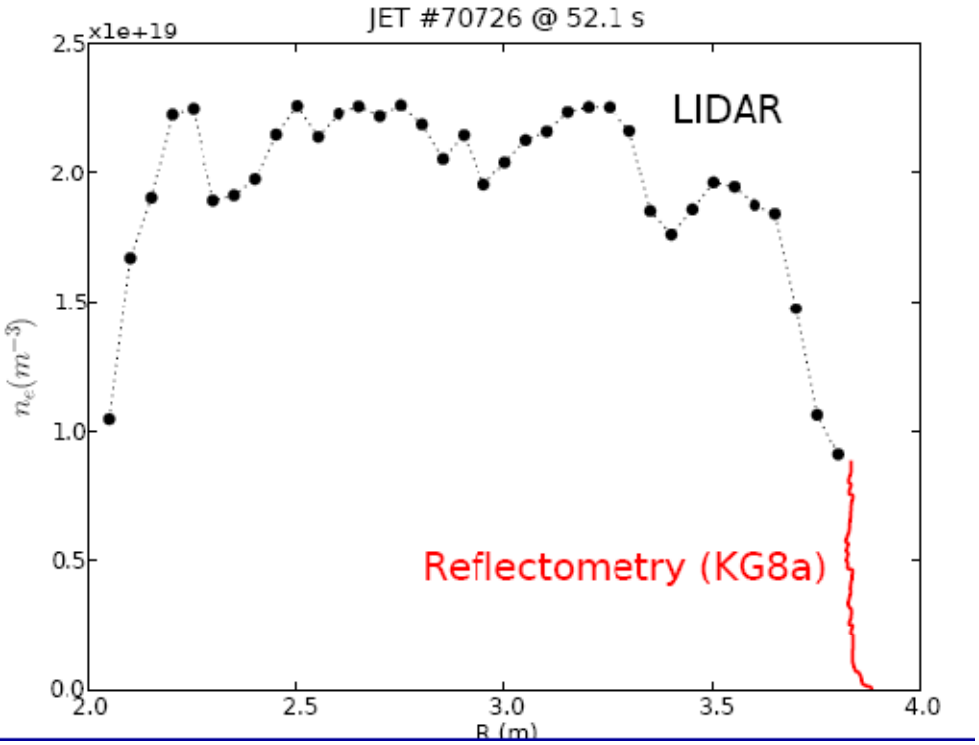

H mode

Broadband reflectometer for COMPASS

(under development with IST Lisboa)

1. **Edge pedestal plasma measurements with spatial resolution Δr≤1cm**
3. **Study of fast transient events with time resolution ~tens of μs**
2. **Correlation properties of plasma turbulence with frequency hopping (low phase noise synthesizers)**

System will have four frequency bands, but together five reflectometers:

Ka in O- as well as X-mode,
K, U, E only in O-mode

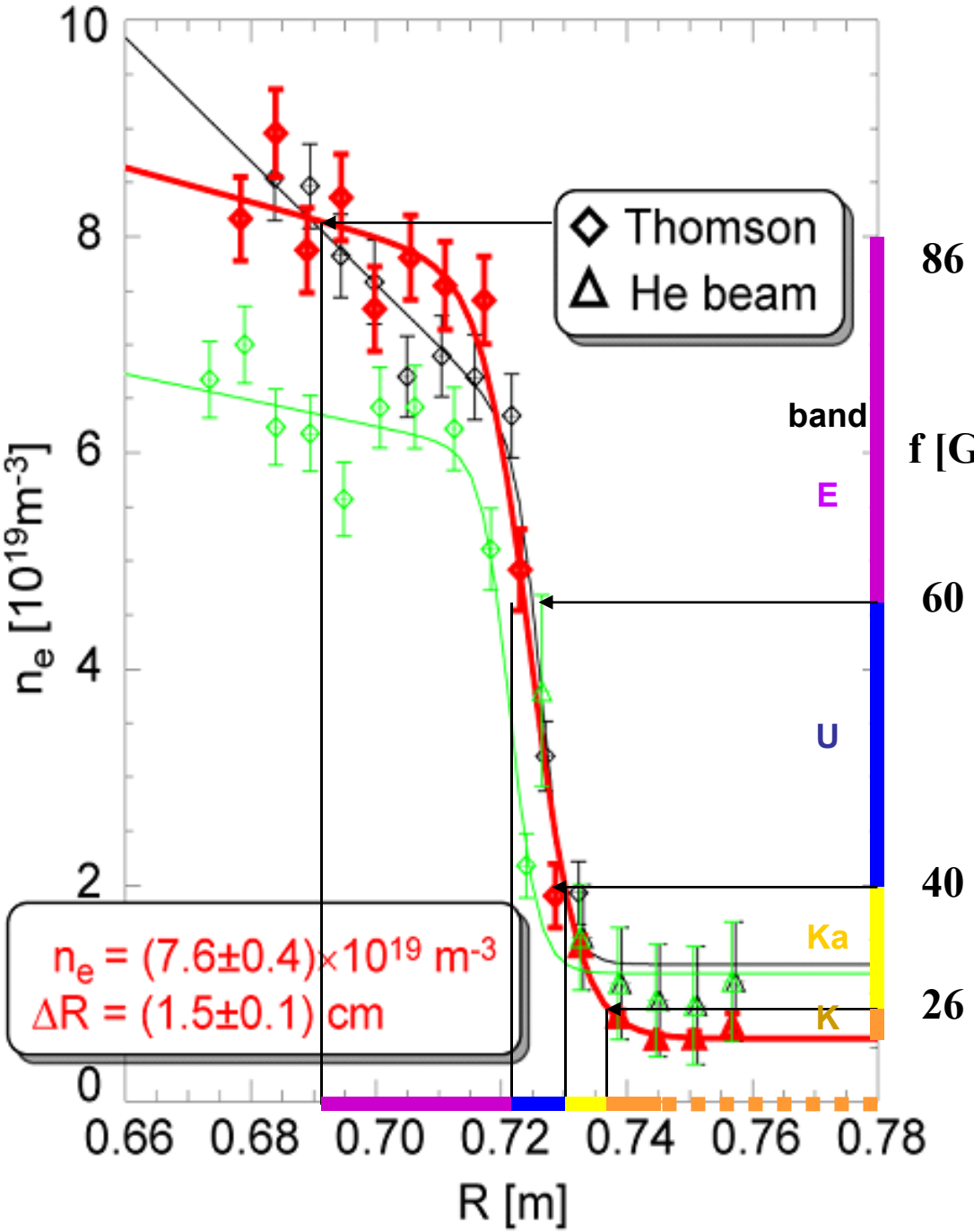

COMPASS:
R = 0.56 m
a = 0.2 m

$$N_{crit}\ [m^{-3}] = 0.0124\ f^2[Hz]$$

Block scheme of the transmitter and receiver of COMPASS reflectometer

(design, under construction)

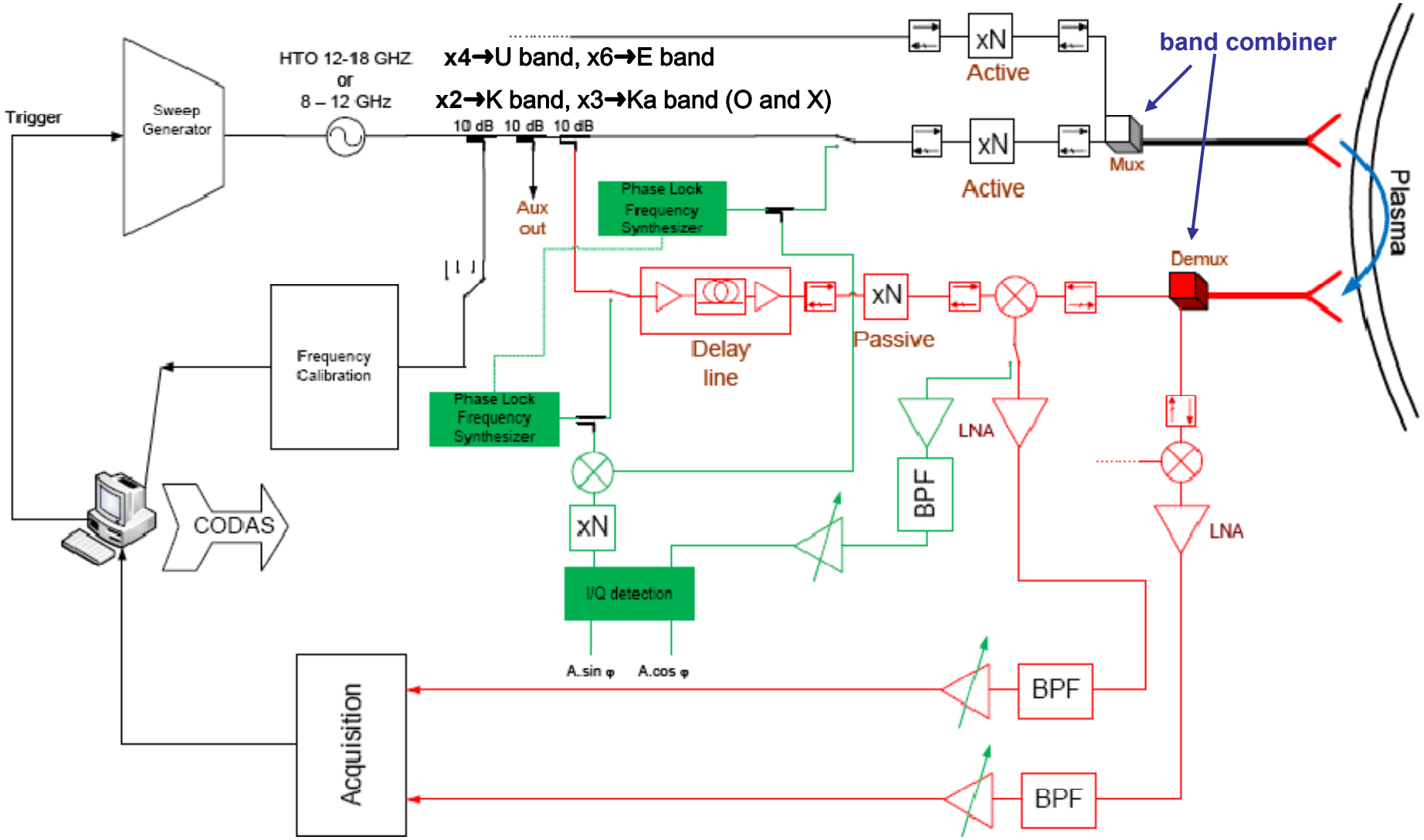

Scattering of the electromagnetic waves

Conservation laws: $k_s = k_i \pm k_f$ $\omega_s = \omega_i \pm \omega_f$ **where indices:** i … incident radiation (wave); s … scattered radiation; f … scattering object

Angle of observation Θ_s determines, what k_f is measured

For optical and microwave band in case of plasma turbulence detection may be seen that:

$\omega_i \gg \omega_f \Rightarrow \omega_s \approx \omega_i$ **and therefore also** $|k_i| \approx |k_s|$ $(k=\omega/v) \Rightarrow$ **vectors** k_i **a** k_s **form an isosceles triangle**

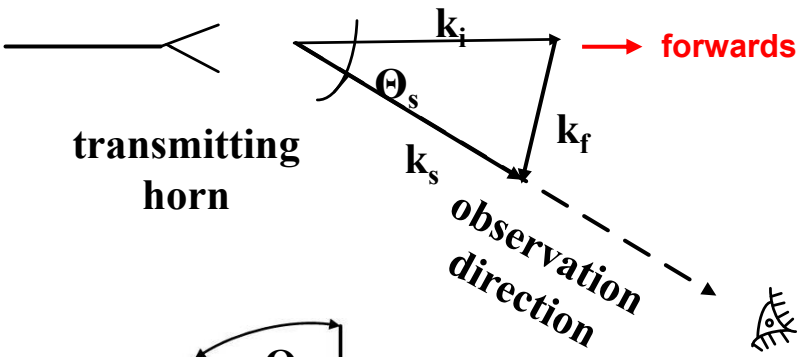

$k_f^2 = k_i^2 + k_s^2 - 2k_i k_s \cos\Theta_s$

$\Rightarrow k_f = 2k_i \sin(\Theta_s/2)$ $(\lambda_f^{min}=(\lambda_i/2))$

$\Rightarrow$ angle of maximum scattering on inhomogeneity with a given λ_f fulfils the following condition

$\Theta_s^{max} = 2\arcsin(\lambda_i/2\lambda_f) \Rightarrow \lambda_i/\lambda_f = 2\sin(\Theta_s/2)$

(so called Bragg condition, according to scattering of electrons or XR on the crystals: for $\omega_i \gg \omega_f$ the most scattered wavelength equals the incident wavelength):

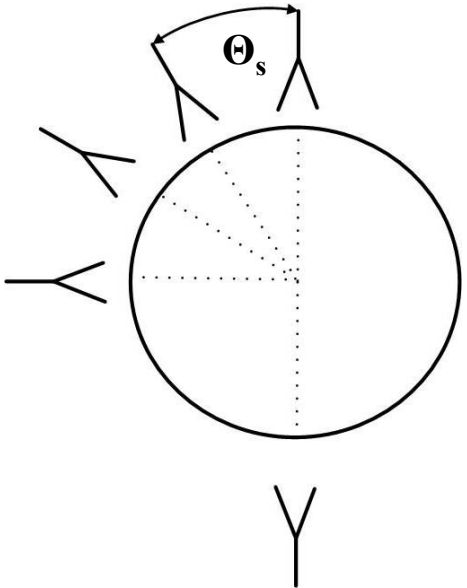

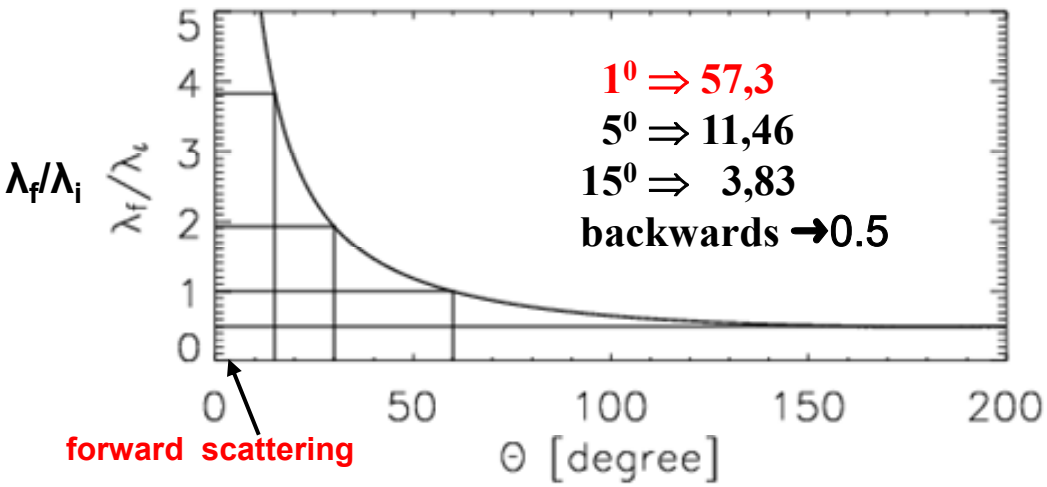

CASTOR microwave scattering at λ=2,6mm

Fizika Plazmy 15 (1989), 515

$$\langle \delta n^2 \rangle = n/(2\pi)^4 \cdot \int_{\omega} \int_{k} S(k,\omega).d^3k.d\omega$$

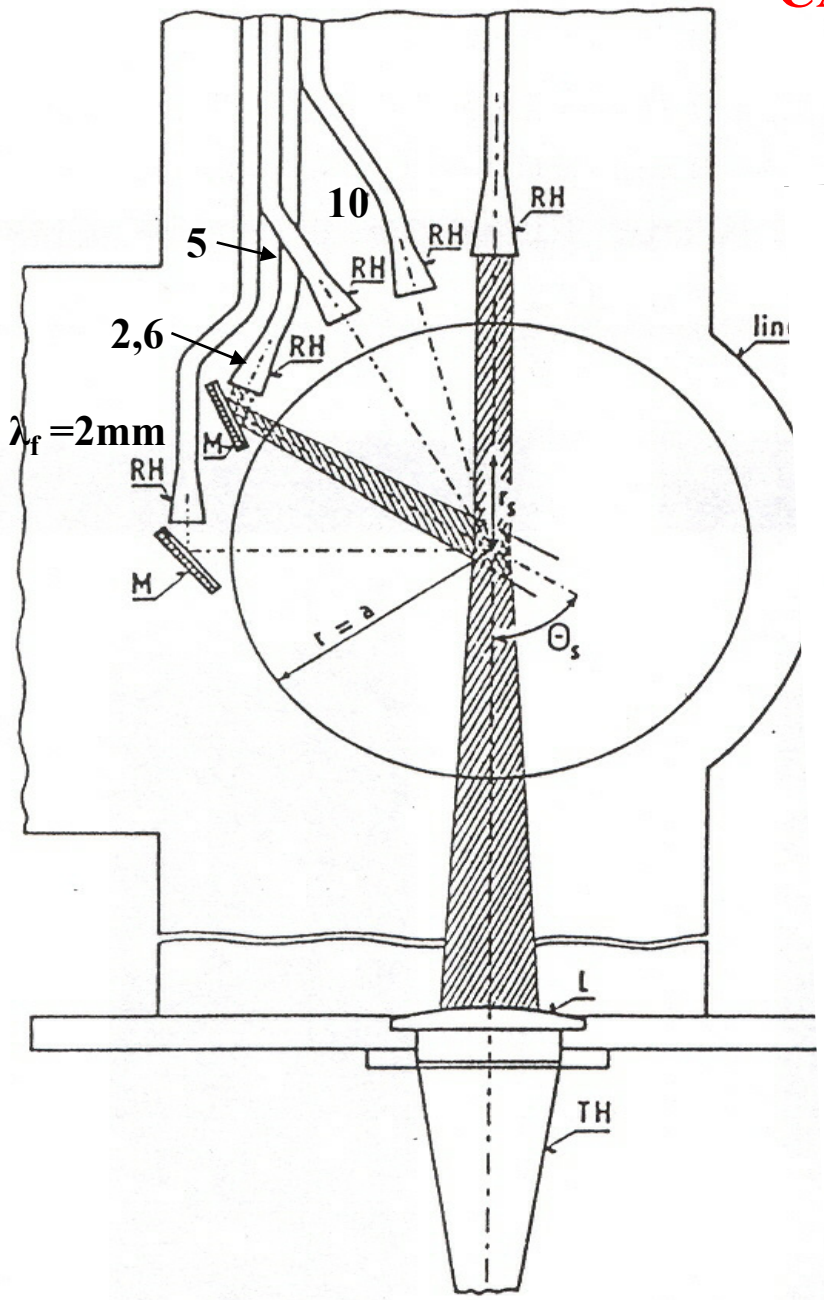

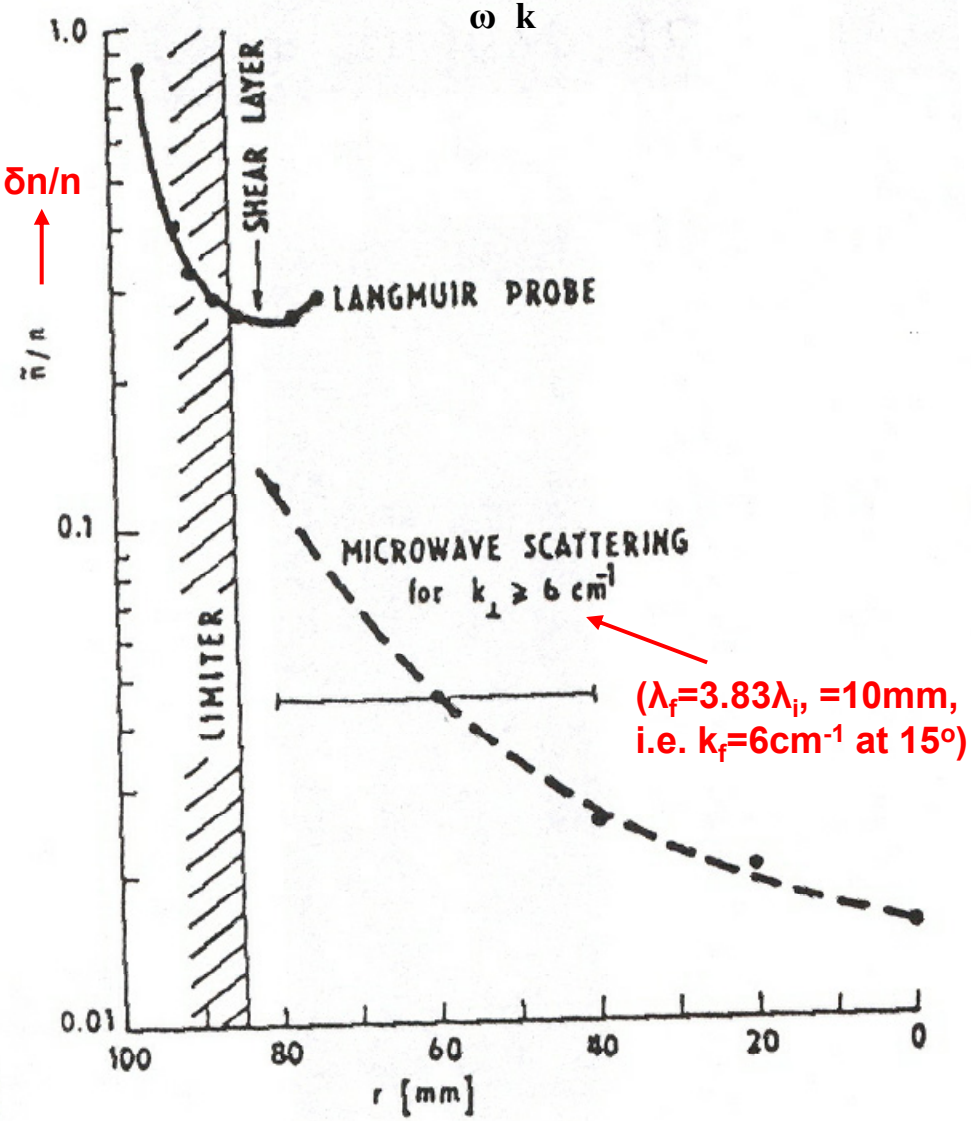

(λ_f=3.83λ_i, =10mm, i.e. k_f=6cm^{-1} at 15°)

Scheme of monostatic Doppler reflectometry

a) microwave beam (λ_o, $f=f_o$) strikes upon a fluctuating reflecting surface ($\Lambda_\perp=2\pi/k_\perp$, amplitude σ), moving across the magnetic field with a velocity $u_\perp$ ($k_\parallel \approx 0$), under angle Θ_t (measured from the normal of incidence)

b) angle Θ_t determines the measured $k_\perp$ fluctuations (Braggs condition), $f_D = \delta f_o$ determines $u_\perp$, intensity of the reflected signal determines the amplitude of fluctuations σ

b) if dimension of the reflecting „spot“ is 2w and wave strikes under angle Θ_t to the magnetic field lines then the space resolution of $k_\perp$ measurement $\Delta k_\perp \approx 2.\sqrt{2}.\cos\Theta_t/w$ and $\delta\omega_D \approx \Delta k_\perp.u_\perp$

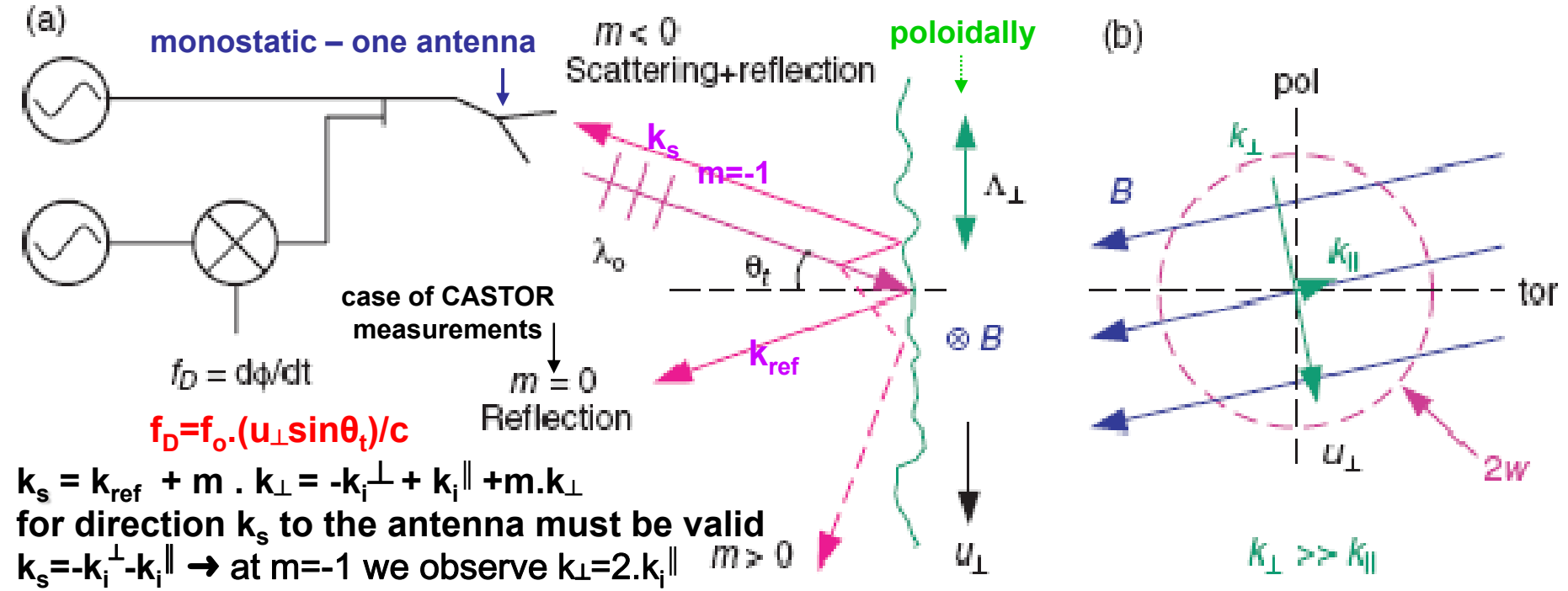

$k_s = k_{ref} + m \cdot k_\perp = -k_i^\perp + k_i^\parallel + m.k_\perp$

for direction k_s to the antenna must be valid

$k_s = -k_i^\perp - k_i^\parallel$ → at m=-1 we observe $k_\perp = 2.k_i^\parallel$

Tokamak AUG – two profiles of $u_\perp$ for different directions of the magnetic field (O-mode reflectometer)

measured at 7,5MW co-NBI, I_p = +0.8MA, just after L→H transition

B_{tor} = -2,6T (red), B_{tor} = +2,6T (blue)

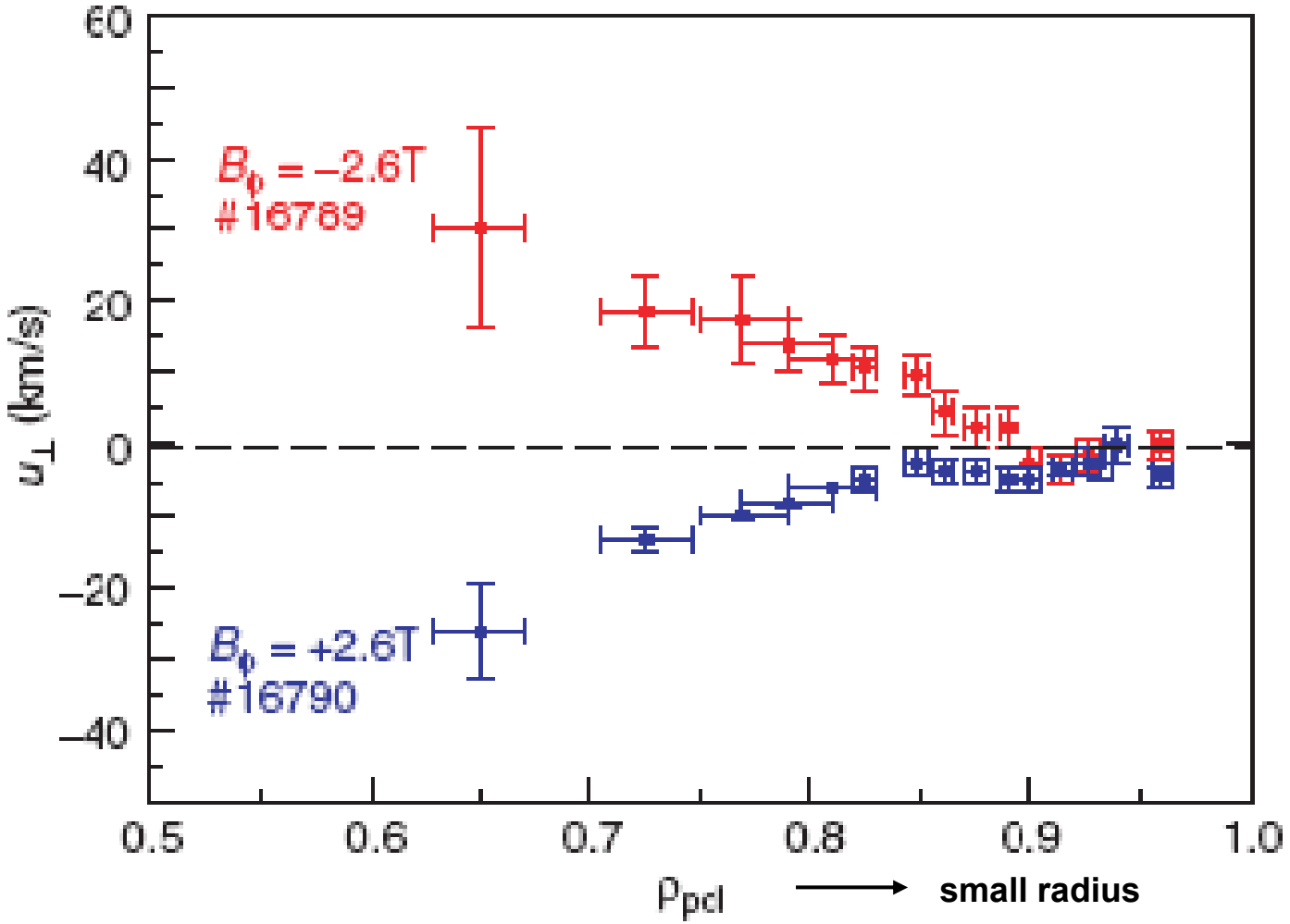

Comparison of microwave reflectometry and interferometry

A) Common features of the both methods:

- in both cases phase interferometric measurements of the probe electromagnetic wave is carried out
- i.e. the both methods are active diagnostic methods
- the probing is realized in contactless way, i.e. both methods are convenient for diagnostics of a hot plasma
- the same RF technique (waveguides, antennas, …) is used
- the same RF generators (frequencies may differ, but maximum several times)
- the same phase detecting systems (interference of the probing and reference waves) are used

Comparison of microwave interferometry and reflectometry

B) **The methods have different characteristics and this fact results in a different application of the both methods:**

	interferometer	versus	reflectometer
• probing wave	passes the medium ⇩		is reflected on the cut-off layer r_{cut} where r_{cut} = function(ω, n_e, B) ⇩
• effect of the the medium is	averaged along the wave path ⇩		extremely well localized ⇩
• utilization	determination of $\langle n_e \rangle_{lin}$		determination of $\delta n_e(r=r_{cut})$
• sensitivity to δ_{ne}	low		high
• data evaluation	simple (low f, small amplitude changes) ⇩		more complex (high f, high amplitude changes) ⇩
• measuring circuit	interferometer with one phase detector		two interferometric branches are needed (I/Q detection principle, on CASTOR sin-cosin scheme)

Planck: $B(\omega,T) = (\hbar/8\pi^3c^2)\omega^3.(1/(e^{\hbar\omega/kTe} - 1)$ for CASTOR, where T_e=100eV:

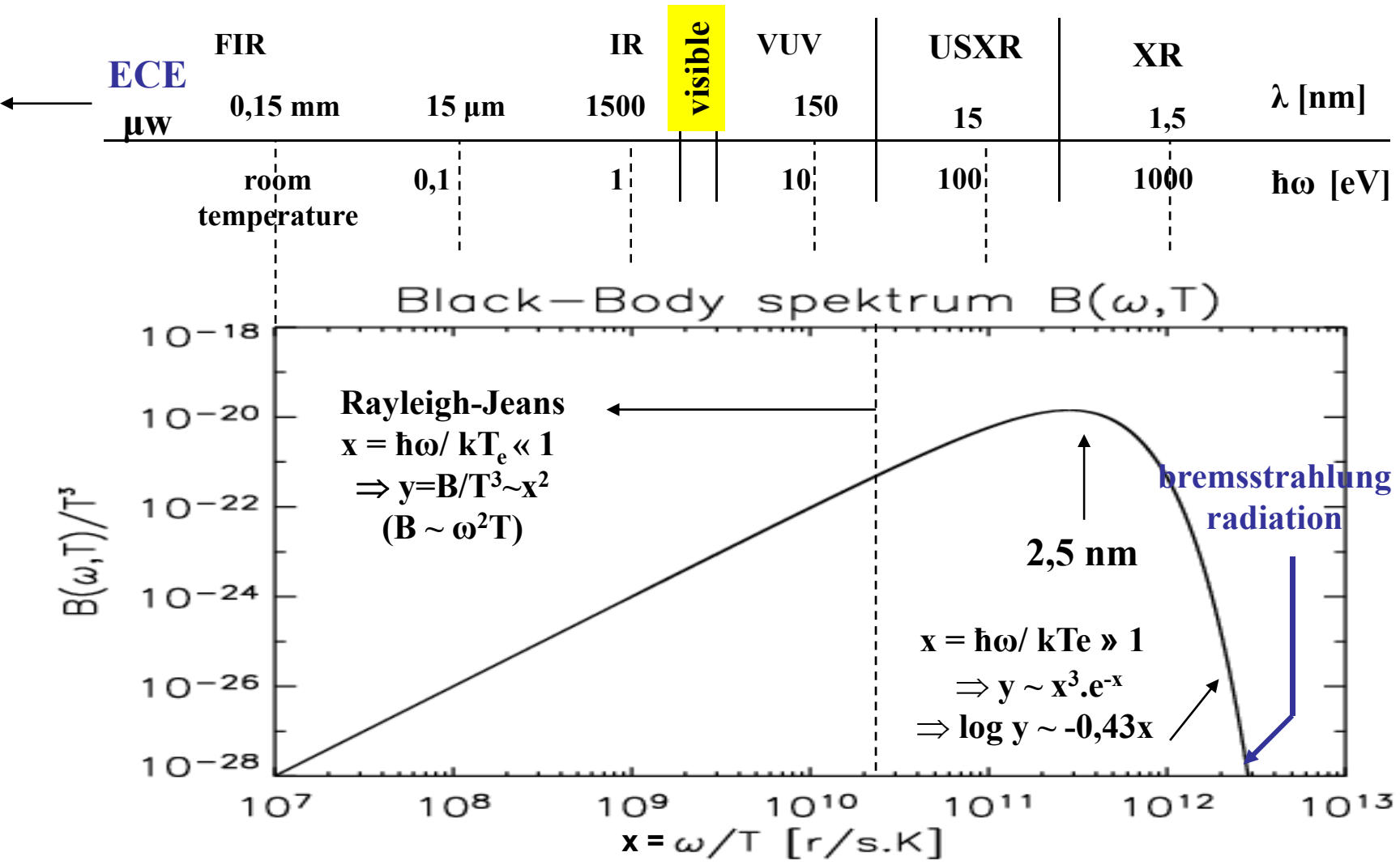

Tokamak DITE – evaluated X-wave ECE spectrum

(and in the case of maxwellian plasma electron temperature profile)

for following parameters on the device axis:

- **density 6.19^{19}m^{-3}**
- **electron temperature 300 eV**
- **magnetic field 2,7 T**

Tokamaks:

$\omega_c(R)=eB(R)/m$ ➜ radius identification

spectral x space resolution: $d\omega/\omega = -dR/R$

1. Tokamaks- spectral x space resolution:

$$d\omega/\omega_{ce} = s.(v_{Te}/c)^2 = -dR/R$$

2. Optical thickness must be: $\tau = \int \alpha_\omega(N,T_e,R,s).dR >> 1$

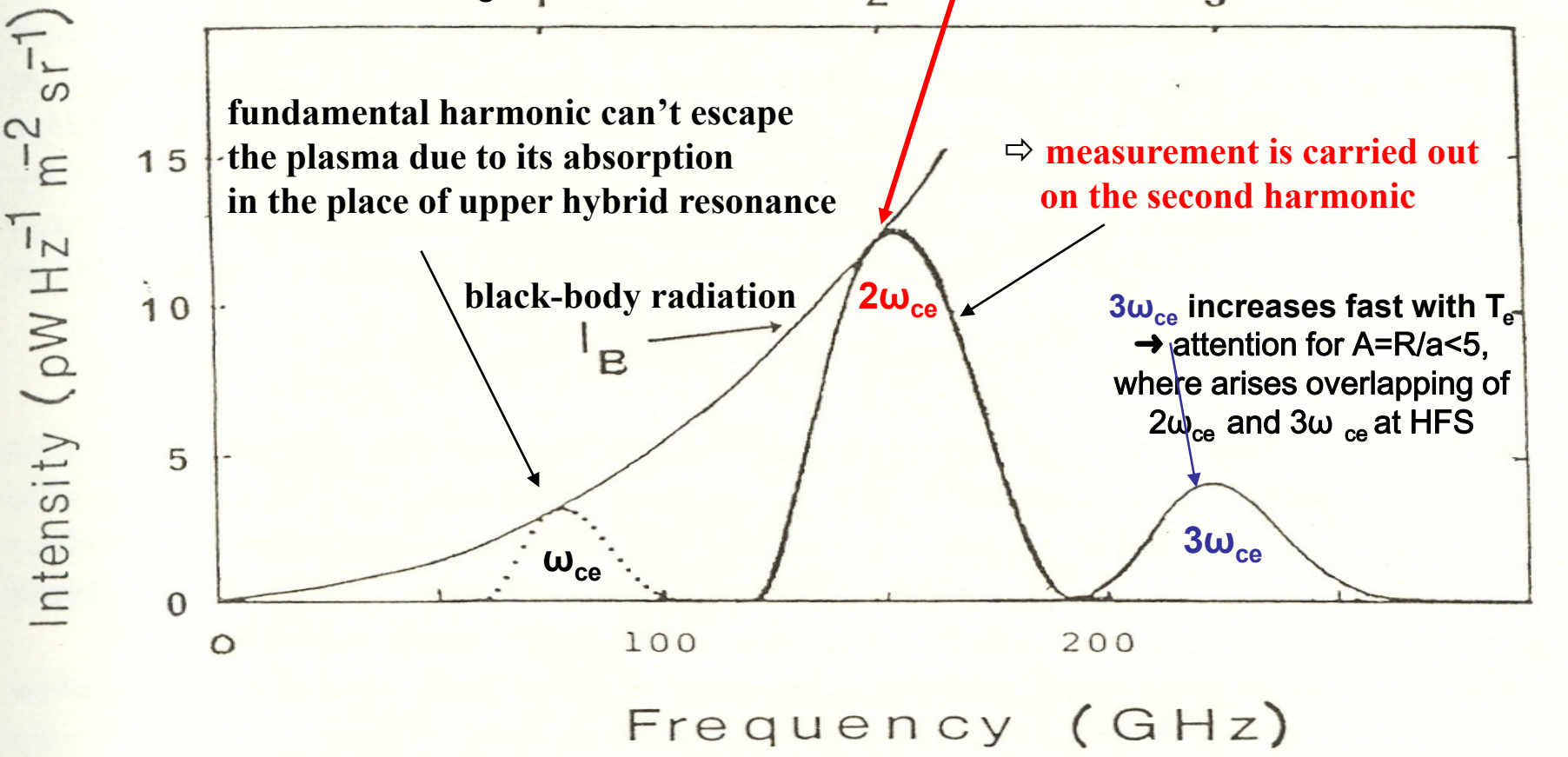

Radiometer for COMPASS: ECE (θ=90°) and EBE (θ≠90°) both polarizations

One 16-channel heterodyne receiver with total bandwidth 15GHz wil be alternately connected to Ka-band or E-band front-end circuits (E-band is divided to two sub-bands using a changeable input BPF)

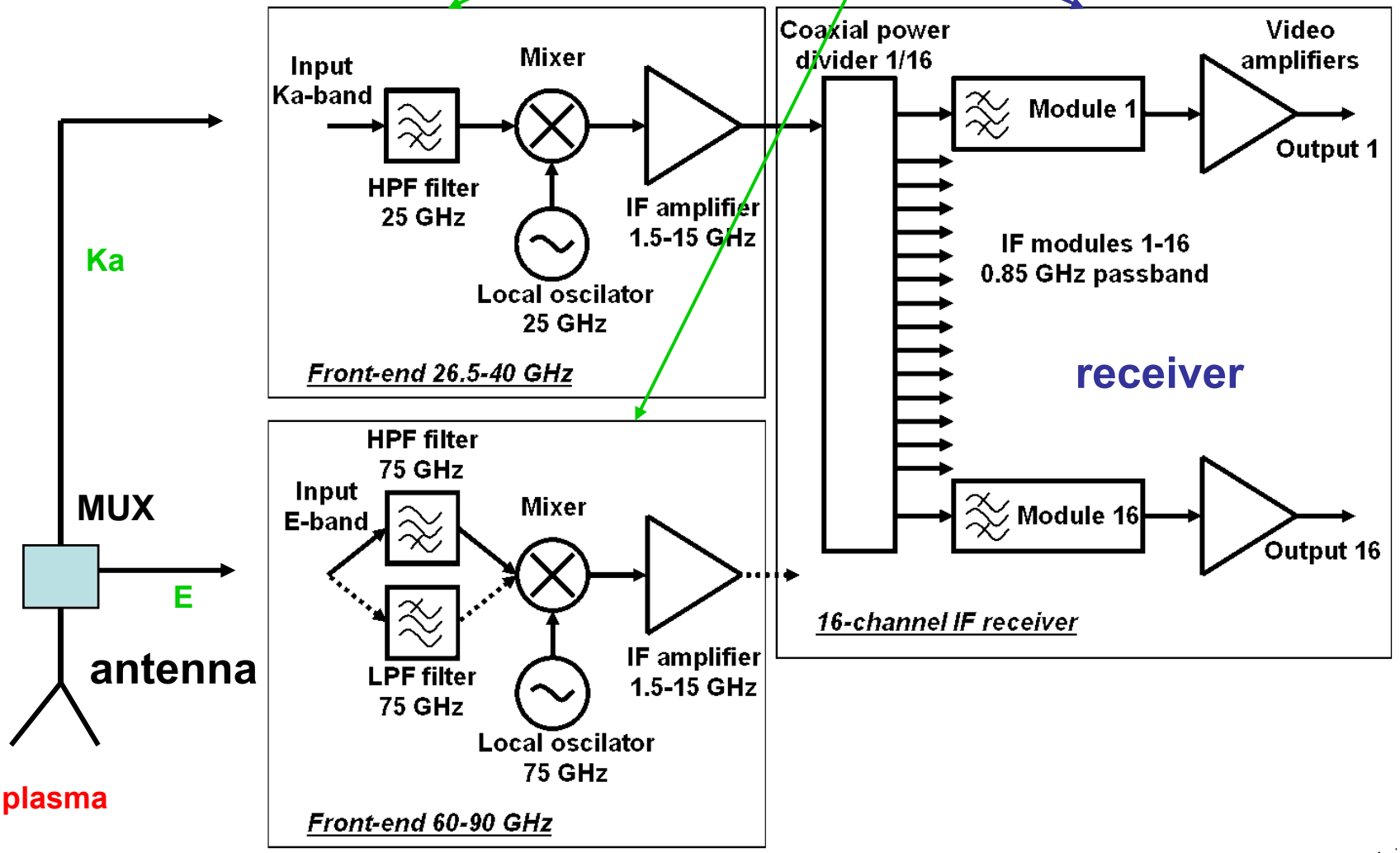

Equipment

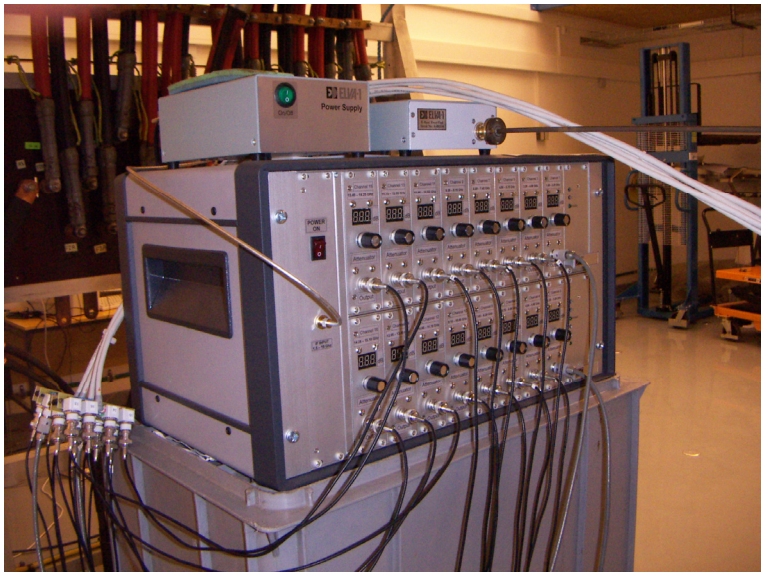

16-channel receiver

GOLA antennas for Ka and E bands

Horn antenna

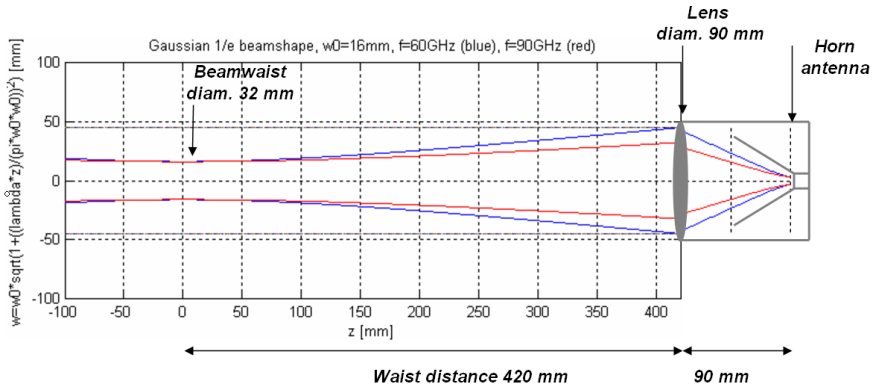

Beamshapes of gaussian-optics lens antenna

First tests on Compass

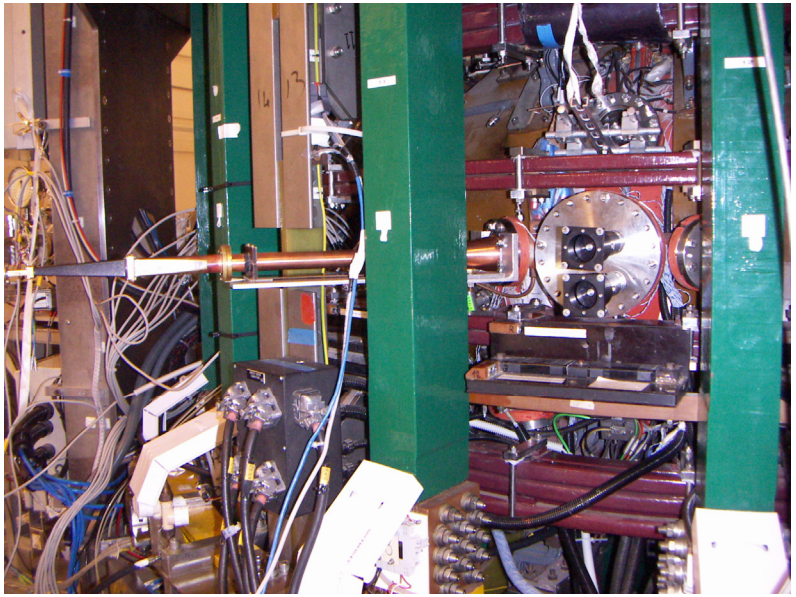

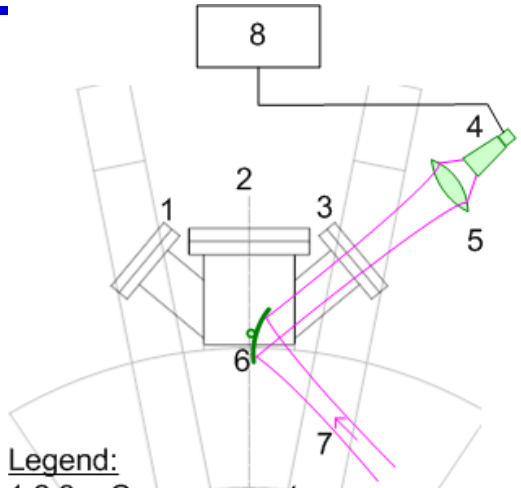

Legend:
1,2,3 – Compass ports
4 – horn antenna
5 – microwave lens
6 – rotatable mirror
7 – beam waist
8 – Radiometer 26.5-40 GHz

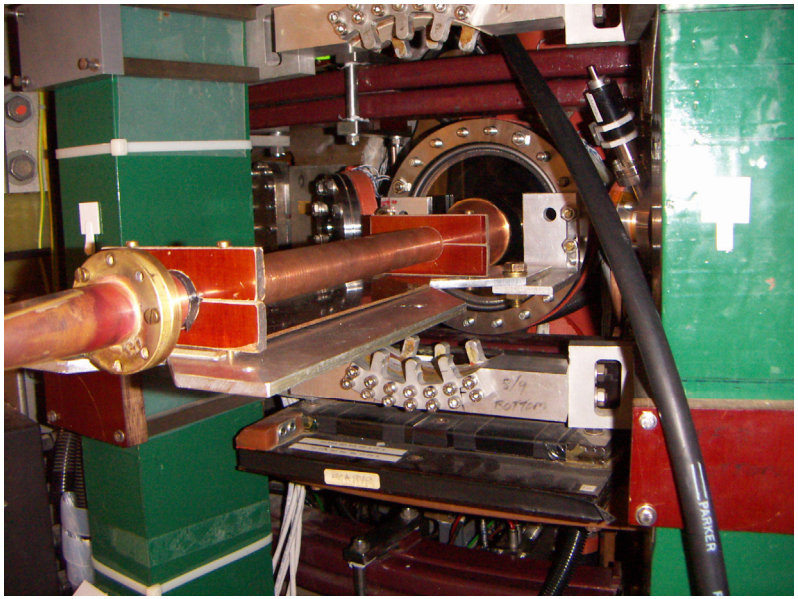

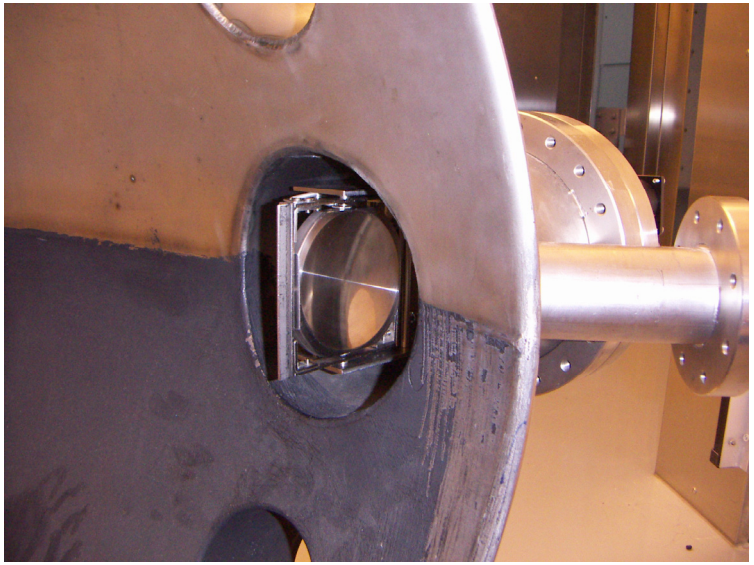

Example of signals from tests on COMPASS

(B_0 = 0.8 T, Ka band, O-mode)

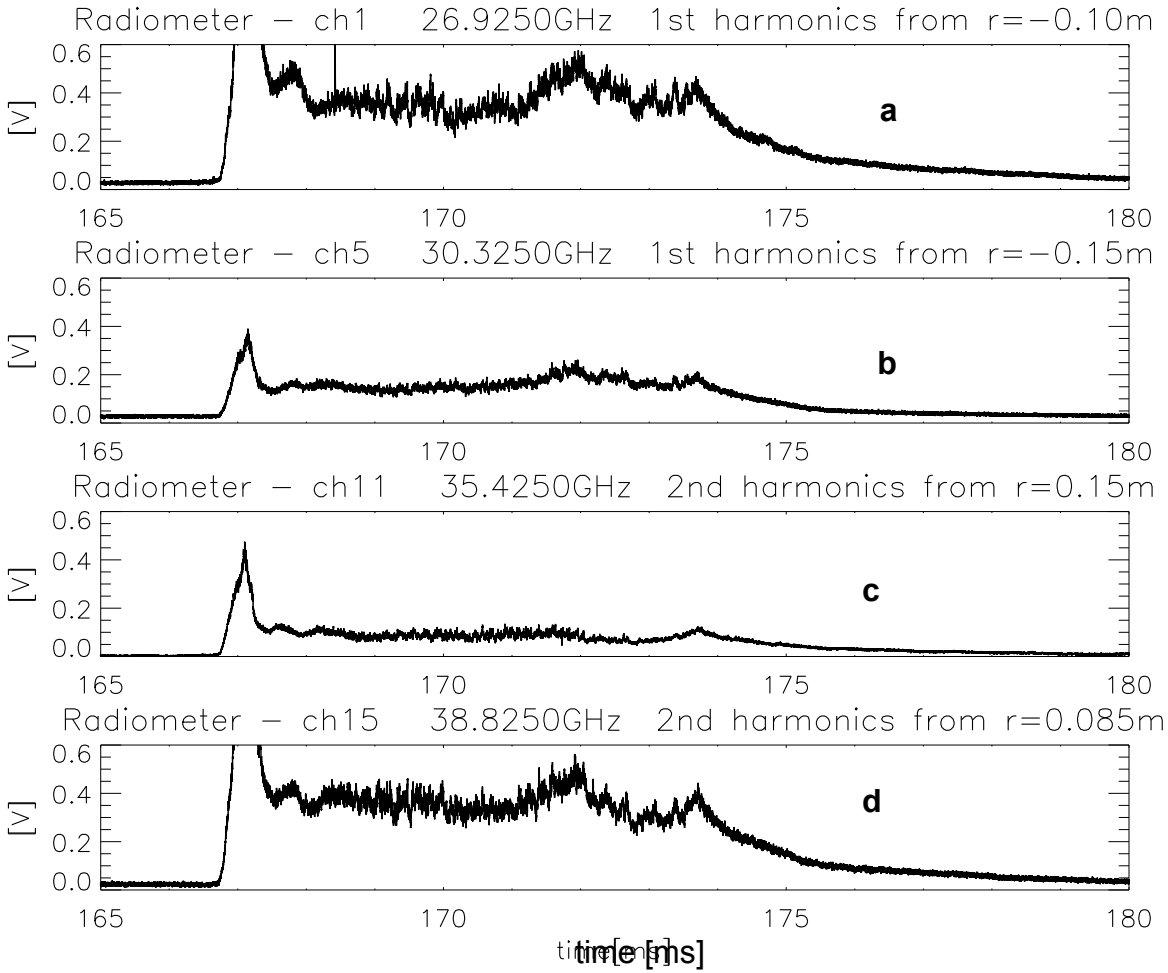

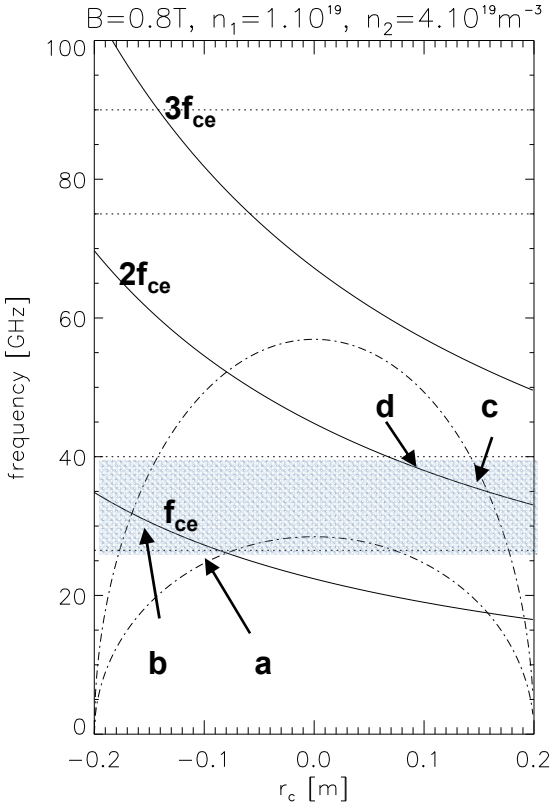

0.8 T / Ka band

COMPASS: A=R/a= 0.56/0.2=2.8

Diagnostic de sondes HF sur le coupleur C3

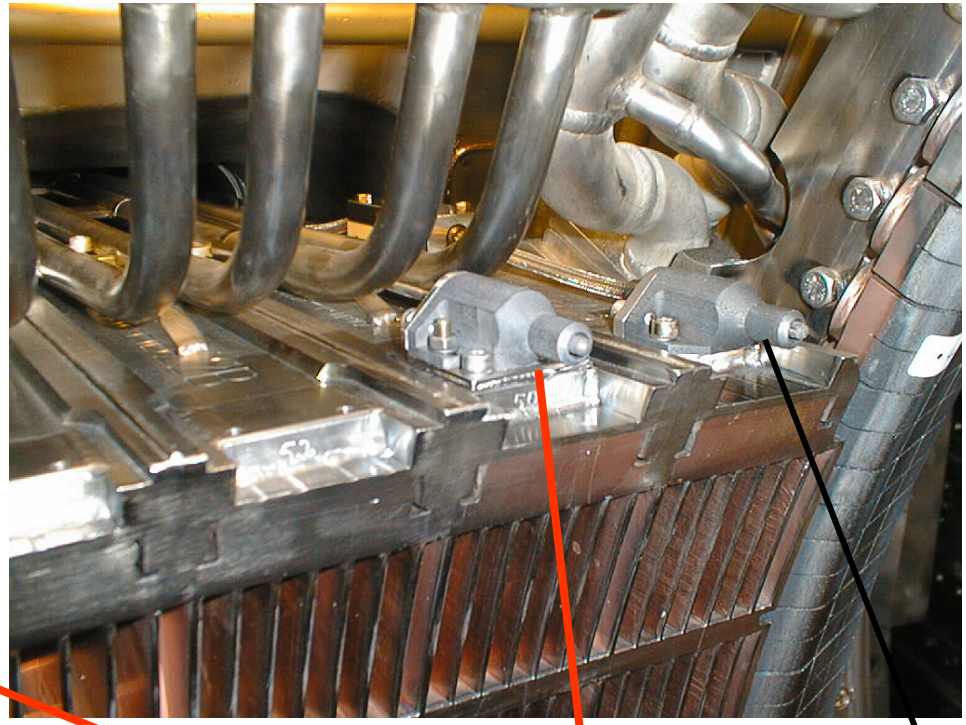

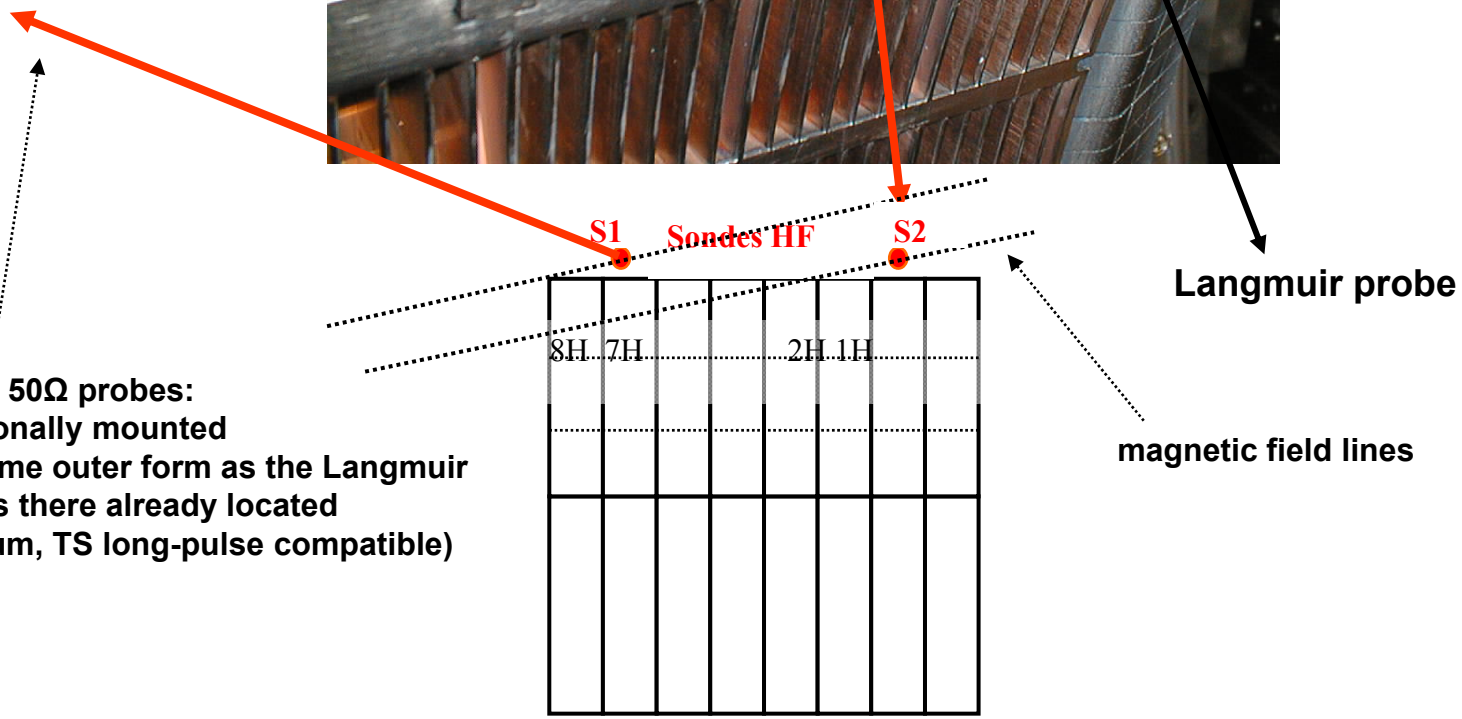

Miniature double 50Ω RF probe for new C4 Tore Supra LHCD launcher

(correlation characteristics of the launched wave as well as production of parasitically accelerated electrons resulting in creation of hot spots observed under high RF powers)

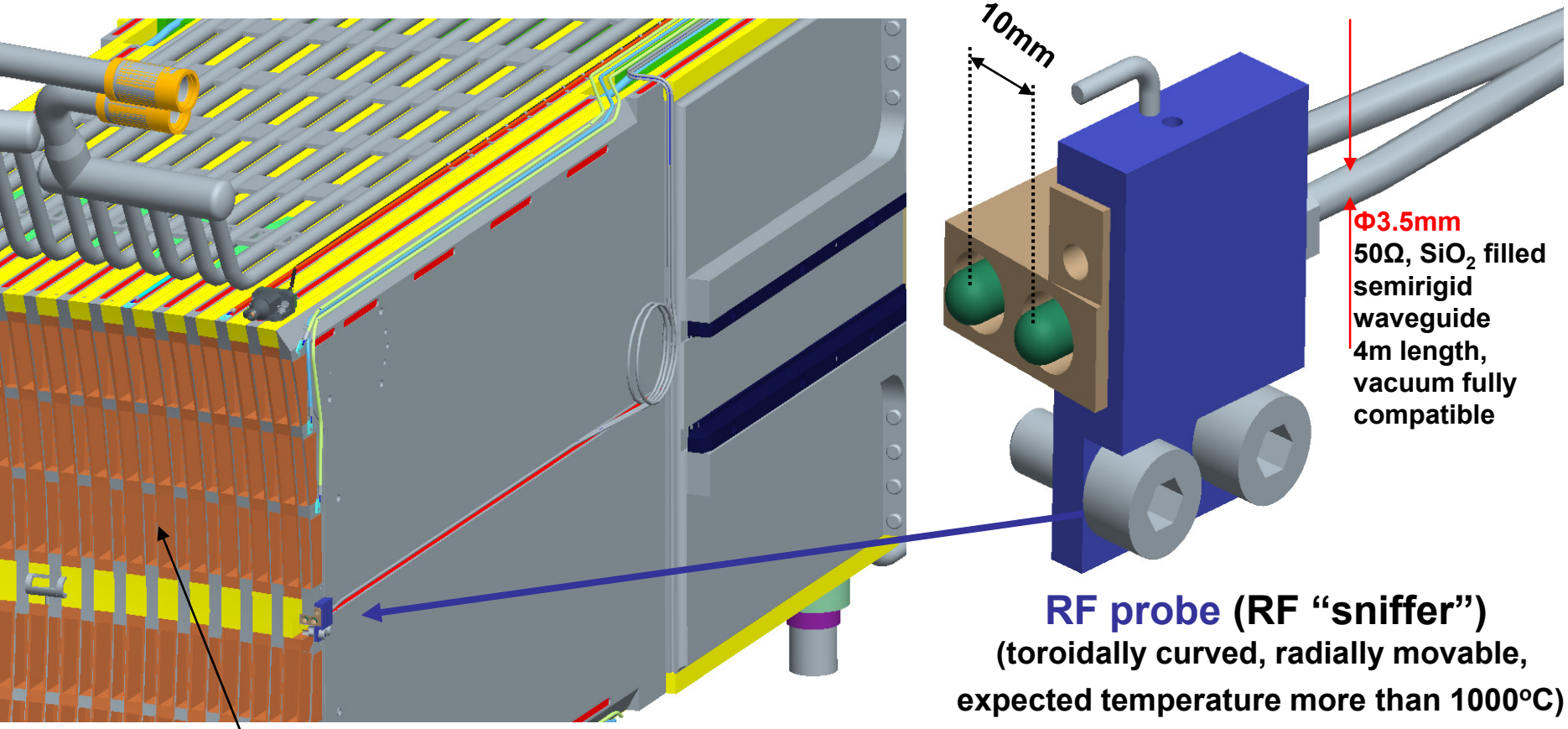

Thanks for your attention